



Feasibility of Integrating Nondestructive Testing Data Analysis Techniques

Research Report 0-4393-1

TxDOT Project Number 0-4393

**Conducted for:
Texas Department of Transportation &
Federal Highway Administration**

August 2005

Center for Transportation Infrastructure Systems
The University of Texas at El Paso
El Paso, TX 79968
(915) 747-6925

This page replaces an intentionally blank page in the original.

-- CTR Library Digitization Team

TECHNICAL REPORT STANDARD TITLE PAGE

1. Report No. FHWA/TX-05/0-4393-1		2. Government Accession No.		3. Recipient's Catalog No.	
4. Title and Subtitle Feasibility of Integrating of Nondestructive Testing Data Analysis Techniques				5. Report Date August 2005	
				6. Performing Organization Code	
7. Author(s) I. Abdallah, D. Yuan, S. Nazarian and C. Ferregut				8. Performing Organization Report No. TX 0-4393-1	
9. Performing Organization Name and Address Center for Transportation Research Systems The University of Texas at El Paso El Paso, Texas 79968-0516				10. Work Unit No.	
				11. Contract or Grant No. 0-4393	
12. Sponsoring Agency Name and Address Texas Department of Transportation Research and Technology Implementation Office P.O. Box 5080 Austin, Texas 78763-5080				13. Type of Report and Period Covered Technical Report Sept. 1, 2002 –August 31, 2003	
				14. Sponsoring Agency Code	
15. Supplementary Notes Research Performed in Cooperation with TxDOT and FHWA entitled "Integration of Nondestructive Testing Data Analysis Techniques."					
16. Abstract TxDOT is increasingly using of nondestructive testing (NDT) for structural evaluation of pavements used in design and rehabilitation selection procedures. The Falling Weight Deflectometer (FWD) is currently the main structural evaluation tool. The Ground Penetrating Radar (GPR) has been introduced to supplement the FWD testing by providing thickness information, defining section breaks, and locating areas of subsurface defects in flexible pavements. The Seismic Pavement Analyzer (SPA) has been demonstrated to provide information about the structural capacity that is not available with the FWD. Each of the three devices has strengths and weaknesses. However, when combined, they can provide a wealth of information not available from a single device. The feasibility of joint analysis of the data obtained from these three devices, as well as others, is addressed in this report.					
17. Key Words Nondestructive Testing, Backcalculation, FWD, GPR, Seismic Pavement Analyzer			18. Distribution Statement No restrictions. This document is available to the public through the National Technical Information Service, 5285 Port Royal Road, Springfield, Virginia 22161, www.ntis.gov		
19. Security Classif. (of this report) Unclassified		20. Security Classif. (of this page) Unclassified		21. No. of Pages 106	22. Price

This page replaces an intentionally blank page in the original.

-- CTR Library Digitization Team

Feasibility of Integrating Nondestructive Testing Data Analysis Techniques

by

Imad Abdallah, MSCE
Deren Yuan, PhD
Soheil Nazarian, PhD, PE
and
Carlos Ferregut, PhD

Research Project TX-0-4393

Integration of Nondestructive Testing Data Analysis Techniques

**Conducted for
Texas Department of Transportation**

Research Report TX 0-4393-1

The Center for Transportation Infrastructure Systems
The University of Texas at El Paso
El Paso, TX 79968-0516

DISCLAIMERS

The contents of this report reflect the view of the authors who are responsible for the facts and the accuracy of the data presented herein. The contents do not necessarily reflect the official views or policies of the Texas Department of Transportation or the Federal Highway Administration. This report does not constitute a standard, a specification or a regulation.

The material contained in this report is experimental in nature and is published for informational purposes only. Any discrepancies with official views or policies of the Texas Department of Transportation or the Federal Highway Administration should be discussed with the appropriate Austin Division prior to implementation of the procedures or results.

NOT INTENDED FOR CONSTRUCTION, BIDDING, OR PERMIT PURPOSES

Imad Abdallah, MSCE
Deren Yuan, PhD
Soheil Nazarian, PhD, PE (69263)
Carlos Ferregut, PhD

Acknowledgements

The authors would like to express their sincere appreciation to the PD of the project John Bilyeu of the TxDOT Construction Division, and German Claros of the Research and Technology Implementation Office for their ever-present support. The project Advisors, consisted of Mike Murphy, Mark McDaniel, Joe Leidy, Dar Hao Chen, Carl Bertrand and Ahmed Eltahan, provided invaluable suggestions to focus the objectives of this project in a manner that is useful to TxDOT day-to-day use.

We are also grateful to a large number of TxDOT district personnel who assisted us with planning and site selection, and field testing.

We would also like to thank Tom Scullion Co-PI of this project and his staff of researchers for providing us with advice and support on all aspects of this project.

Reuben Williams and Moein Ganji, graduate research assistants at UTEP assisted us in this project.

Abstract

TxDOT is increasingly using of nondestructive testing (NDT) for structural evaluation of pavements used in design and rehabilitation selection procedures. The Falling Weight Deflectometer (FWD) is currently the main structural evaluation tool. The Ground Penetrating Radar (GPR) has been introduced to supplement the FWD testing by providing thickness information, defining section breaks, and locating areas of subsurface defects in flexible pavements. The Seismic Pavement Analyzer (SPA) has been demonstrated to provide information about the structural capacity that is not available with the FWD. Each of the three devices has strengths and weaknesses. However, when combined, they can provide a wealth of information not available from a single device. The feasibility of joint analysis of the data obtained from these three devices, as well as others, is addressed in this report.

Executive Summary

Nondestructive testing (NDT) technology has made substantial progress in the last two decades. Currently, four NDT devices, the Falling Weight Deflectometer (FWD), the Ground Penetrating Radar (GPR), the Seismic Pavement Analyzer (SPA), and the Portable Seismic Property Analyzer (PSPA), are available to TxDOT for collecting field data. Each of these technologies has strengths and weaknesses. However, when combined, they can provide a wealth of information not available when one method is used alone.

The ultimate NDT tool for the evaluation of all pavement systems in Texas would be a device that integrates these NDT tools. The first step toward a fully integrated hardware is a robust integration software. The objective of this project is to harvest the strength of different NDT methods and combine them in a way as to improve the parameters used in pavement design and evaluation. This project will examine the strengths and weaknesses of each device to develop a work plan for integrating information collected from each device in a practical manner.

Developing an algorithm for combining data from different NDT methods with the objective to assess the state of a pavement requires specialized technical capabilities beyond the requirements of conventional data analysis. It requires: (a) a good understanding of each of the NDT techniques being considered, (b) in-depth knowledge of probability and statistical techniques, cross-correlation techniques and techniques for normalizing and re-sampling; and (c) a good understanding of advanced analysis techniques such as artificial neural networks and expert systems. In that context, combining the data from different methods falls under the following three broad categories a) sequential ordinary inversion (backcalculation), b) joint inversion, and data fusion.

In this document, the feasibility of the concept of integration was demonstrated. The different integration schemes that were investigated are described. Several options that are selected for implementation are detailed. Finally a work plan for the next stage is provided.

Implementation Statement

At this stage of the project the tools and algorithms are underdevelopment and are not ready for implementation.

Table of Contents

List of Figures.....	xiii
List of Tables	xv
Chapter 1 - Introduction	1
Objective	1
Organization of Report.....	2
Chapter 2 - Background.....	3
Introduction.....	3
Nondestructive Testing Methods	3
Falling Weight Deflectometer	3
Strength and weaknesses.....	4
Seismic Pavement Analyzer	4
Strengths and weaknesses	10
Portable Seismic Pavement Analyzer.....	10
Strengths and weaknesses	11
Ground Penetrating Radar	11
Strengths and weaknesses	12
Integration Algorithms.....	12
Sequential Analysis	12
Joint Analysis	12
Data Fusion.....	13
Chapter 3 - Data Collection and Data Analysis	17
Introduction.....	17
Preliminary Survey	17
Data Collection	18
Data Analysis.....	20
Robustness in Current Analysis Practices.....	22

Repeatability of NDT devices.....	22
Significant Parameters of NDT Analysis Programs	24
Harmonizing Field Testing Protocols.....	30
Chapter 4 - Development of Integration Algorithms.....	33
Introduction.....	33
Overall Integration Scheme	33
Sequential Integration Algorithms.....	34
Joint Inversion.....	36
Data Fusion.....	39
Chapter 5 - Feasible Integration Techniques Based on Case Studies.....	41
Introduction.....	41
Case Study - El Paso District Parking Lot.....	41
Data Analysis.....	42
SPA-SASW Analysis.....	42
SMART Analysis.....	45
FWD Analysis.....	46
JIM analysis	48
Comparison of Results from the Different Analyses.....	48
Case Study - Ride Rut Facility at Riverside Annex.....	52
Field Testing.....	53
Data Analysis.....	54
Conventional Analyses	54
JIM analysis	55
Comparison of Results from Different Analyses.....	57
Sequential Analyses.....	60
Summary of Case Studies.....	60
Chapter 6 - Work Plan for Implementing Integration Algorithms	63
References	67
Appendix A - Sample Survey.....	71
Appendix B - Results of Survey.....	79
Appendix C - Results of Data Analysis Using SMART, MODULUS, and JIM for the Ride Rut facility	89

List of Figures

Figure 2.1 -	Falling Weight Deflectometer.....	4
Figure 2.2 -	Seismic Pavement Analyzer	5
Figure 2.3 -	Master curve concept	8
Figure 2.4 -	Portable Seismic Pavement Analyzer	10
Figure 2.5 -	Ground Penetrating Radar.....	11
Figure 2.6 -	Human data fusion center	14
Figure 2.7 -	Data fusion center for pavements	15
Figure 3.1 -	NDT devices used by TxDOT personnel.....	18
Figure 3.2 -	NDT devices in which TxDOT Personnel are satisfied with their data collection scheme.....	19
Figure 3.3 -	Source of information used to provide the thickness and initial modulus for each layer in backcalculation analysis.....	20
Figure 3.4 -	Use of GPR or seismic results in modulus backcalculation	21
Figure 3.5 -	Repeatability based on FWD	23
Figure 3.6 -	Repeatability based on SPA.....	23
Figure 3.7 -	Results of repeatability test from GPR at the Ride Rut facility.	24
Figure 4.1 -	Overall schematic of proposed integration tools	34
Figure 4.2 -	Sequential integration process using MODULUS for calculating layer moduli	35
Figure 4.3 -	Joint inversion algorithm flowchart.....	37
Figure 4.4 -	Joint inversion method using data measured from both FWD and SPA.....	37
Figure 4.5 -	Comparing results of JIM with conventional method to evaluate stability of the algorithm	38
Figure 4.6 -	Comparing the convergence of JIM with conventional methods	39
Figure 4.7 -	Illustrative example of data fusion.....	40
Figure 5.1 -	FWD and SPA at El Paso District parking lot.....	42

Figure 5.2 -	Dispersion curves from SASW at El Paso District parking lot	43
Figure 5.3 -	Typical results from SASW data reduction processes at El Paso District parking lot	44
Figure 5.4 -	Variations in moduli from JIM along El Paso District parking lot.....	49
Figure 5.5 -	Variations in layer thicknesses from JIM and SMART along El Paso District parking lot	50
Figure 5.6 -	Comparison of moduli from MODULUS, SMART and JIM at El Paso District parking lot	51
Figure 5.7 -	Comparison of deflection basin mismatches at El Paso District parking lot.....	52
Figure 5.8 -	Schematic of the test setup and test section at the Ride Rut facility.....	53
Figure 5.9 -	FWD and SPA at the Ride Rut facility	53
Figure 5.10 -	Variation in moduli of pavement layers from JIM at the Ride Rut facility	56
Figure 5.11 -	Variations in layer thicknesses from JIM and SMART at the Ride Rut facility	57
Figure 5.12 -	Comparison of moduli obtained from MODULUS, SMART and JIM at the Ride Rut facility.....	58
Figure 5.13 -	Comparison of deflection basin mismatches at the Ride Rut facility	59
Figure 5.14 -	Comparison of moduli from MODULUS based on sequential analysis algorithms at the Ride Rut facility	61
Figure 6.1 -	Framework of the proposed integration algorithm	64
Figure 6.2 -	Flowchart of proposed software integration tools	65

List of Tables

Table 3.1 - Repeatability of PSPA at the Ride Rut facility	24
Table 3.2 - Repeatability of GPR at the Ride Rut facility	24
Table 3.3 - Results of parametric study using SASW for the inversion process	26
Table 3.4 - Results of parametric study using MODULUS for the backcalculation process.....	29
Table 3.5 - Results of parametric study using EVERCALC for the backcalculation process.....	30
Table 5.1 - Results of SASW data reduction process at El Paso District parking lot.....	45
Table 5.2 - Design moduli from SMART at El Paso District parking lot	46
Table 5.3 - Measured FWD field data normalized to 9000 lbs at El Paso District parking lot	47
Table 5.4 - Backcalculated Moduli from FWD at El Paso District parking lot.....	47
Table 5.5 - Design moduli from JIM at El Paso District parking lot.....	48
Table 5.6 - Results of SASW data reduction process the Ride Rut facility.....	55

Chapter 1

Introduction

Nondestructive testing (NDT) technology has made substantial progress in the last two decades. TxDOT extensively utilizes the Falling Weight Deflectometer (FWD) in their day-to-day activities. In the last decade, two new technologies, the Ground Penetrating Radar (GPR) and the seismic techniques as those used in the Seismic Pavement Analyzer (SPA) and Portable Seismic Pavement Analyzer (PSPA) have shown great promise. These tools are also being implemented at a rapid rate in the day-to-day activities of TxDOT. Each of the technologies introduced above has strengths and weaknesses. However, when combined, they can provide a wealth of information not available when one technology is used alone. The goal of this project is to determine whether combining information from the three different NDT devices would provide a more accurate depiction the pavement behavior than current practices.

Objective

The first task of this project is to identify the strength, weaknesses in the FWD, SPA/PSPA and GPR data analyses. The areas of improvement required for each technology are different. For the FWD, further development in the analysis procedures is needed to improve the stability and capabilities of current programs. Nonetheless, the greatest obstacle to a reliable implementation of the FWD is accurate determination of layer thickness and depth to shallow bedrock. The GPR measures the electric properties of the layers that can be translated to layer thickness and the uniformity of the pavement in terms of moisture and density. However, electric properties are not directly related to the mechanical properties used in structural evaluation. Seismic methods provide the thickness and moduli of different layers. However, the GPR is more convenient for thickness determination. In addition, the seismic moduli are small-strain moduli.

The main objective of this project is to develop a comprehensive NDT tool. One of the main tasks that will be addressed in this project is the feasibility of combining NDT methods. This is

addressed in the first year of this project. The focus and challenge in the first year of this project was on:

- a) identifying the strengths and weakness of each of the NDT methods,
- b) selecting various feasible alternatives for combining NDT analyses,
- c) implementing the alternatives selected in Item b and
- d) verifying the accuracy and robustness of each recommended integration algorithm with field data.

Also addressed in this project are the means and ways to merge the technology to ultimately be capable of having a pavement analysis tool using the strength of existing NDT methods. This leads to the second stage, which is ultimately to:

- a) improve synthesis, interpretation, and display of the data collected by the FWD, GPR, and SPA/PSPA,
- b) improve software for data analysis for each, all or any combination of the three technologies, and
- c) develop user's manuals, training schools, and associated materials.

Organization of Report

Chapter 2 contains a review of relevant literature regarding the FWD, SPA/PSPA and GPR as well as a general description of the methods for the interpretation of data from the devices. The strengths and weaknesses of each interpretation method are presented. That chapter also includes background and description of data integration strategies. Finally, an introduction of the data fusion techniques is presented.

Chapter 3 provides information about data collection and data analysis. A preliminary survey of TXDOT personnel conducted as part of this study is presented in that chapter. A discussion on harmonizing field-testing protocols with the three NDT devices is also included in that chapter.

The development of integration algorithms and the proposed integration schemes are presented in Chapter 4. The joint inversion is discussed in that chapter, as is the use of data fusion.

Chapter 5 contains the results of feasible integration techniques based on case studies. A discussion of the analyses and results for all sites tested are also presented. The strengths and limitations of the algorithm based on these studies are included.

The work plan for implementation of the integration algorithm is included in Chapter 6.

Chapter 2

Background

Introduction

In this chapter, a summary highlighting the main features and limitations of each nondestructive test method investigated is provided. First, a brief overview of each NDT device is presented followed by a rundown of the different analysis tools used for data reduction.

The second part of this chapter contains a discussion based on the integration techniques that were investigated. Also, a brief background on the probabilistic techniques utilized to examine and understand the limitations of each NDT method are provided. The last part of the chapter includes a brief discussion on the indicators used to verify the feasibility of the integration methodology.

Nondestructive Testing Methods

Falling Weight Deflectometer

The Falling Weight Deflectometer (FWD) is the most popular NDT device. As shown in Figure 2.1, the FWD applies an impulse load to the pavement, and seven or more sensors measure the deflections of the pavement. The deflections obtained from the sensors are analyzed to determine the layer moduli of the pavement. Normally, a backcalculation program is employed to implement this analysis.

The FWD data processing usually requires a backcalculation algorithm to obtain material properties from the deflection basin. The determination of pavement moduli using the static layer elastic backcalculation method is, by far, the most widely used procedure (Bush, 1980; Lytton, et al., 1985; Uzan and Lytton, 1990). The application of layered theory for in-situ material characterization requires the estimation of only one unknown parameter, the Young's modulus,

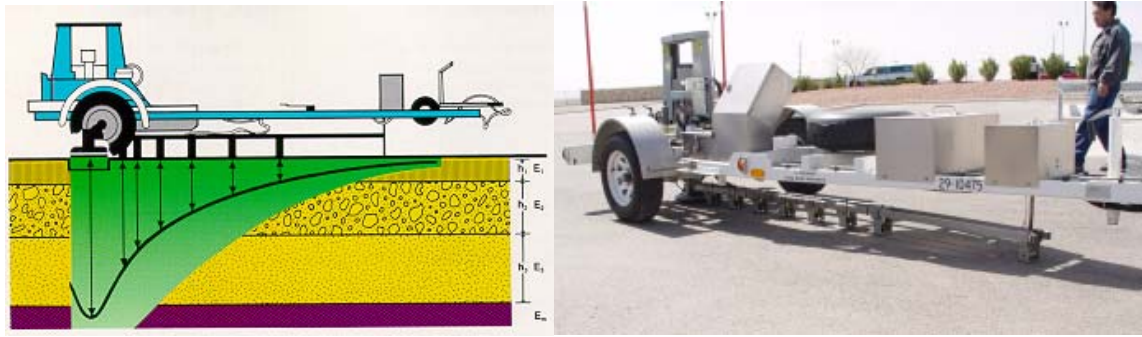


Figure 2.1 - Falling Weight Deflectometer

of each layer. The Poisson's ratio can be assumed from the literature. The following assumptions are made in layered theory solutions (Uddin and McCullough, 1989):

- The material in each layer is linear elastic, homogeneous, and isotropic.
- The layers overlaying the elastic half space are weightless, are finite in thickness, but are extended to infinity in the horizontal plane.
- A uniform static load is applied on a circular area of the surface.
- The inertia effect is neglected.
- The normal stress outside the loaded area and the shearing stress at the top of the surface layer are negligible.
- The stresses and displacements approach zero at large depths.

Strength and weaknesses

One of the strengths or advantages of the FWD device is that it imposes loads that approximate wheel loads. On the other hand the state-of-stress within pavement strongly depends on moduli of different layers, and hence is unknown.

As for the analysis process, the computer program MODULUS has been tailored for TxDOT. The default parameters set in the program, make it easy to analyze most of the flexible pavement systems in Texas. As far as the limitations of MODULUS, pavement systems with shallow bedrock cannot be easily analyzed. Also the program cannot reasonably accurately estimate the AC moduli of layers less than 3 in. thick. Another limitation is with four-layer pavements systems. The solutions sometimes are unreliable especially for stabilized layers.

Seismic Pavement Analyzer

The Seismic Pavement Analyzer (SPA) is a trailer-mounted nondestructive testing device, as shown in Figure 2.2. Its operating principle is based on generating and detecting stress waves in a layered medium. Several seismic testing techniques are combined. A detailed discussion on the background of the device can be found in Nazarian et al. (1995).

The SPA is mainly designed to determine the variation in modulus with depth and to diagnose the structural condition of pavements. The SPA records the pavement response produced by

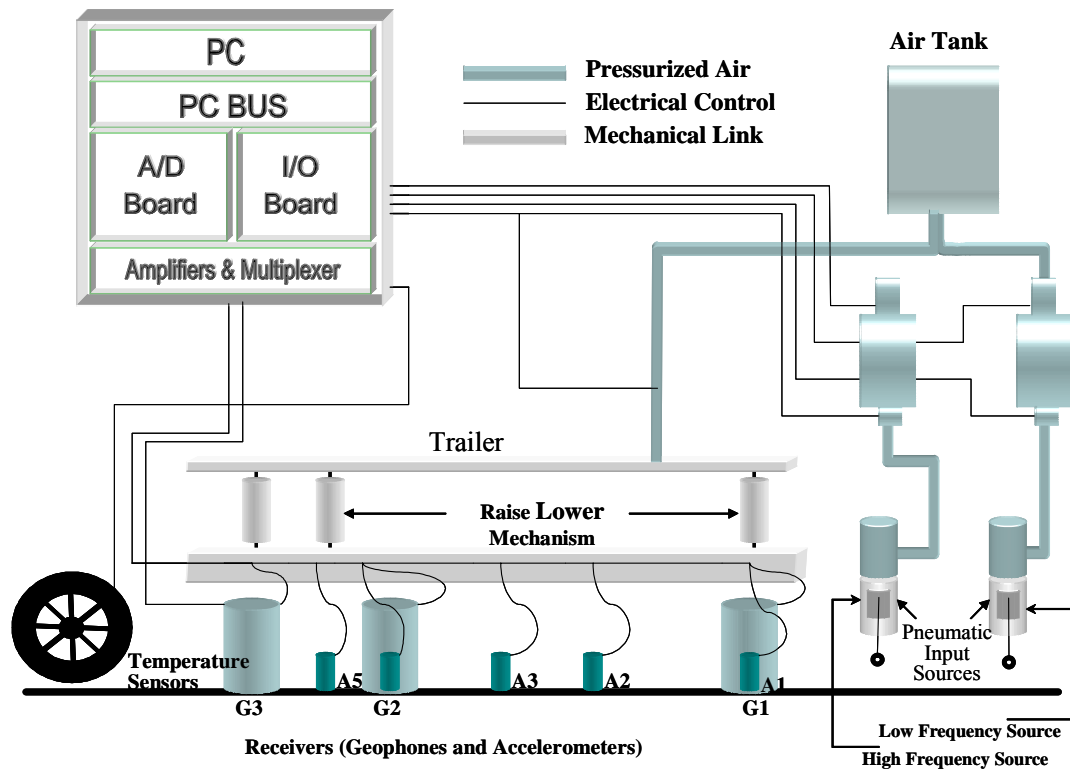
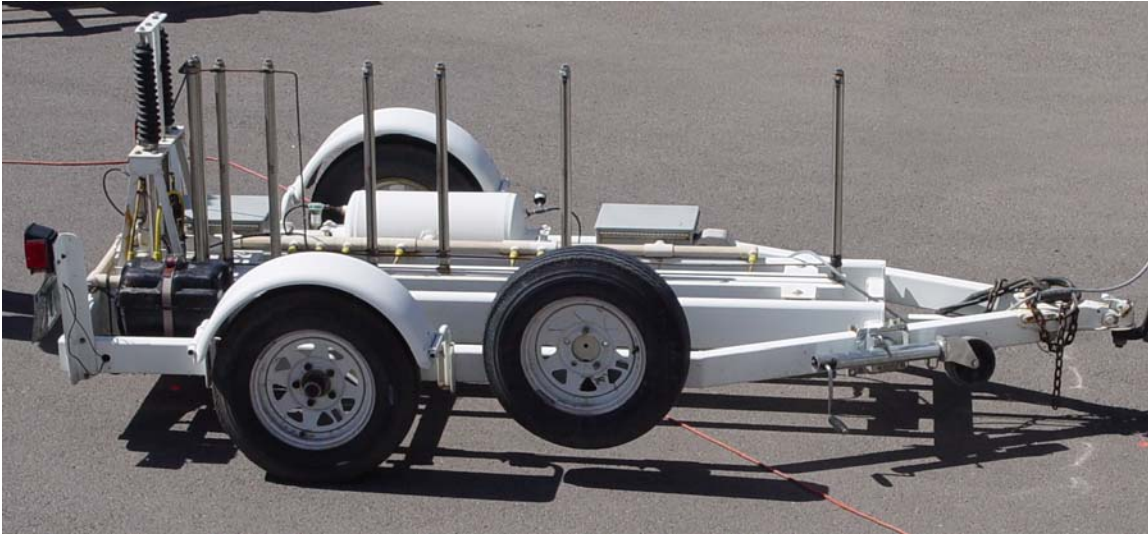


Figure 2.2 - Seismic Pavement Analyzer

high- and low-frequency pneumatic hammers on five accelerometers and three geophones. The equipment has been used in several applications such as analyzing pavement conditions in project-level surveys, diagnosing specific distress precursors to aid in selecting a maintenance treatment, and monitoring pavement conditions after construction as a quality control tool.

The SPA lowers several transducers and sources to the pavement. Surface deformations are recorded digitally. The deformations are induced by a large pneumatic hammer, which generates

low-frequency vibrations, and a small pneumatic hammer, which generates high-frequency vibrations.

The SPA is similar in size to the FWD. However, the SPA uses more transducers with higher frequencies and more sophisticated interpretation techniques. The measurement is rapid. A complete testing cycle at one point takes less than one minute (lowering sources and receivers, making measurements, and withdrawing the equipment).

Pavement properties estimated by the SPA include: Young's modulus and thickness of the top pavement layer; Young's modulus and thickness of base layer; and Young's modulus of subgrade.

The Spectral-Analysis-of-Surface-Waves (SASW) method is used in the SPA to determine the modulus profiles of pavement sections by measuring the dispersive nature of surface waves. The procedure includes collecting data, determining the experimental dispersion curve, and obtaining the stiffness profile.

In data collection, the transfer function and the coherence function between pairs of receivers are determined. The phase information of the transfer function and the coherence functions are used to determine a representative dispersion curve in an automated fashion (Nazarian and Desai, 1993). Finally, the shear wave velocity (V_s) of different layers can be determined from the dispersion curve using an automated inversion process (Yuan and Nazarian, 1993). From the shear wave velocity, the elastic modulus or seismic modulus is calculated based on the following relationship:

$$E = 2\rho V_s^2(1 + \nu) \quad (2.1)$$

where E is the elastic or seismic modulus, ρ is density, V_s is the shear wave velocity, and ν is Poisson ratio.

Since the SASW analysis is based on the state of stress close to zero, CTIS with support from TxDOT has developed a tool that uses results from the SASW analysis to determine layer moduli for the state of stress under the traffic load. The program is named SMART. The other major input that is required in the program is laboratory parameters based on the dynamic modulus test for AC layer or resilient modulus test for base and subgrade layers. The program provides default values that can be used if laboratory tests are not performed. The material models used in SMART are detailed in TXDOT Report 1780-5 (Abdallah et al., 2003). For clarity, a brief explanation on the material models used is presented.

Viscoelastic Model: The viscoelastic model is incorporated to adjust the AC layer moduli. The AC modulus is strongly dependent on temperature and frequency of load application. Aouad et al. (1993), Li and Nazarian (1994) and several other investigators have demonstrated the variation in modulus with temperature and frequency. The algorithm built in the program incorporates three options for the viscoelastic behavior.

The first option is a simplified equation suggested by Li and Nazarian (1994) to adjust for temperature. The modulus of AC is adjusted to a reference temperature of 77° F. That relationship is presented as:

$$E_{77^{\circ} F} = \frac{E_t}{1.35 - 0.0078(t - 32)} \quad (2.2)$$

where E_{77} is the adjusted modulus at 77° F, E_t is the measured seismic modulus at temperature t , and t is the temperature in Fahrenheit. The adjustment for frequency is done based on work by Aouod et al. (1993).

The second and third options to adjust for viscoelasticity are based on the master curve concept. The master curve, which is developed based on the principals of viscoelastic and time-temperature superposition, can be used to adjust moduli for frequency and temperature. Witczak et al. (1999) describe the newer methodology used in the development of master curves. A typical distribution of complex modulus with time and temperature of an asphalt concrete mixture is shown in Figure 2.3. The general practice has been to perform the complex modulus testing at various temperatures with similar loading times. This is illustrated in Figure 2.3a. An algorithm, using a time-temperature shift factor, shifts the data using the reference temperature as a baseline of some sort. Figure 2.3b shows the data at various temperatures shifted left or right of the reference temperature. The result is an experimental curve that can be fitted. The final step in the process is to fit a master curve using a curve fitting technique similar to the one presented in Figure 2.3c. The master curve can then be shifted to any other temperature. As a result, modulus values at any frequency temperature can be estimated.

A popular sigmoidal function proposed by Ferry (1970) can be used to generate a master curve. The sigmoidal function is in the form of:

$$\log(E^*) = \delta + \frac{\alpha}{1 + e^{\beta + \gamma \log t_r}} \quad (2.3)$$

where E^* = dynamic modulus, t_r = loading period, δ = Minimum value of dynamic modulus, α = Maximum value of dynamic modulus with β and γ = sigmoidal function shape parameters.

The two ways that the program adjusts the asphalt modulus based on the master curve differ on the method upon which the sigmoidal parameters α , β , γ and δ are obtained. These parameters can be preferably obtained from laboratory testing as in the example illustrated on Figure 2.3. In the absence of lab testing the relationships that are suggested by Mirza and Witczak (1995) to relate the common volumetric information obtained during mix design to these four parameters. Abdallah et al. (2003) contains a detailed description of the subject.

Nonlinear constitutive model: The nonlinear constitutive model adopted for the base, subbase and subgrade layers by most agencies and institutions can be generalized as:

$$E = k_1 \sigma_c^{k_2} \sigma_d^{k_3} \quad (2.4)$$

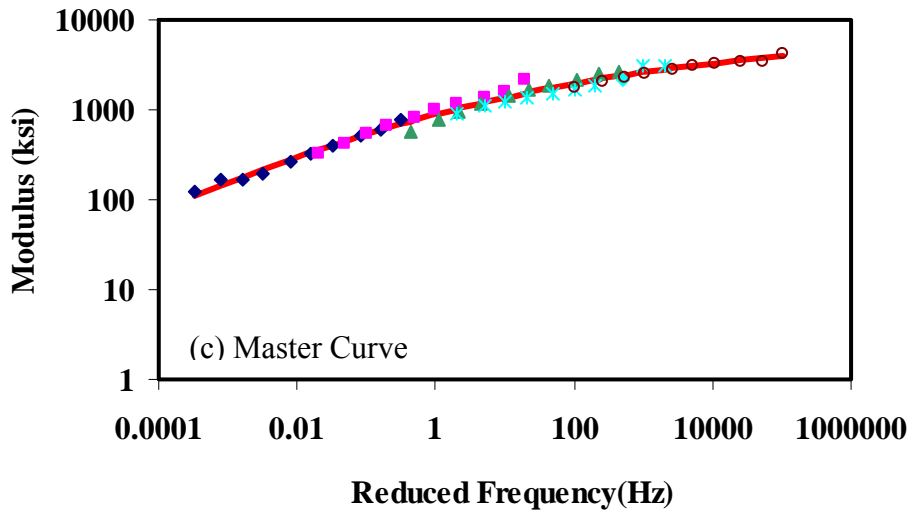
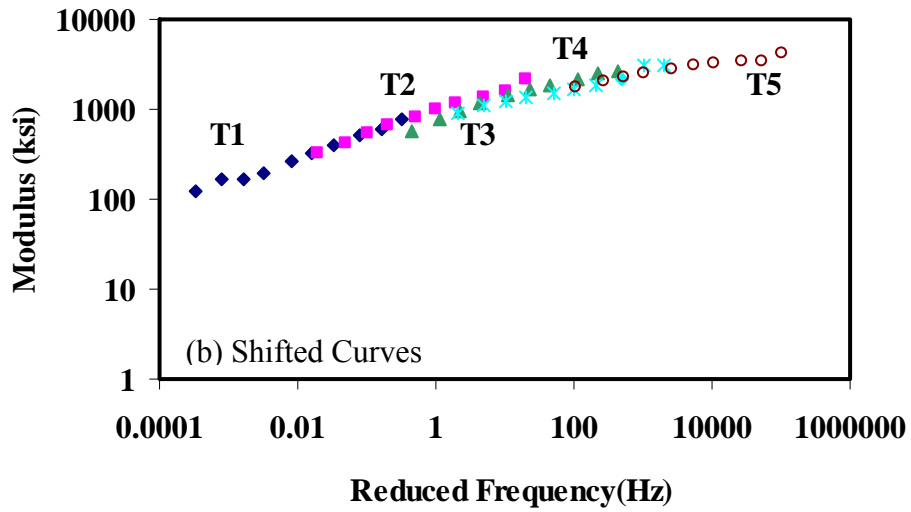
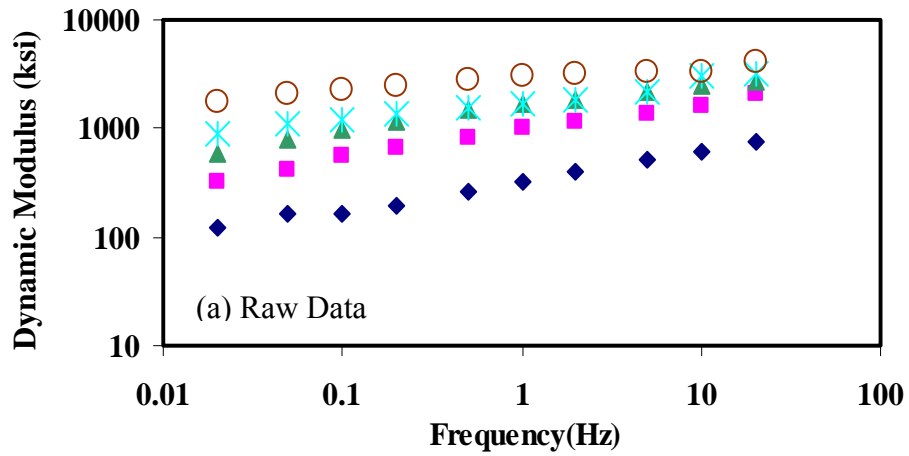


Figure 2.3 - Master curve concept

where k_1 , k_2 and k_3 are coefficients preferably determined from laboratory tests. In Equation 2.4 the modulus at a given point within the pavement structure is related to the state of stress. The advantage of this type of model is that it is universally applicable to fine-grained and coarse-grained base and subgrade materials. The accuracy and reasonableness of this model are extremely important because they are the keys to successfully combining laboratory and field results. Barksdale et al. (1997) have summarized a number of variations to this equation. Using principles of mechanics, all those relationships can be converted to the other with ease. The so-called two-parameter models advocated by the AASHTO 1993 design guide can be derived from Equation 2.4 by assigning a value of zero to k_2 (for fine-grained materials) or k_3 (for coarse-grained materials). As such, considering one specific model does not impact the generality of the conclusions drawn from a given model.

The purpose of this study is to relate seismic modulus with the load-induced nonlinear modulus while predicting k_2 and k_3 parameters considering state of stress under the external load imparted by a FWD or truck load. Ke et al. (2002) derived such a relationship, which is in the form of:

$$E = E_{seis} \left(\frac{\sigma_{c-ult}}{\sigma_{c-init}} \right)^{k_2} \left(\frac{\sigma_{d-ult}}{\sigma_{d-init}} \right)^{k_3} \quad (2.5)$$

where E is the resilient modulus at a given depth under FWD or truck load, E_{seis} is the seismic modulus of the layer, k_2 and k_3 are statically determined coefficients. σ_{c-init} and σ_{c-ult} are respectively the initial and ultimate confining pressures. Parameters σ_{d-init} and σ_{d-ult} are the initial and ultimate deviatoric stresses, respectively. The derivation of Equation 2.5 is included in TxDOT Report 1780-2 (Ke et al., 2002).

The above procedure is implemented in a software package called SMART (Seismic Modulus Analysis and Reduction Tool) that uses seismic moduli and well-substantiated nonlinear relationships to provide representative moduli for pavement design and analysis (Abdallah et al., 2003). Research Report 1780-4 (Abdallah and Nazarian, 2003) contains the users' manual of SMART.

In SMART, the structural model is based on an iterative process. To implement the algorithm, nonlinear layers are divided into several sublayers. One stress point is chosen for each nonlinear sub-layer. An initial modulus is assigned to each stress point. The stresses and strains are calculated for all stress points using a multi-layer elastic computer program. The confining pressure and deviatoric stress can be calculated for each stress point. A new modulus can then be obtained from Equation 2.5. The assumed modulus and the newly calculated modulus at each stress point are compared. If the difference is larger than a pre-assigned tolerance, the process will be repeated using the updated moduli. The above procedure is repeated until the modulus difference is within the tolerance and, thus, convergence is reached. Finally, the required stresses and strains are computed using final moduli for all nonlinear sublayers. The limitations and advantages of this procedure are described in detail in Abdallah et al. (2003).

Strengths and weaknesses

The attraction in utilizing the SASW test in pavement evaluation is the fact that it measures a fundamentally correct parameter (i.e., linear elastic modulus). The inherent weakness or limitation of the SASW analysis is that the state-of-stress during seismic tests differs from the state-of-stress under actual load. This problem has been remedied by the development of SMART, which essentially determines the design moduli under the state of stress induced by actual loads, from seismic modulus. Other weakness with the SASW method is that user intervention is still required for more complex pavement systems.

Portable Seismic Pavement Analyzer

Although the Portable Seismic Pavement Analyzer (PSPA) is designed to determine the average modulus of the top pavement layer such as asphalt layer or a concrete layer, it is an NDT seismic-device, which is increasingly being used by TXDOT. The PSPA, shown in Figure 2.4, consists of two receivers (accelerometers) and a source packaged into a hand-portable system, which can perform high frequency seismic tests. The device is operable from a computer.



Figure 2.4 - Portable Seismic Pavement Analyzer

The operating principle of the PSPA is based on generating and detecting stress waves in a medium. The Ultrasonic Surface Wave (USW) method, which is an offshoot of the SASW method (Nazarian et al., 1997), can be used to determine the modulus of the material. The major distinction between these two methods is that in the USW method the modulus of the top pavement layer can be directly determined without an inversion algorithm. The entire process, from initiating the testing sequence to collecting and saving the data, takes a few seconds. Baker et al. (1995) provides a detailed account of the data collection and data reduction process with PSPA. The result of PSPA is the modulus of the top pavement layer. Since PSPA is used to determine the same fundamental properties as the SPA but only for the top layer, SPA will be the focus of the integration routines keeping in mind that PSPA results could also be used in the process.

Strengths and weaknesses

The Windows version of the PSPA data collection and analysis program has been developed. Several applications are built into the program that automatically sets-up configuration based on application required. Also a batch mode is incorporated into the program, which allows for reducing data for an entire pavement section and generating a tab delimited text file reporting the results in minimal time. One of the main concerns that PSPA analysis is similar to that of SASW analysis. The modulus obtained is the linear elastic modulus, without adjustment factors. Since PSPA is mainly used for determining the properties of the asphalt layer, in flexible pavements, the results needed to reflect the viscoelastic behavior of the layer.

Ground Penetrating Radar

Ground Penetrating Radar (GPR) is an automated nondestructive testing tool for evaluating pavements. Its primary use is to measure pavement layer thickness and detect subsurface information in the pavement. Figure 2.5 shows a GPR unit in operation. Also presented in the figure is a sample of the results depicting the layer thickness of a pavement systems using COLORMAP, a data interpretation program used to reduce GPR results.

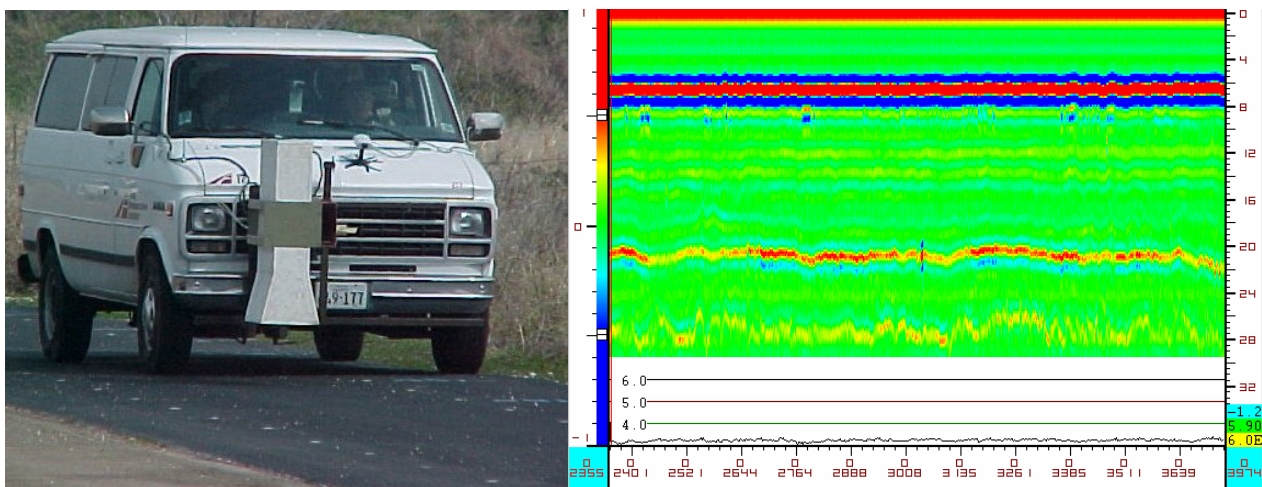


Figure 2.5 - Ground Penetrating Radar

Pavement layer thickness is one of the crucial input parameters used by all pavement analysis programs. For the purpose of analysis, the thickness of a flexible pavement layer is determined either from design specifications or coring information. The thickness based on design specification can only be used as an approximation due to the variability exhibited with construction practices, traffic and environmental factors. On the other hand, coring does provide means to accurately determine the pavement thickness. The problem with coring is time and money. GPR provides an alternative means of determining pavement layer thickness.

GPR operates by transmitting short pulses of electromagnetic energy into pavement using an antenna attached to a survey vehicle. GPR operates at highway speed by transmitting and

receiving 50 pulses per second. The effective depth penetration is close to two feet. Saarenketo and Scullion (1994) reported less than 3% error, for the asphalt-concrete (AC) layer, based on validation studies. Further details on GPR can be found in Scullion et al. (1997).

Strengths and weaknesses

GPR passes electromagnetic wave unimpeded through each paving materials. The speed at which it travels is related to the dielectric constants of the layer. However, the wave is partially reflected upon encountering a change in properties of the pavement, more specifically a change in electrical properties or “dielectric” of the materials. Therefore, GPR will only work in layered pavement constructed with different dielectric values.

Integration Algorithms

To develop an integrated NDT tool two items have to be addressed: a) integration of the data and analysis of existing NDT methods and b) synchronizing the data collection scheme of the NDT devices. The later will be discussed in Chapter 3. The two main integration methods that can be used for pavement analysis are: a) sequential analysis and b) Joint Inversion.

Sequential Analysis

In engineering problems, multi-faceted data are typically collected independently and interpreted separately. An experienced engineer can then combine the sometimes conflicting or mutually exclusive results from different tests to come up with an assessment of the problem. Similarly, the sequential inversion consists of a series of independent analysis that are systematically and logically tied together. For example, one can reduce the GPR data to obtain the thickness of each layer, use the PSPA to obtain the modulus of the ACP layer, and then input the determined thickness and moduli with FWD deflection data in the MODULUS program to obtain moduli of the base and subgrade.

The premises of sequential analysis, as this project was concerned, is to compliment the input of the existing FWD analysis used by TxDOT with results from other NDT devices (i.e., SPA or GPR). This system is adequate and reasonable as long as all methods used are robust and always provide the necessary information.

Joint Analysis

Unlike sequential analysis, in joint analysis, the data from different methods are interpreted simultaneously. In that manner, the results are harmonized and are made consistent using not only objective criteria, but also subjective adjustments. Consider a pavement section at which FWD, SPA and GPR data are available. The engineer would like to determine the modulus and thickness of each layer. As indicated before, when the FWD is interpreted alone, the thickness has to be estimated. Any uncertainty in thickness may significantly impact the backcalculated moduli. Today, one can use the GPR to obtain the thickness of the layers and input them to the backcalculation program. This will reduce the uncertainty in the input thickness; however, due

to the nonuniqueness of the backcalculation algorithms, one is not ensured that the estimated moduli are accurate. To improve the analysis, one can presumably also include the dielectric properties of each layer determined by GPR. One knows that higher dielectric values correspond to wetter material and as such lower moduli. Even though this is a subjective criterion, it can guide the backcalculation of the FWD moduli through joint inversion. However, this is not effectively possible when data are reduced sequentially or independently.

If the SPA data are available, one can harmonize the results even further since the SPA provides the moduli and thickness of each layer also. When the results of the FWD, GPR and SPA are combined, the moduli from the SPA and FWD and dielectric values of GPR have to corroborate with one another and the thickness from the GPR and SPA should agree. In that manner, at least in theory, the results should be more accurate and representative.

The use of joint inversion in the geophysics problems was first suggested in the 1970s (Vozoff and Jupp, 1975), gained its initial momentum in the mid-1980s and, has gained popularity in the last decade.

Dobroka et al. (1991) described an algorithm for joint inversion of seismic and electric data to estimate the depth to rock-coal interface and the hardness of the coal. They reported that the interpreted results were, by far, more accurate when compared to that from either seismic or electric data alone. In addition, they indicated that the inversion process was more robust for the joint inversion. Notice that this is very applicable to our problem since SPA provides seismic information and GPR the electric properties.

Hering et al. (1995) fully described the idea beyond the joint inversion process for SASW tests and resistivity sounding. They showed how incorporating the data from the two methods could improve the interpretation, especially in the presence of noise (uncertainty) in the data.

Misiek et al. (1997) applied the algorithm developed by Hering et al. to a five-layer structure and a three-layer structure. They showed that even though the results were not as definitive as when Hering used synthetic data, the joint inversion provided better results as compared to each individual one.

A large number of other examples in geophysical literature can be found that joint inversion has been carried out between different seismic methods (e.g. surface wave and refraction) or different methods like seismic and resistivity. We focused our literature review to seismic and electric because that is the closest to joint inversion of SPA and GPR results.

Data Fusion

In its most general form, data fusion is the process of integrating the data from diverse NDT methods applied to a pavement into a consistent description of its condition and its properties. Algorithms for data manipulation that facilitate the incorporation of multiple-NDT data were originally developed at Boeing (Nelson et al., 1989; Georgeson et al., 1989). Recently, Boeing (Nelson et al., 1997) developed a data fusion software package heavily devoted to the

visualization of nondestructive evaluation (NDE) results and no effort is made to interpret the data. Osegueda et al. (2000) developed data fusion algorithms to process information coming from several NDT tests to assess the state of damage of aerospace structures in real time. The techniques and algorithms used in that study was investigated and is being implemented in this project.

The human brain is probably the best analogy to a data fusion system (see Figure 2.6). Our sensors (eyes, ears, nose, mouth etc.) provide the information (sight, hearing, smell, taste etc.) to our brain where information gets fused and a decision is made. Figure 2.7 illustrates the data fusion problem for pavement characterization where the human sensors have been replaced by the NDT techniques and the data fusion center is composed of a series of algorithms that process the information coming from the various NDT conducted on the pavement. The output of this system could be the condition of the pavement, the material properties or an action to be taken.

Methods of data fusion can range from simplistic algorithms such as averaging to complex mathematical models such as Artificial Neural Network (ANN) models. Abdallah et al. (2001) demonstrate that the deflection and seismic data can be combined to determine the thickness and moduli with better accuracy than from each analysis alone.

Popular methods of data fusion are summarized in Table 2.1. The table lists the different fusion methods with the type and representation of sensor information including the noise level and the algorithm of fusion. Several of these techniques that have been investigated to determine their applicability to this project are discussed later in this report.

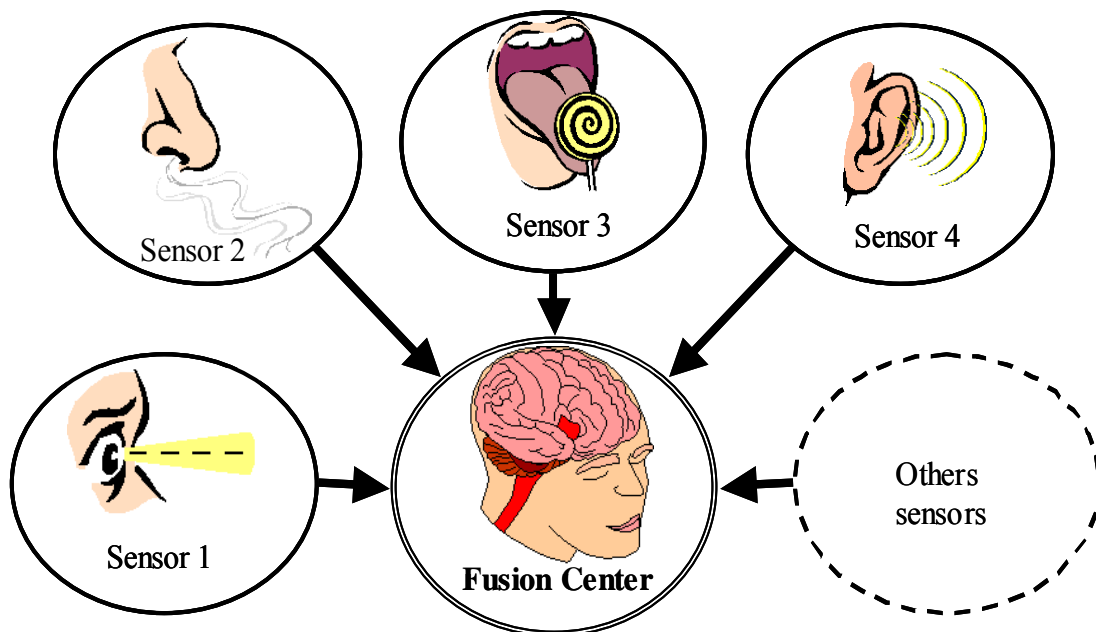


Figure 2.6 - Human data fusion center

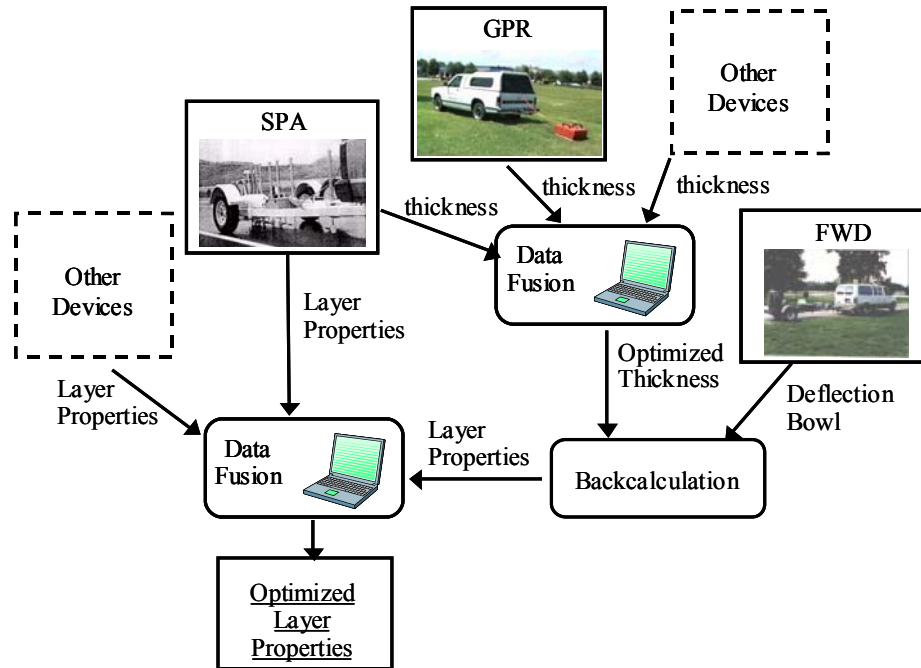


Figure 2.7 - Data fusion center for pavements

Table 2.1 - Data fusion methods

Method	Type of Sensory Information	Information Representation	Uncertainty	Fusion Technique
Weighted average	redundant	raw sensor readings	–	weighted average
Kalman filter	redundant	probability distribution	additive Gaussian noise	filtering of system model
Bayesian estimate using consensus sensors	redundant	probability distribution	additive Gaussian noise	maximum Bayesian estimate of consensus sensor
Multi-Bayesian	redundant	probability distribution	additive Gaussian noise	maximum Bayesian estimate
Statistical decision theory	redundant	probability distribution	additive noise	robust minimax decision rules
Evidential reasoning	redundant & complementary	proposition	level of support versus ignorance	logical inference
Fuzzy logic	redundant & complementary	proposition	degree of truth	logical inference
Production rules	redundant & complementary	proposition	confidence factor	logical inference

Chapter 3

Data Collection and Data Analysis

Introduction

To focus the efforts in merging the NDT technologies identified in the previous chapter, several steps were taken. The first task in this project was to conduct a survey to assess the existing needs for an integration tool. The focus group of this survey was TxDOT personnel that are most familiar and have hands-on experience with NDT technologies.

Two other preliminary activities were conducted at the early stages of this project to focus the improvements needed to current NDT methods. The first was a set of meetings amongst the project team members (UTEP, TTI and TXDOT). The meetings focused on determining the areas of improvements on current analysis methods and suggestions on the most effective path for integration. The second effort was to conduct a study to evaluate the analysis process used in each method. The final area of investigation was harmonizing the data collection process from all NDT devices which is the key to the success of NDT data integration.

Preliminary Survey

In an effort to better serve the needs of TxDOT in developing an integrated analysis tools using NDT data, a survey was conducted to obtain information on the current needs and uses of the NDT technology. General question in data collection and data analysis were posed. A copy of the survey is included in Appendix A.

The survey was distributed to over thirty of TxDOT personnel. A total of 16 responses were received. The results of the survey are compiled and summarized in Appendix B. Few of the critical questions and their compiled results are highlighted below.

Data Collection

As expected, the data collection portion of the survey showed that the FWD is the most widely used NDT device by TxDOT personnel. Figures 3.1 and 3.2 indicate that every respondent has used the FWD for data collection and of whom 75% are satisfied with the FWD data collection scheme. As for the GPR, 45% of the respondents have used it for data collection and of those 60% we satisfied with its current data collection scheme. The results for the SPA/PSPA showed that it was the least used devices compared to the other two. The biggest complaint with the SPA and PSPA was not necessarily to improve the data collection scheme, but that too few devices were in the inventory to ever develop confidence in their use.

Q1.1. Please select NDT devices that you have used for data collection?
 FWD GPR

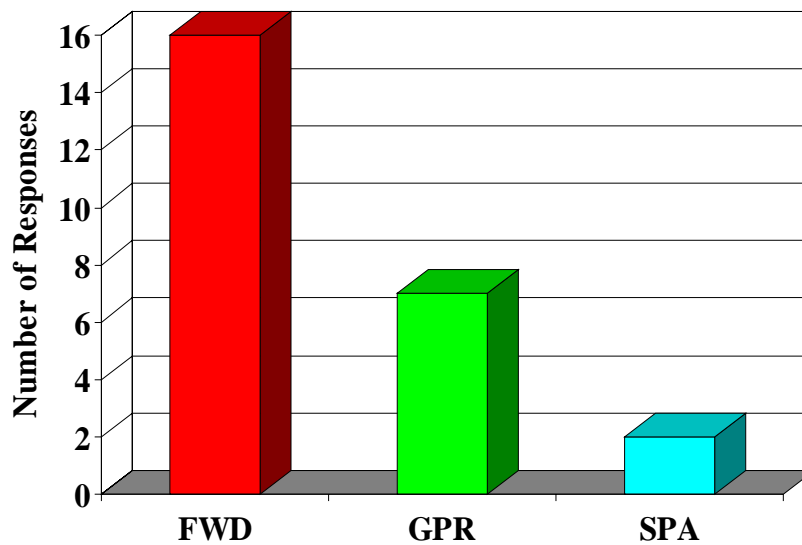


Figure 3.1 - NDT devices used by TxDOT personnel

The other statistic that is relevant in Figure 3.2 was the “no opinion” response. A large percentage of the respondents seem to have no opinion about the data collection methods of GPR and SPA. This could very well be that these individuals are not directly involved with collecting data. However, it is more likely that with more training the percentage of “no opinion” responses will decrease.

In general, the main feedback from the data collection portion of the survey suggests that some adjustments to the current data collection scheme would help and many of the respondents’ comments indicate to use one machine for data collection.

Also based on the information of this part of the survey, the research team will work very closely together with individuals from TxDOT that are directly involved in other projects to develop a data collection scheme that can be used with the integration analysis tool that will be developed from this project.

Q1.3. Are you satisfied with the current data collection process for;

FWD? Yes No No Opinion

GPR? Yes No No Opinion

SPA? Yes No No Opinion

PSPA? Yes No No Opinion

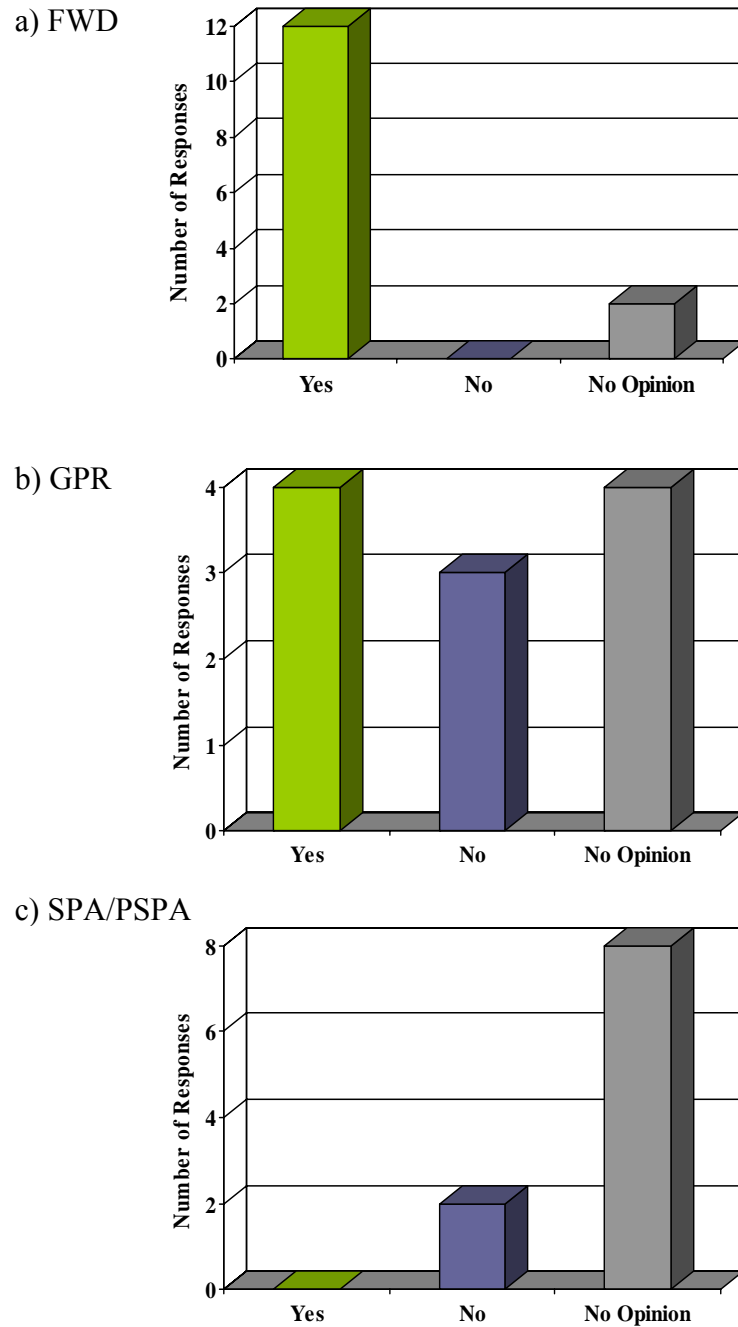


Figure 3.2 - NDT devices in which TxDOT Personnel are satisfied with their data collection scheme

Data Analysis

The questions on the data analysis portion of the survey were a bit more extensive. The goal was to gather information based on current TxDOT practices. The questions varied from the type of analyses performed to detail inputs used in the analysis (i.e., thickness and Poisson's ratio). Also asked in the survey was if any of the users manually integrated data from the various NDT devices and to identify limitation in the current analyses where improvements can be made.

Again, the detail compilation of the results can be found in Appendix B. Two of the questions were related to the source of a priori information used in the current backcalculation process. The results are presented in Figure 3.3.

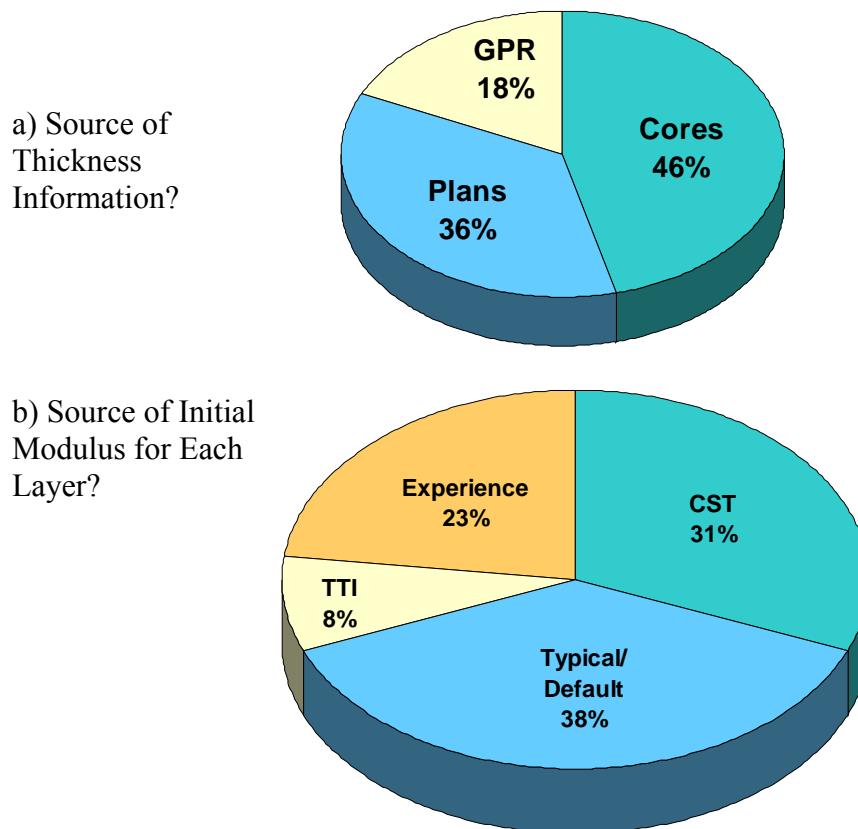


Figure 3.3 - Source of information used to provide the thickness and initial modulus for each layer in backcalculation analysis.

Figure 3.3a shows that the majority of the thickness information is obtained from coring followed by construction or design plans with 18% of the time using results of the GPR. The source from which the initial moduli are obtained is reflected in Figure 3b. About 38% reported using default or typical values, 31% reported using values based on construction information, 23% used their own experience to set initial values, and 8% based their initial input according to the TTI recommendations.

Another set of questions dealt with using the GPR/Seismic results in the FWD backcalculation. Based on Figure 3.4, it seems that some level of data integration is currently being performed. Six out of sixteen respondents have used the results of the GPR in the FWD backcalculation program and four out of sixteen have used result of the seismic in modulus backcalculation. Therefore by developing a tool that allows easy access to the different NDT data could prove useful in enabling more of TxDOT personnel to integrate NDT data.

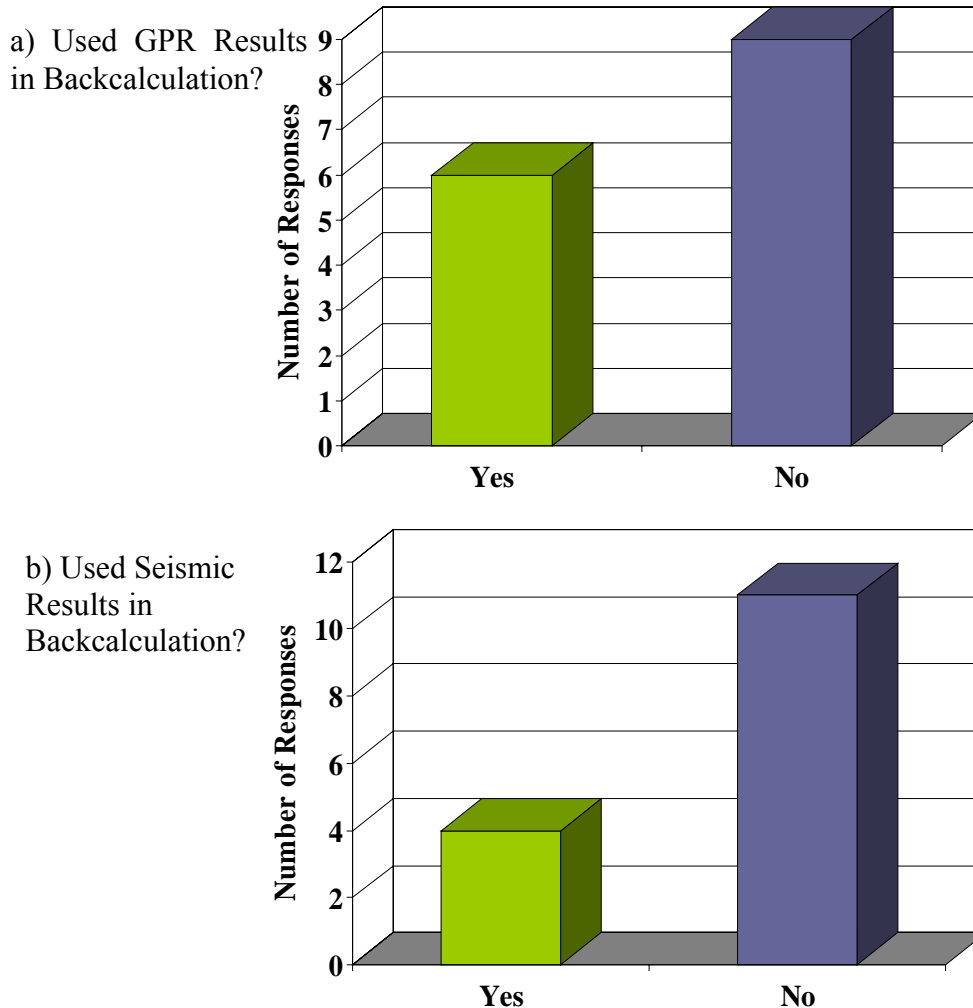


Figure 3.4 - Use of GPR or seismic results in modulus backcalculation

The general consensus of the second part of the survey was that a data integration tool seems a logical progression. One of the concerns of the integration tool was that adequate training would be needed to build confidence in the analysis.

Even though there were only sixteen respondents, the information was useful to the research team in terms of focusing the efforts in the future tasks. A second survey with a selected group might be carried out in the next phase of the project to provide more feedback on the proposed analysis tools.

Robustness in Current Analysis Practices

One of the tasks in the development of a data integration tool was to identify weaknesses in current analysis practices. This task was not to necessarily identify areas of improvement in existing analysis, but it was more a preliminary effort to identify and document the main strengths and limitations of the FWD backcalculation process (MODULUS) and the inversion process (SASW). To carry out this task, a study was performed to first check repeatability of each device and its corresponding analysis process, and second to identify input parameters that are sensitive to the analysis process.

Repeatability of NDT devices

In the development of each of the NDT devices, several studies were conducted to evaluate the repeatability of the devices and their respective data reduction algorithms. One point or station at two sites (TxDOT parking lot in El Paso and Ride Rut facility at Riverside Annex of Texas A&M University) was selected for the repeatability study. The test was repeated twenty times at the same location with the FWD, SPA, and PSPA (PSPA repeatability test was only performed at the Ride Rut facility). The GPR tests were repeated three times at the Ride Rut facility. The data from each test was reduced and the results are presented in the next set of graphs. Only data from the Ride Rut facility is presented since the variability results from both sites were very similar.

Figure 3.5 shows the results from the FWD process. Figure 3.5a is the raw deflection data collected and measured at the same drop height. The coefficient of variation (COV) is less than 2% for all seven deflections. With such high repeatability the analysis “backcalculation program” was very consistent as presented in Figure 3.5b.

Similar accuracy is shown for the SPA results. Figure 3.6a shows raw dispersion curve for the repeatability test. The quality of the data was of very high quality as depicted by the overlap of the data. Likewise, the analysis program “SASW” dispersion results of the dispersion test were very consistent.

Table 3.1 shows the repeatability of the PSPA. The coefficient of variation for seismic modulus of the AC layer is 4% with an average value of 1363 ksi. The variabilities of shear wave velocity and the design modulus were 2% and 4%, respectively. The PSPA results were based on repeating the test for a single location 20 times at the Ride Rut facility.

The GPR repeatability was close to 2% for both the AC layer and base layer thickness. These results were determined by averaging out the data from three runs and then calculating the statistics across the section at one-foot increment at the Ride Rut facility. The results are presented in Table 3.2. Figure 3.7 compares the nominal thickness with the GPR results of the stations tested along the test section. The points plotted in the figure show the location of the test stations measured for the FWD, SPA and GPR. The accuracy of the results from both NDT devices will be verified shortly upon core sampling and laboratory testing.

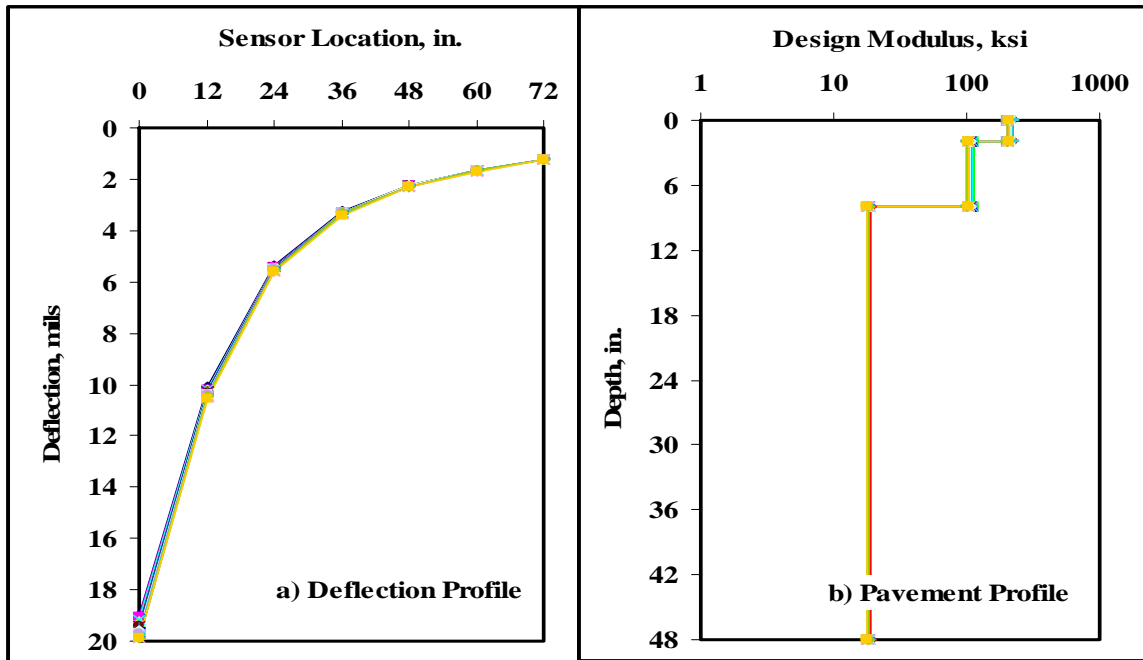


Figure 3.5 - Repeatability based on FWD

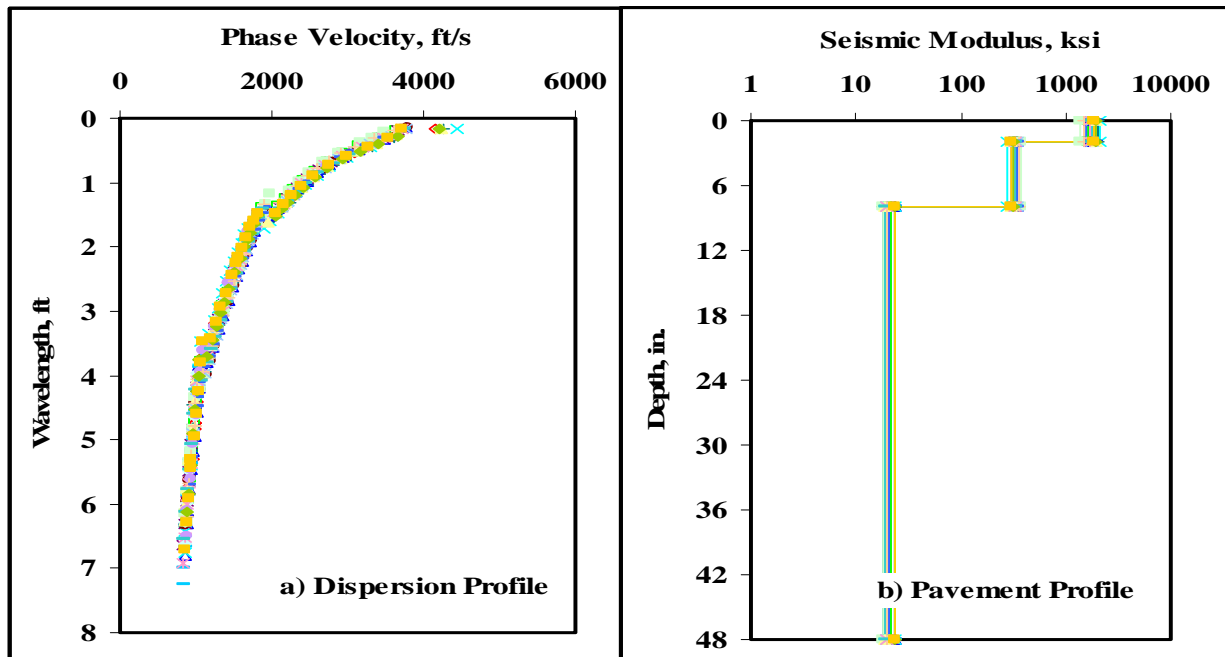


Figure 3.6 - Repeatability based on SPA

Table 3.1 - Repeatability of PSPA at the Ride Rut facility

Statistics	Seismic Modulus, ksi	Shear Wave Velocity, ft/s	Design Modulus, ksi
Minimum	1279	3730	400
Maximum	1430	3944	447
Average	1363	3850	426
Stdev.	48	68	15
COV	4%	2%	4%

Table 3.2 - Repeatability of GPR at the Ride Rut facility

Statistics	COV of AC Layer	COV of Base Layer
Minimum	0%	0%
Maximum	9%	16%
Average	2%	2%

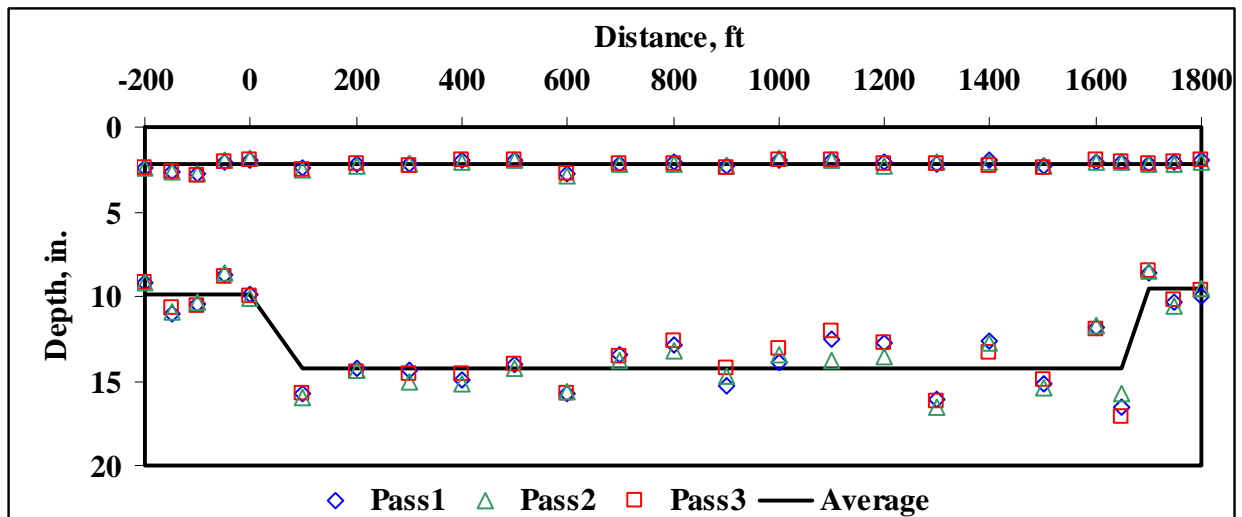


Figure 3.7 - Results of repeatability test from GPR at the Ride Rut facility.

Significant Parameters of NDT Analysis Programs

As stated, one part of the study was to identify the robustness of the current analysis practices and the limitations of each analysis algorithm. This study was focused on identifying input parameters that are sensitive or significant. The goal was to optimize the development of the integration algorithm scheme by focusing the integration on parameters that impact the analysis.

A parametric study was performed for both the SASW inversion and the MODULUS backcalculation programs. To carry out this study, thickness and modulus of each layer were varied. In the SASW program, data from the repeatability test was used as the pavement response. Other inputs used in the SASW program are a priori information of pavement layers. This information is the best guess of thickness, modulus, density, and Poisson's ratio of each layer. A benchmark was needed to be established as a way of comparing the results. In the absence of exact thickness and modulus values at this time, a benchmark was determined based on the average values of the repeatability test. The a priori information was set to the average values from the repeatability test and the resulting pavement profile was used as the baseline for comparison.

The first part of the analysis was the case where all variables (thickness and modulus of each layer) were simultaneously varied as a worst case scenario. The remaining input parameters were fixed to constant values. This is in the case where no a priori information about the condition of the pavement is available. The inversion process for this case was performed twice: a) when both layer thickness and layer moduli were estimated and b) when only layer moduli were estimated. In the second part, only specific parameters were varied one at a time by $\pm 30\%$ and then by $\pm 50\%$ before performing the analysis with all remaining variables fixed. These cases simulate situations where information about modulus or thickness of other layers is known from other sources. The outputs (essentially modulus and thickness of each layer) were compared to the baseline values. The results of this analysis are summarized in Table 3.3. Assuming the average values are the true representation of the pavement analyzed, a comparison can then be made from the table to identify parameters that are sensitive in the SASW analysis. The misestimation error for each estimated parameter is also included in Table 3.3.

The first two sets of results are for varying all parameters by $\pm 30\%$ and then by $\pm 50\%$ (worse case scenarios). In the first set, both the layer thickness and moduli were estimated. In general, the predicted and measured dispersion curves converged with an RMS error of less than 1 except for the case where the parameters were perturbed by -50% (RMS error was 2). In that case, the maximum number of iterations was reached. Had the operator allowed more iterations, the RMS error would have been reduced. The misestimation errors were less than 20% when the a priori information were less than the actual values. This is a well-known phenomenon in the SASW inversion. The thicknesses are within 10% except for the case when the RMS error is high.

In the second set of results, the thickness of AC and base layers were varied but not estimated. Only the modulus of the layers was calculated. In most cases, the misestimation of the moduli increased compared to the first set of results. From Table 3.3, the highest variability observed is 56% for the modulus of base when the a priori is -30% of the actual value. And similar to the results of the first set, perturbing the parameters by -50% results in a higher RMS error. This shows the impact of the thickness in the SASW analysis. If there are uncertainty in the thicknesses, it is best to allow the inversion process to estimate both thickness and modulus.

In the next set of results, the thickness of the AC and base layers were maintained at their actual values and only the layer moduli were estimated. In most cases, the misestimation errors of the moduli greatly reduced. Again, the impact the thickness in the analysis seems very important.

Table 3.3 - Results of parametric study using SASW for the inversion process

Parameters Perturbed	Modulus, ksi						Thickness, ksi				Iteration	RMS Error	
	AC		Base		Subgrade		AC		Base				
Average Value	1800	-	1	0.9	25	-	2	-	6	-	1	0.9	
Layer Thickness and Moduli	+30%	1954	9%	302	8%	20	20%	1.8	10%	7.3	22%	6	0.9
	+50%	2070	15%	307	7%	18	28%	1.8	10%	7.2	20%	6	0.8
	-30%	1526	15%	383	16%	25	0%	1.9	5%	5.3	12%	5	0.9
	-50%	1443	20%	371	12%	26	4%	1.5	25%	4.5	25%	10	2
Layer Thickness and Moduli	+30%	1540	14%	245	26%	20	20%	-	-	-	-	10	1.2
	+50%	1496	17%	158	52%	32	28%	-	-	-	-	10	1
	-30%	1861	3%	515	56%	32	28%	-	-	-	-	4	0.9
	-50%	1946	8%	371	12%	29	16%	-	-	-	-	10	3.3
Layer Moduli	+30%	1818	1%	334	1%	21	16%	-	-	-	-	3	0.9
	+50%	1735	4%	358	8%	20	20%	-	-	-	-	4	0.9
	-30%	1638	9%	334	1%	25	0%	-	-	-	-	3	0.9
	-50%	1696	6%	338	2%	23	8%	-	-	-	-	6	0.9
AC Modulus	+30%	1915	6%	311	6%	25	0%	-	-	-	-	3	0.9
	+50%	1811	1%	328	1%	23	8%	-	-	-	-	6	0.9
	-30%	1538	15%	362	10%	21	16%	-	-	-	-	3	0.9
	-50%	1569	13%	372	13%	20	20%	-	-	-	-	8	0.9
Base Modulus	+30%	1722	4%	353	7%	21	16%	-	-	-	-	2	0.9
	+50%	1724	4%	351	6%	21	16%	-	-	-	-	3	0.9
	-30%	1752	3%	323	2%	26	4%	-	-	-	-	10	0.9
	-50%	1712	5%	335	2%	24	4%	-	-	-	-	5	0.9
Subgrade Modulus	+30%	1771	2%	340	3%	24	4%	-	-	-	-	2	0.9
	+50%	1717	5%	354	7%	24	4%	-	-	-	-	2	0.9
	-30%	1784	1%	329	0%	23	8%	-	-	-	-	1	0.9
	-50%	1796	0%	323	2%	23	8%	-	-	-	-	3	0.9
AC Thickness	+30%	1489	17%	279	15%	27	8%	-	-	-	-	10	1.2
	+50%	1416	21%	206	38%	35	40%	-	-	-	-	10	1.3
	-30%	2158	20%	404	22%	18	28%	-	-	-	-	10	1
	-50%	2954	64%	429	30%	19	24%	-	-	-	-	10	1.3
AC Thickness	+30%	1998	11%	302	8%	18	28%	1.8	10%	-	-	10	1
	+50%	2000	11%	294	11%	18	28%	1.8	10%	-	-	10	1
	-30%	1729	4%	373	13%	24	4%	1.8	10%	-	-	3	0.9
	-50%	1404	22%	420	27%	28	12%	1.5	25%	-	-	10	1.4
Base Thickness	+30%	1750	3%	312	5%	15	40%	-	-	-	-	2	0.9
	+50%	1812	1%	281	15%	15	40%	-	-	-	-	2	0.9
	-30%	1661	8%	418	27%	32	28%	-	-	-	-	3	0.8
	-50%	1498	17%	540	64%	41	64%	-	-	-	-	3	0.7
Base Thickness	+30%	1832	2%	332	1%	23	8%	-	-	6.4	7%	3	0.9
	+50%	1847	3%	332	1%	20	20%	-	-	7	17%	3	0.9
	-30%	1759	2%	384	16%	24	4%	-	-	5.3	12%	3	0.9
	-50%	1660	8%	449	36%	32	28%	-	-	3.8	37%	3	0.9
Base & Subgrade Modulus	+30%	-	-	337	2%	22	12%	-	-	-	-	4	0.9
	+50%	-	-	335	2%	22	12%	-	-	-	-	6	0.9
	-30%	-	-	325	2%	24	4%	-	-	-	-	3	0.9
	-50%	-	-	320	3%	26	4%	-	-	-	-	6	0.9

From Table 3.3, the highest misestimation error is 20% for the modulus of subgrade when the a priori of 50% greater than the actual value was used.

The next three sets of results simulate the case when only one of the layer moduli is varied. The misestimation errors reduced, especially when the a priori information was less than the actual one. Also reflected in the results is the impact of the upper layer moduli. The uncertainty in the modulus of the AC layer has a large impact on the base and subgrade layer results. On the other hand, the variation of the base moduli only impacts the results of subgrade moduli and not as much the AC layer moduli. This is supported with results of varying the subgrade moduli. The moduli of the AC and base show the least misestimation errors. Even the subgrade modulus is estimated with fairly-good accuracy. This suggests that the more certainty there is in the upper layer the better estimation of the modulus profile, which supports the need for data integration.

The next set of results deals with the variation in the thickness of the AC and base layers. Four cases were considered: 1) varying the AC thickness but only estimating the layer moduli, 2) varying the AC thickness while estimating the AC thickness and layer moduli, 3) varying the base thickness but only estimating the layer moduli, and 4) varying the base thickness while estimating the base thickness and layer moduli. The first two cases, where the AC thickness was varied, the results show the impact that the uncertainty in layer thickness has on the estimation of the moduli. Performing the inversion with a constrained “bad guess” of the thickness increases the error of the modulus profile by a factor of two compared to when the thickness was not constrained. This shows the importance of knowing or estimating the AC layer thickness in the SASW analysis. Again when the a priori thickness is off by more than 50%, the convergence is not complete.

The two sets of results dealing with the variation of the thickness of the base layers show similar pattern. Again, the results show the impact of the uncertainty in the base layer thickness on the estimation of the results. Performing the inversion with a constrained “bad guess” of base thickness increases the error in the estimated moduli, especially for the base and subgrade layer. Also, the results indicate that the worse the a priori “first guess” is, the larger the error in the estimated moduli will be. This shows the importance of knowing the base layer thickness in SASW analysis. Another observation from the results of the AC modulus shows that not knowing the base thickness has less impact on the top layer (AC layer) than the moduli of the other layers.

The last set of results is to simulate the case when the thickness of the layers is well known and the modulus of the top layer is well known from other sources. In this case the thickness of the AC and the base could be provided from coring data and/or GPR results and the modulus of the AC layer is provided from the PSPA results. The results in Table 3.3 are very promising with the largest misestimation error of 12% for the modulus of the subgrade. The modulus profile is very consistent with the average values. This is an indication of the benefits of data integration.

The same process, with a slightly different approach, was performed in identifying the significant parameters in the MODULUS program. The reason for the different approach was based on the way a priori inputs are introduced into MODULUS. The a priori inputs are not actual seed values but a range (minimum and maximum values) for the AC, base and subbase

layers (subgrade input allows for a seed value). In this case, as long as the actual value being predicted is within the range, the analysis is comparable. However, one should have in mind that MODULUS assigns the seed value for the subgrade internally. Therefore, as long as the deflections are not changed, the results from MODULUS should converge to a given value but not necessarily to the actual value. As such, one expects very consistent results from that program.

The results are summarized in Table 3.4. The first set of results corresponds to the case when the layer moduli and thicknesses were varied. The misestimation errors for the moduli are rather large, except for the subgrade. Comparing the results from this set to the second and third set, where layer thicknesses are known, it can be observed that a large percentage of the variability is attributed to the thickness. The difference between the second and third set is the a priori input of the subgrade (one case was perturbed by -50% and the second case was perturbed by 50%). The results when the thickness is known shows significantly reduced variability. Again, the importance of thickness in pavement analysis is crucial, and integrating reliable thickness data into the analysis could prove useful.

The next three sets of results shows the impact of changing modulus of each layer. This analysis was performed differently than SASW analysis since MODULUS does not allow for varying modulus of one layer without constraining the other layers. In this case the moduli of the other layers were constrained and only modulus of one layer was backcalculated. The backcalculated modulus is the modulus that was varied in the input. The results show that if the modulus of the other layer is known then the variability of the moduli is improved compared to backcalculating moduli of all layers. The AC is backcalculated with a misestimation error of 3%, base and subgrade were estimated exactly. This supports the integration of reliable modulus data into the analysis. Modulus of AC from other sources such as seismic analysis could produce such reliable backcalculation results.

The last two sets are when only one of the thicknesses is not known. The results again show the impact of the thickness on the analysis. For this pavement, the thickness of base largely impacts the results compared to the thickness of the AC layer.

A popular backcalculation program, EVERCALC (Sivaneswaran et al., 1999), was also used to further study the impact of thickness and modulus on the backcalculation process. In EVERCALC, the user has full control on the input parameters similar to the SASW program. This case study will be a more realistic representation of what one should expect from actual field data. The results are presented in Table 3.5. The results for varying all relevant parameters, similar to MODULUS, show large misestimation errors as compared to the second set where the thicknesses are known.

For the next three sets, the impact of varying one parameter on the estimated modulus profile is exhibited. The misestimation errors were at the most 10%. This shows the impact of data integration when reliable layer moduli data is available from other sources, the convergence is improved and the results are more reliable.

The next two sets of data show the impact of the thickness of each of the layers. The misestimation of the thickness of the AC or base layer impacts the estimated modulus of that layer the most. Also layer thickness does not seem to have an effect on the subgrade modulus. In fact none of the variations in all the sets seem to impact the subgrade layer moduli.

The last example demonstrates the same scenario preformed for SASW. That is the case when the thickness of the layers is known and the modulus of the AC is also known. The base modulus seems to converge within 10%. Again, the need for data integration could prove very useful as demonstrated in this study.

This study proved very useful. Although some results were obvious, the study was beneficial to setup guidelines for algorithms for integration of data from the various NDT devices. Aside from improving accuracy, perhaps analysis time would also be reduced.

Table 3.4 - Results of parametric study using MODULUS for the backcalculation process

Parameters Perturbed		Modulus, ksi						Absolute Error per Sensor
		AC		Base		Subgrade		
Average Value		300	-	93	-	18	-	4.02
Layer Thickness and Moduli	+30%	210	30%	65	30%	17.3	4%	1.5
	+50%	223	26%	51	45%	17.3	4%	2
	-30%	390	30%	121	30%	19.1	6%	10
	-50%	450	50%	140	51%	22	22%	19
Layer Moduli with -50% Subgrade Modulus	+/-50%	283	6%	94	1%	18	0%	4
Layer Moduli with +50% Subgrade Modulus	+/-50%	370	23%	86.5	7%	17.6	2%	3.62
AC Modulus	+/-30%	291	3%	-	-	-	-	4
	+/-50%	293	2%	-	-	-	-	4
Base Modulus	+/-30%	-	-	93	0%	-	-	4
	+/-50%	-	-	93	0%	-	-	4
Subgrade Modulus	+/-30%	-	-	-	-	18	0%	4
	+/-50%	-	-	-	-	18	0%	4
AC Thickness	+30%	210	30%	84	10%	17.6	2%	3.45
	+50%	150	50%	85	9%	17.7	2%	3.23
	-30%	390	30%	107	15%	18	0%	4.2
	-50%	450	50%	120	29%	18.2	1%	5.4
Base Thickness	+30%	210	30%	75	19%	17.4	3%	0.8
	+50%	395.5	32%	59	37%	17.2	4%	0.95
	-30%	389	30%	140	51%	18.1	1%	6.17
	-50%	663	121%	140	51%	14	22%	23

Table 3.5 - Results of parametric study using EVERCALC for the backcalculation process

Parameters Perturbed		Modulus, ksi						RMS Error
		AC		Base		Subgrade		
Average Value		477	-	93	-	17	-	6
Layer Thickness and Moduli	+30%	321	33%	61	34%	18.1	6%	3.0
	+50%	270	43%	51	45%	18.0	6%	2.6
	-30%	731	53%	213	129%	17.1	1%	9.3
	-50%	1000	110%	300	223%	17.5	3%	12.5
Layer Moduli	+30%	450	6%	101	8%	16.9	1%	7.4
	+50%	449	6%	102	10%	16.9	1%	7.4
	-30%	450	6%	101	8%	17.0	0%	7.4
	-50%	443	7%	102	10%	16.9	1%	7.4
AC Modulus	+30%	448	6%	101	9%	16.9	1%	7.4
	+50%	450	6%	100	7%	17.0	0%	7.4
	-30%	450	6%	101	8%	16.9	1%	7.4
	-50%	449	6%	102	9%	16.9	1%	7.4
Base Modulus	+30%	449	6%	102	10%	16.9	1%	7.4
	+50%	447	6%	102	10%	16.9	1%	7.4
	-30%	449	6%	102	10%	16.9	1%	7.4
	-50%	449	6%	100	7%	17.0	0%	7.4
Subgrade Modulus	+30%	449	6%	102	10%	16.9	1%	7.4
	+50%	448	6%	102	10%	16.9	1%	7.4
	-30%	448	6%	103	10%	16.9	1%	7.4
	-50%	447	6%	102	10%	16.9	1%	7.4
AC Thickness	+30%	316	34%	81	13%	18.1	6%	3.9
	+50%	269	44%	73	22%	18.1	6%	3.8
	-30%	730	53%	116	25%	16.9	1%	7.5
	-50%	1000	110%	128	38%	17.0	0%	7.6
Base Thickness	+30%	450	6%	75	19%	16.8	1%	6.1
	+50%	450	6%	65	30%	16.8	1%	5.5
	-30%	450	6%	178	91%	17.1	1%	9.1
	-50%	1000	110%	283	204%	16.8	1%	10.8
Base & Subgrade Modulus	+30%	-	-	102	10%	16.9	1%	7.4
	+50%	-	-	102	10%	16.9	1%	7.4
	-30%	-	-	102	10%	16.9	1%	7.4
	-50%	-	-	102	10%	16.9	1%	7.4

Harmonizing Field Testing Protocols

One of the most critical aspects of a successful data integration tool is a good data collection protocol. Ideally integrating the hardware of the different NDT devices is optimal for using a data integration program. However, complete hardware integration is not in the plans for the near future. As such a protocol will be developed to ensure convenient use of the integration tools.

Currently the testing procedures are different for different devices. As such, a substantial amount of time is spent in comparing the results of each of the analysis. The reason for this is

mainly due to referencing of test points or “stations”. As an example, the FWD uses distant measuring instrument (DMI) as reference for each station tested. Any other information about the station or the test process is found in the comment portion. The SPA uses counters as reference stations. In practice the DMI information and any other information is provided in the comment section. Therefore, any coordination of the data from the two devices requires unnecessary manipulation of data files to extract information and link results. This process becomes more complicated if data from one of the devices was repeated, skipped or corrupt.

To determine the best scenario and ensure data synchronization from the different devices, the setup scheme from each device will be investigated. Every step from the lineup of the testing devices, to time it takes to perform a testing sequence, to the information the operator includes in the comments will be checked. A protocol will be suggested at the end of this project to provide optimal data collection process when the devices are used together. This protocol will ensure data synchronization from the different devices when the joint analysis is performed.

As a part of this project, three sites were tested using several NDT devices. In two of the sites no traffic control was required. The third site required a moving traffic control. In all three cases, close attention was given to the flow of data collection. Some of the concerns observed were documented and are summarized below.

Testing time and order of NDT devices: The time it takes for each NDT device to perform a test becomes very important when dealing with multiple devices. If four devices are being used then the rate of testing becomes crucial especially when traffic control is involved. Based on our documentation, the time it takes to test for each device per station is: 1) less than a minute for FWD (four drops per station), 2) less than a minute for SPA, 3) less than 30 seconds for PSPA, and 4) negligible for GPR. This means if conditions are perfect, the total test time is between three and a half to four minutes. This does not include driving time, alignment, and setup time between each station. In sections that were tested for this project using all four devices, the test time documented seemed accurate. The order of testing that was used in the field was decided at the test site. In one case where traffic control was not needed, the GPR was used first. Then the series of tests starting with the SPA followed by the FWD followed by the PSPA were carried out. Since time was not a factor and the test per station per device was repeated three times, the total test time was not recorded. In such instances different combination of the device line up would have worked.

However, when traffic control is required, the lineup becomes crucial. On SH47 in Bryan Texas, moving traffic was used. The setup of testing in this instance was as follows: 1) the GPR scanned through the entire section since it did not need traffic control, 2) the FWD was second followed by the SPA and PSPA. In this particular site, the SPA and PSPA tests were carried out concurrently (test time for both devices was close to one minute). Having the SPA and PSPA work together proved very efficient and could be setup easily having one person running both operations. In the case of SH47, two persons were used, one to drive and the other to run the test. This lineup of the four devices worked well. The total time per station, from aligning over the test point to performing the test for all devices, took between two to four minutes. The device lineup and the testing time required will be further verified before a final recommendation is made.

Referencing stations: Referencing is a major issue when it comes to data analysis. The FWD referencing is standardized using DMI. The SPA and PSPA use counters to mark each station and the comment fields are usually used to include the referencing to match the FWD. These counters are the name of the file where the data is stored. As accurately as operators try to coordinate their efforts in referencing each station, there always seems to be some ambiguity in the data. This was the case even with the test sites specifically tested for this project. The situation becomes more difficult, in the analysis stage, when tests are repeated, skipped or the raw data is ambiguous. A more efficient way of referencing will be established and used in the second phase of this project. If the modified procedure proves to be useful in reducing ambiguities in data comparison, it will be recommended as part of the testing protocol.

Other observation: As part of optimizing data collection some coordination amongst the operators is needed. This training is not necessarily to operate the machine, but to work together as one unit with the other operators to ensure that a) testing time is kept to minimum, b) everyone knows what the other is including in their comments (i.e., temperature measurement and visual distresses), c) there is consistency in the unit system, and d) all the data is saved into one media right after the testing is complete.

An attempt will be made to streamline data collection in all these areas. Before visiting the next test site, a tentative protocol will be established and used to resolve some of the problems that currently exist.

Chapter 4

Development of Integration Algorithms

Introduction

The main objective of this project is to develop tools that will improve the decision making process by combining information from different NDT devices. The following three general algorithms are proposed for further development under this project: a) Sequential Integration, b) Joint Inversion, and c) Data Fusion. To understand the protocols involved in each integration algorithm, a conceptual explanation is included followed by a specific implementation plan. The algorithms proposed were the result of several discussions among the researchers of this project and TxDOT staff to ensure their practicality and applicability to day-to-day operation of TxDOT.

Overall Integration Scheme

The focus of this project is to integrate information from four specific NDT devices: a) FWD, SPA, GPR, and PSPA. Figure 4.1 illustrates the overall integration scheme and the flow of information. The current analysis methods are illustrated to the left of the figure and the proposed analysis methods to the right. In current state, the analysis from each NDT device is performed separately usually by different persons. The engineer in charge then compares and analyzes the results from each method manually and subjectively. The flow of information for the current process is indicated by dotted lines. In the proposed data integration method, the data from each device are passed into an integration center where all the reduction, analysis and harmonization of the data are performed.

The integration techniques investigated in this project are: a) Sequential Integration, b) Joint Inversion and c) Data Fusion. The data fusion technique is useful when more than one set of results are obtained. The lower portion of Figure 4.1 depicts the flow and function of data fusion. If the user, for example, performs four different analyses (i.e.; conventional analyses and integrated analyses). The outcome is four sets of results. The benefit of using data fusion is to rationally extract and estimate more-reliable set of results that can be used for evaluation. The following sections provide illustrations of each of the proposed algorithms.

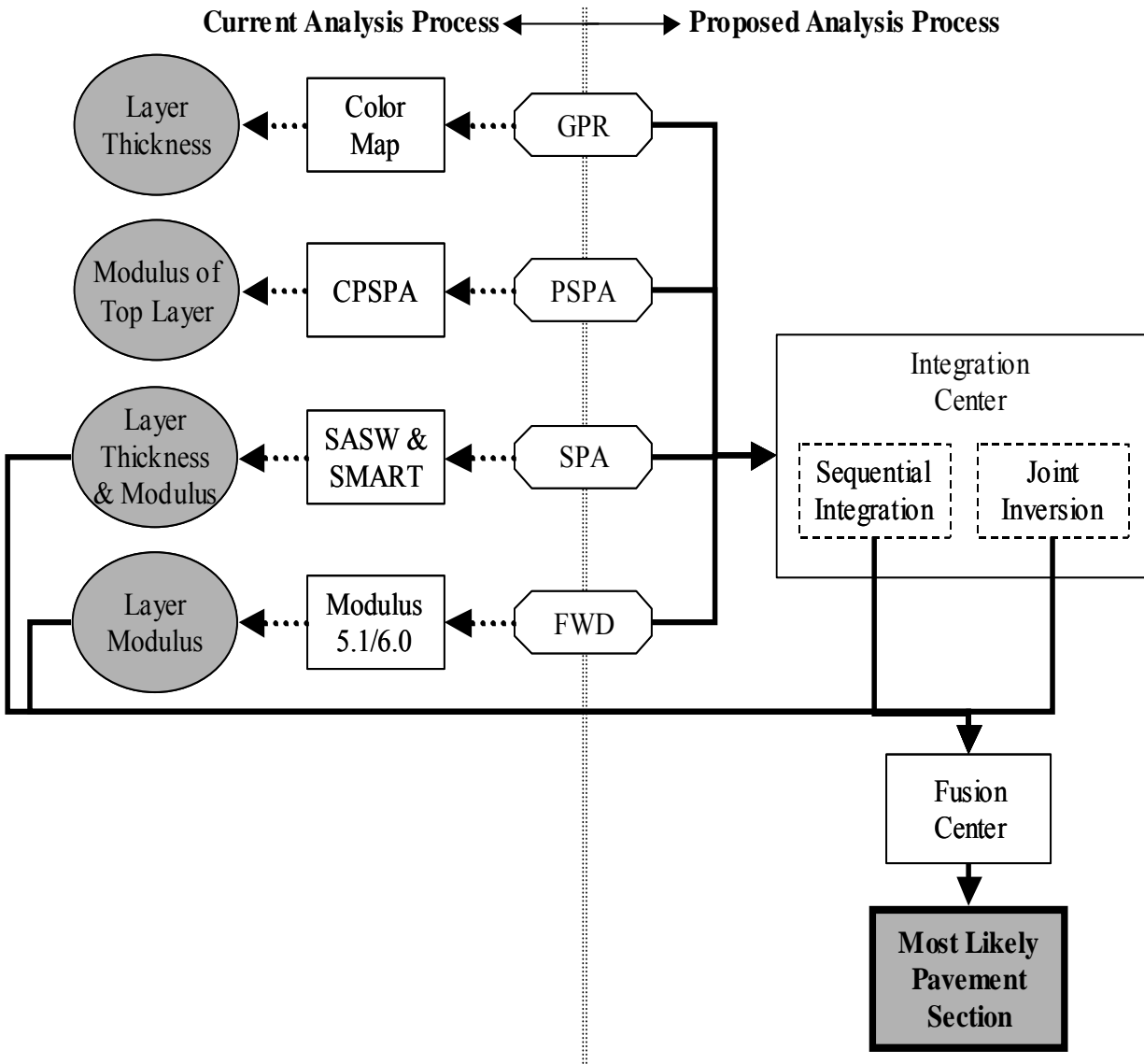


Figure 4.1 - Overall schematic of proposed integration tools

Sequential Integration Algorithms

The idea of sequential analysis is to feed the reliable parameters from one or more NDT device(s), as input into a main analysis program. In this project several sequential integration techniques were researched. Figure 4.2 illustrates the use of the sequential integration with MODULUS as the primary analysis tool since it is currently the main structural analysis program at TxDOT.

Thin pavements is one case where sequential analysis can prove beneficial. Instead of fixing the AC layer modulus to a default value, the modulus from the PSPA at each test point can serve as

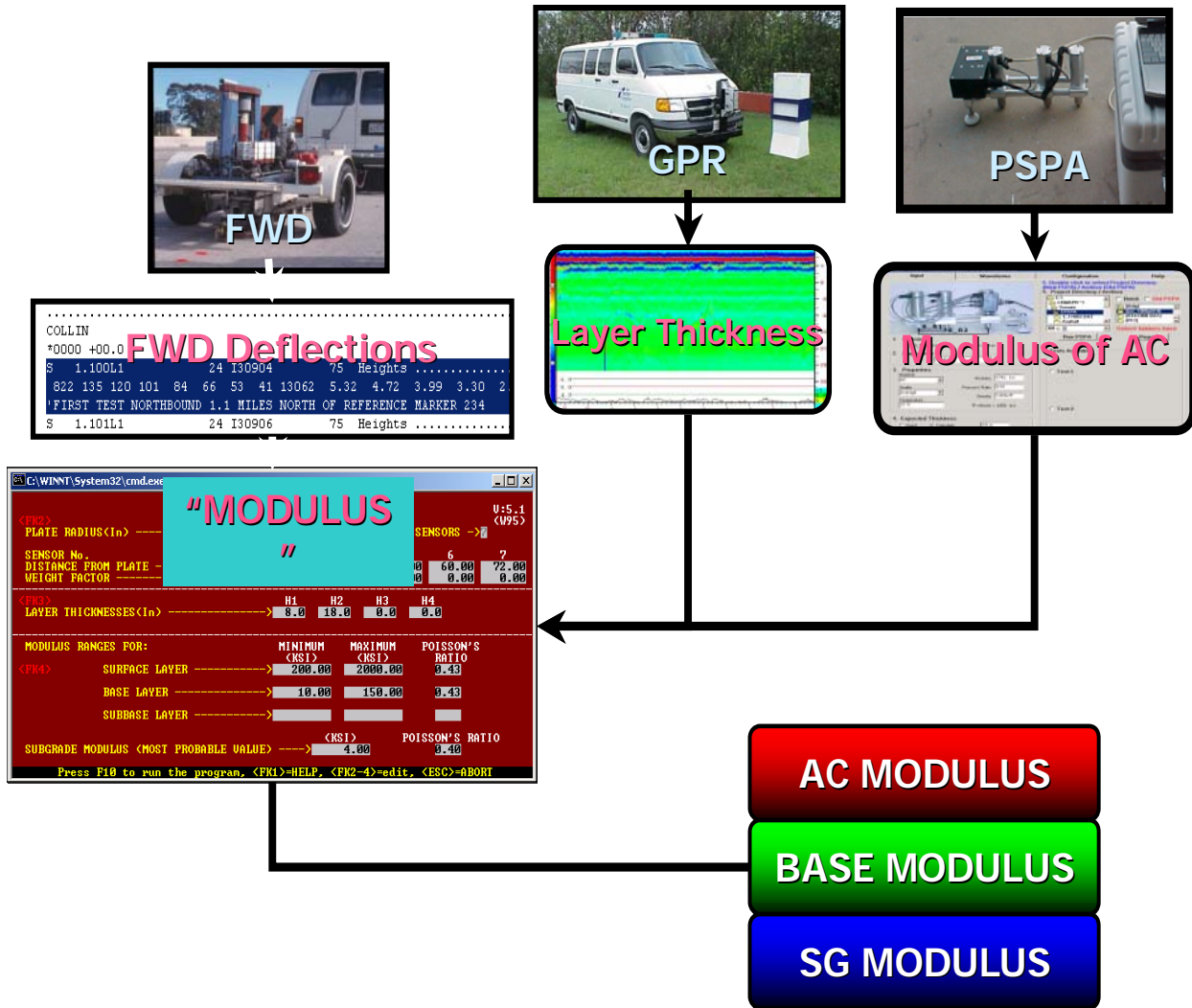


Figure 4.2 - Sequential integration process using MODULUS for calculating layer moduli

fixed a priori information in MODULUS. In addition, the thickness of the AC and possibly (base layers) at each station obtained from the GPR data can be fed to MODULUS.

Figure 4.2 illustrates the use of AC modulus from PSPA and the AC and base thickness from GPR. This process of feeding the information from GPR and SPA/PSPA can be very tedious if performed manually with the current version of MODULUS. However, if this sequential integration is implemented, the flow of information is performed in the background under the control of the user. The analysis part would remain the same; only the background preprocessing would change.

The sequential integration could be expanded to using PSPA and GPR in SMART, however due to the limited resources and the time frame of this project, the only proposed scheme is to integrate results of GPR and SPA/PSPA into MODULUS.

Joint Inversion

The idea of joint integration, as discussed in Chapter 2 has been around since the seventies. The theory behind joint inversion is that the information from different sources measuring the same phenomenon could be used jointly to support each other in describe that phenomenon. Wu (2001) developed an algorithm using joint integration technique for pavements. The work focused on combining seismic and deflection data to determine the moduli of flexible pavement layers. Wu used the artificial neural network technology to develop models that would combine seismic dispersion curve and deflection basin as input to predict moduli of pavement layers. Certainly that work could apply to this project and could be an option when developing the integration tool. However, the approach taken for joint inversion technique under this project, as shown in Figure 4.3, is different. Both the seismic dispersion curve and the FWD deflections are used as input. The output is moduli of pavement layers. The algorithm is an iterative process that uses single value decomposition routine (SVDC) to minimize the errors.

Figure 4.3 illustrates the flow of information and the process used to determine pavement layer moduli. Initially inputs from the FWD measurements are fed into the FWD forward model subroutine (BISAR) and inputs from the SPA measurements are fed into the seismic forward model subroutine with the initial pavement properties such as seed modulus, thickness, Poisson's ratio, and density of each layer. The function of each forward model is to calculate a theoretical response (i.e., deflection bowl for the FWD and dispersion curve for the seismic). The results of the two forward models are compared to the measured values. The error between the theoretical and measured results is calculated. If the error is less than a specified tolerance, the design moduli are reported. However, if the error is greater than the tolerance, the pavement parameters are adjusted and the process is repeated until the error is small enough.

The overall schematic of the joint inversion method (JIM) is presented in Figure 4.4. This algorithm has been developed and is currently being tested and optimized. The accuracy with which pavement layer properties are estimated on synthetic data has been investigated. As an example, the results from a typical three-layer flexible pavement are presented in Figures 4.5 and 4.6. The deflection bowl and dispersion curve were generated using the corresponding forward models. To test the stability of the software, the estimated AC, base and subgrade moduli from JIM are compared to those when only the FWD deflections and only the dispersion curve are used. Estimated layer moduli after each iteration are shown in Figure 4.5. The results from JIM as well as the other methods are all stable. Figure 4.5 also provides an indication of input from which device dominates the inversion process for each layer. It can be observed that the SASW method plays a more predominant role for the AC and base moduli and the FWD is predominant in the estimation of the subgrade modulus.

The convergence of JIM, SASW and FWD results are compared in Figure 4.6. The RMS errors as a function of the number of iterations are shown in the figure. The RMS errors from JIM, similar to the other methods, decrease rapidly with the number of iterations.

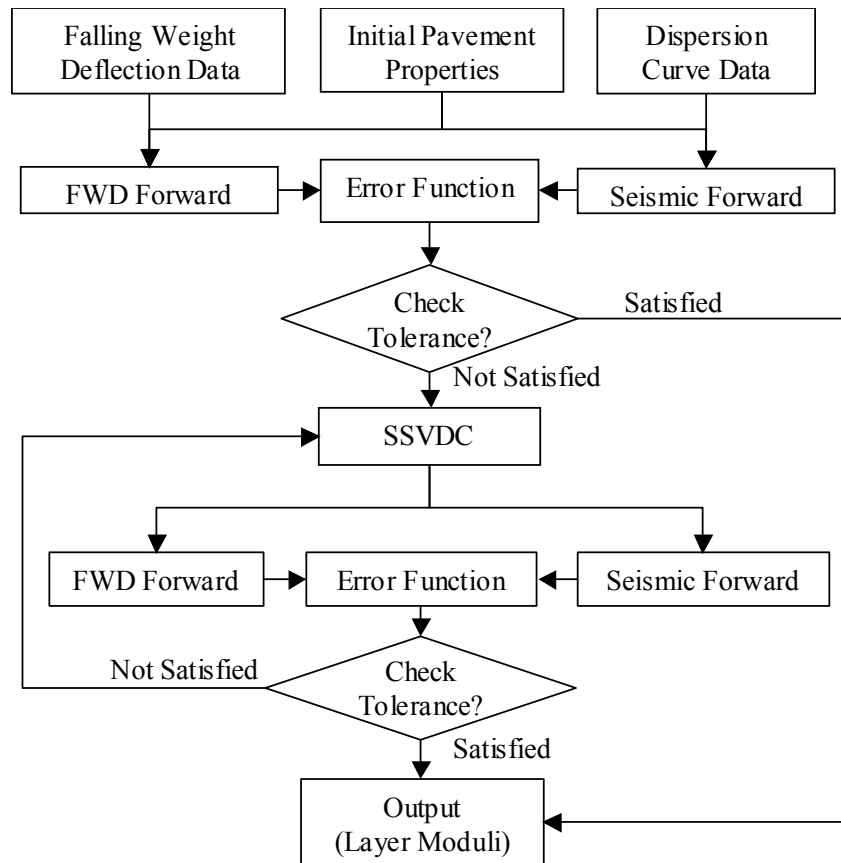


Figure 4.3 - Joint inversion algorithm flowchart

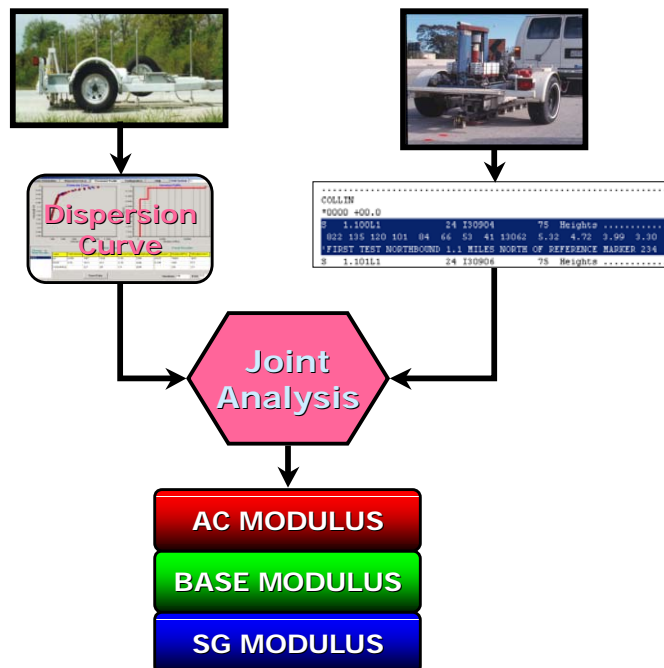


Figure 4.4 - Joint inversion method using data measured from both FWD and SPA

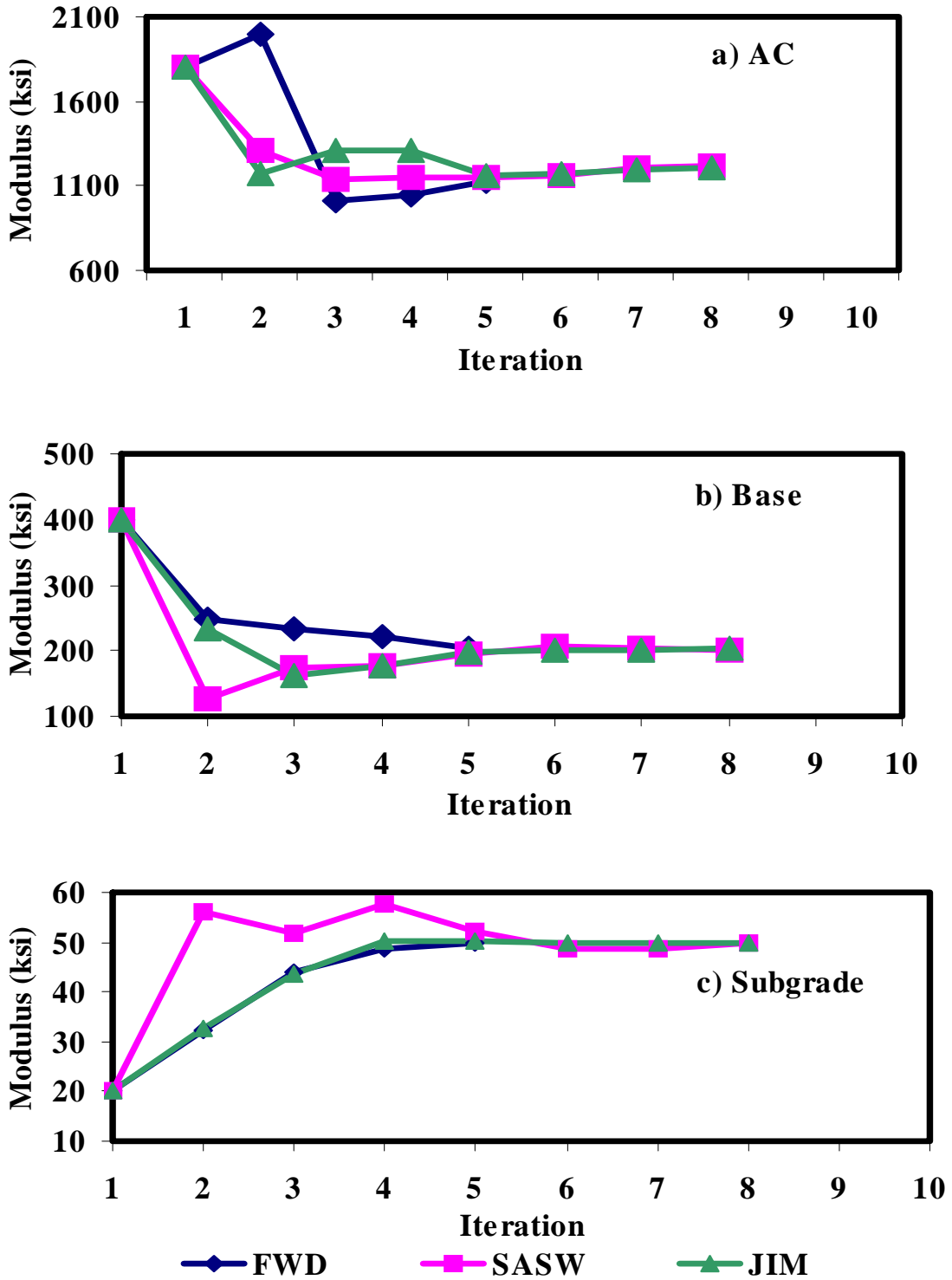


Figure 4.5 - Comparing results of JIM with conventional method to evaluate stability of the algorithm

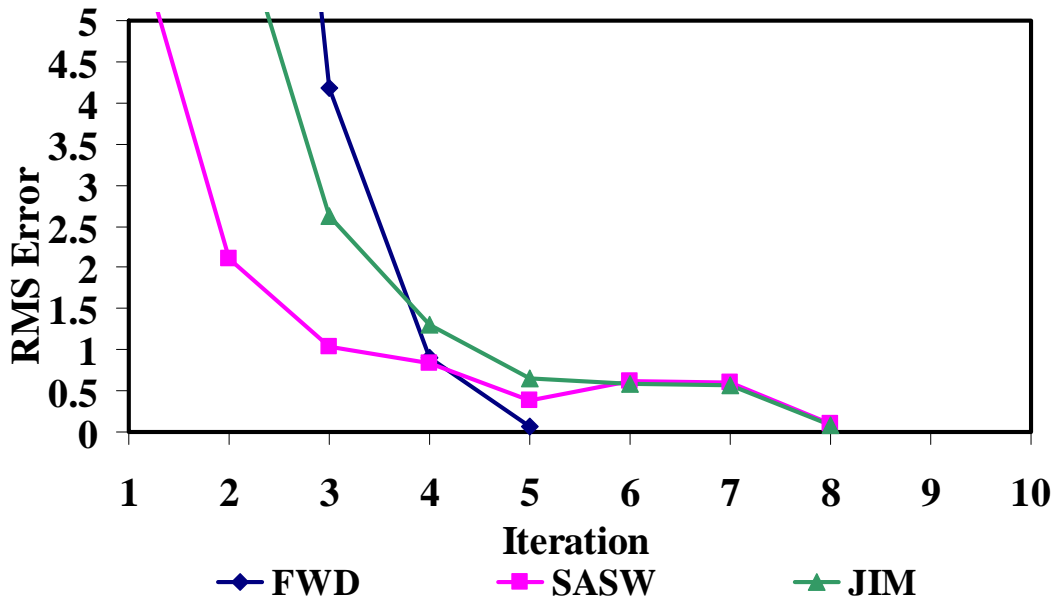


Figure 4.6 - Comparing the convergence of JIM with conventional methods

Data Fusion

Data fusion is the synergistic use of information from multiple sources in order to assist in the overall understanding of a phenomenon. This concept fits very well with the objectives of this project. In a perfect world, using data from several devices collected at the same location should yield the same results. This is hardly the case as applied to the NDT of pavements. The decision on the most appropriate structural parameter is usually made based on engineering judgment. Data fusion can be applied to help in arriving to a rational response. Based on past experience, the most trusted results are considered more favorably to obtain the most likely or most probable outcomes.

Figure 4.7 contains a conceptual example of using data fusion. The probability density function of a parameter measured with five devices is shown in the figure. Devices 1, 2 and 4 have similar mean values when compared to results from Devices 3 and 5. One solution might be to eliminate the results of Devices 3 and 5 and average the remaining three devices. Another solution might be to average results of all devices (this is the simplest form of fusion). Yet another solution might be to report the results ranging from 350 to 650 based on the lowest and highest mean value. If data fusion is applied considering the standard deviation as a weighing factor the fused results show a mean value of 450 (shown in the figure as fused results). Notice that the results of Devices 3 and 5 did not impact the fused results as much as the other three. This happens because the standard deviation associated with these two devices are greater (i.e., the distributions is much wider).

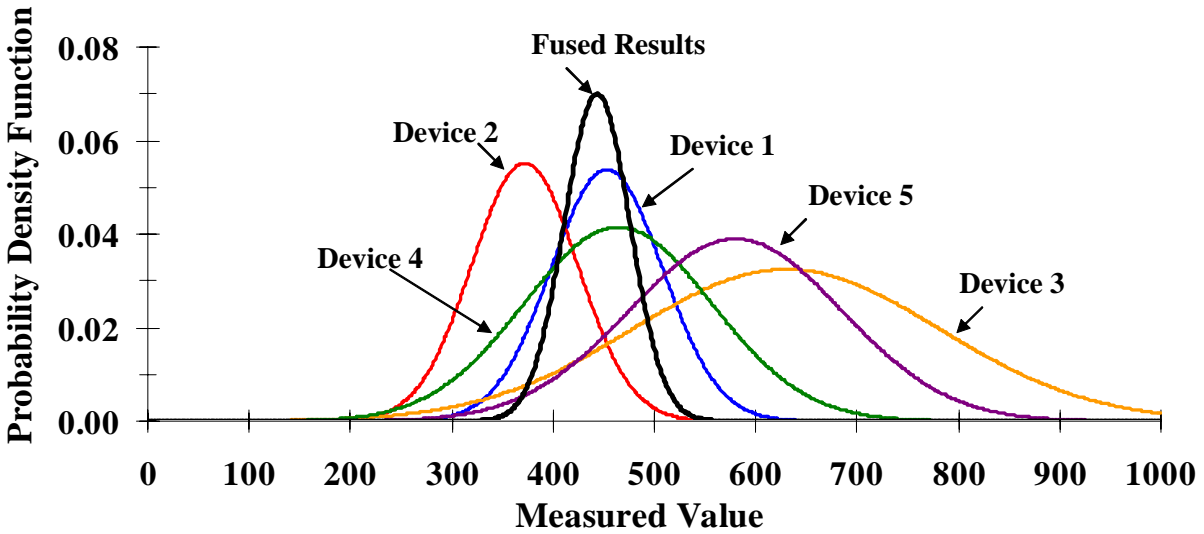


Figure 4.7 - Illustrative example of data fusion

As discussed in Chapter 2, there are several techniques to fuse information. The simplest is taking an average of the sample set. On the other extreme, a network of neural processing elements can be developed. Few of the algorithms listed in Table 2.1 are being investigated at this point to determine the most applicable and practical fusion methods. Another consideration is identifying the information that should be fused.

Two main categories of information can be fused: 1) the information that is fed into the system (i.e., input data such as thickness or deflections) and 2) the information that is provided by the system (i.e., the moduli of the layers). To easily distinguish between the two, the term input fusion will be used in the first instance and the term decision fusion in the second instance. At this point in the research, “decision” fusion is being investigated and it will be part of the final integration tool. Input fusion is not practical for NDT of pavements since it requires more field testing which can become expensive and impractical from a users point of view.

Chapter 5

Feasible Integration Techniques Based on Case Studies

Introduction

As discussed in Chapters 3 and 4, several sites were tested to demonstrate the feasibility of integrating NDT data. At each site, several NDT devices were utilized. The data integration processes, presented in Chapter 4, were applied to the data. The procedures and results for two sites are presented next.

Case Study – El Paso District Parking Lot

The first site was located in the TxDOT El Paso District parking lot. The pavement section at this site nominally consisted of a 2-in.-thick asphalt-concrete pavement (ACP) layer over 6 in. of granular base, over a sandy subgrade. The section was 400 ft in length divided into twenty test points.

The main goal at this site was to demonstrate the feasibility of JIM and data fusion algorithms. The FWD and SPA were used at this site, and the GPR and PSPA were excluded. Figure 5.1 shows the two NDT devices at this site. FWD tests were carried out at four load levels at each test point. The data associated with a load of approximately 9000 lb was used in the analysis because it simulates the load applied by a typical truck.

Each of the twenty points was tested three times using first the FWD followed by the SPA. This process was repeated twice. The data from the repeated tests was used to verify the repeatability of each device, to evaluate the feasibility of fusing raw data before the analysis is performed, and to obtaining statistical data that might be required for fusion techniques. The last point was tested 20 times with each device to quantify the repeatability of the devices as presented in Chapter 3.

As stated in Chapter 2, the two devices utilized dissimilar identification for each test location. To ensure data integrity, each device operator included additional information in the comment

section of each record. The comments included a uniform numbering scheme to easily identify each location, temperature of AC measured with a digital thermometer embedded in the ACP layer, and any visible distresses that were observed. No trenching or coring was performed at this site, therefore laboratory tests were not done. However, because of the geographical location, the typical properties of the base and subgrade are well-known to the researchers.



Figure 5.1 - FWD and SPA at El Paso District Parking Lot

Data Analysis

The procedure used to analyze the data can be summarized in following steps:

- Step 1: Determine the seismic modulus profile from SPA using SASW software.
- Step 2: Determine design modulus profile using the results of Step 1 in SMART software.
- Step 3: Determine modulus profile from FWD using MODULUS.
- Step 4: Determine the design modulus profile using the measured dispersion curves and the deflection basins using JIM.

Each step in the data analysis process is elaborated below.

SPA-SASW Analysis

The reduction of the SASW data is a two step process (Nazarian et al., 1995). The first step consists of constructing an idealized dispersion curve (variation in phase velocity with wavelength). Once a dispersion curve is determined, an inversion (backcalculation) algorithm is used to estimate the shear wave velocity profile of the pavement section. The shear wave velocities were converted to seismic modulus as described in Chapter 2.

The results from this step at this test site are presented in Figures 5.2 and 5.3. The measured dispersion curves for the twenty points are shown in Figure 5.2. The dispersion curves are more similar at short wavelengths as compared to the intermediate and long wavelengths. This pattern

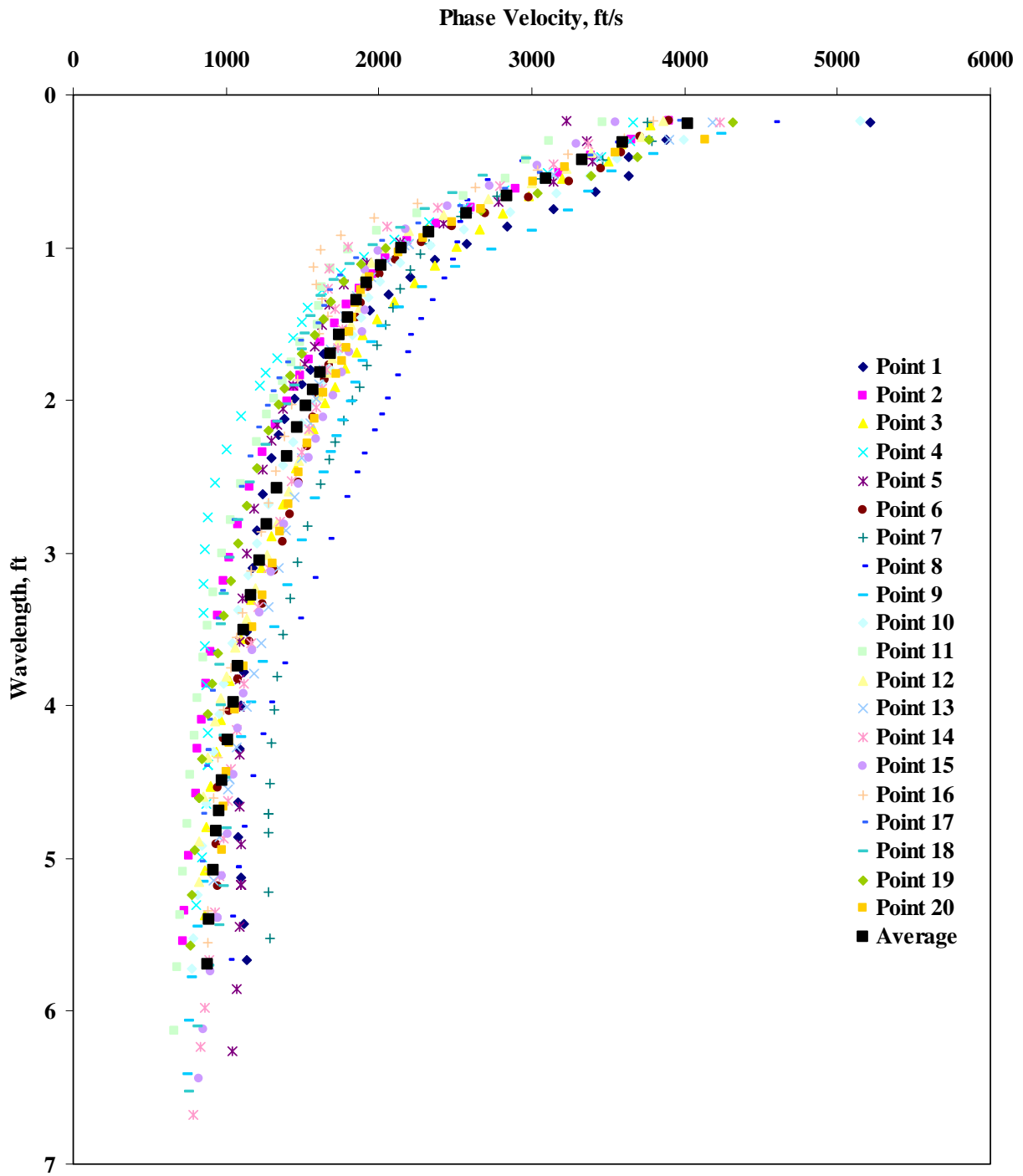


Figure 5.2 - Dispersion curves from SASW at El Paso District Parking Lot

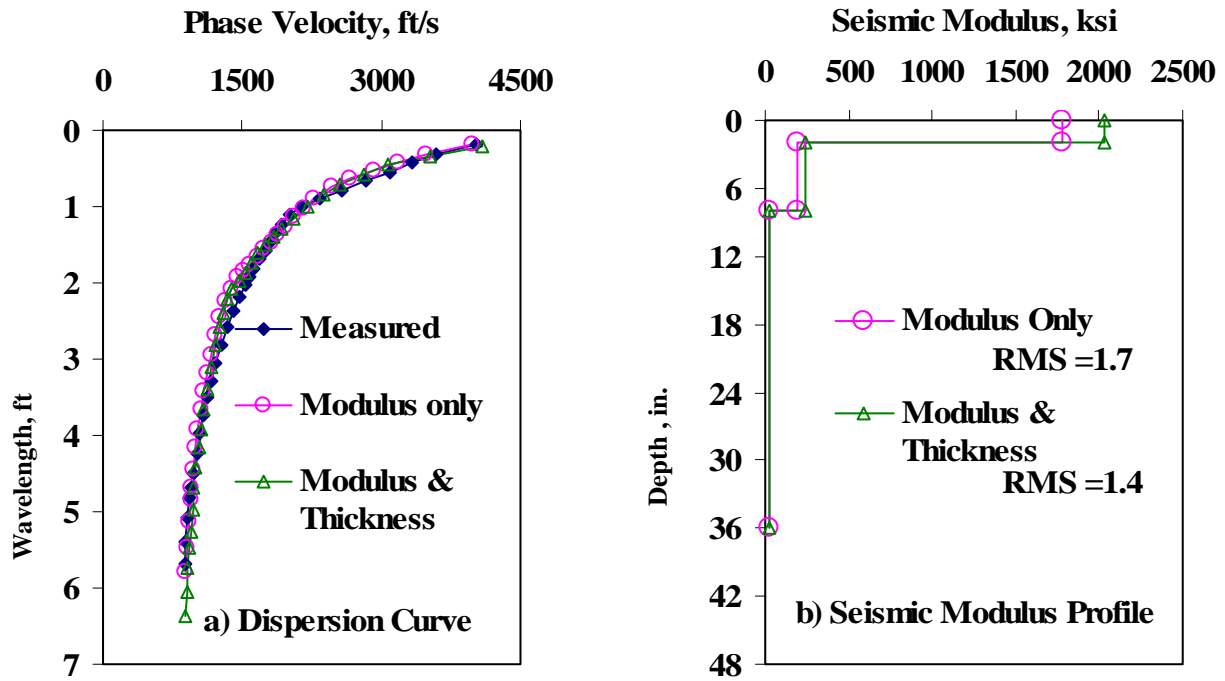


Figure 5.3 - Typical results from SASW data reduction processes at El Paso District Parking Lot

provides a preliminary indication that the ACP is more uniform across the section as compared to the base and subgrade layers.

The inversion algorithm in the SASW program allows users to select any combination of layer thickness or shear wave velocity to be estimated. Typically, the inversion process is performed to determine the modulus of each layer. However, if the thickness is not well known both thickness and modulus can be estimated. For this case study, the inversion process was performed twice. The first was based on the assumption that the thickness of the AC layer and the base layer were known, and only the moduli were estimated. In the second case, the thickness and modulus of each layer were estimated.

The dispersion curve and seismic modulus profile at the last location of the site (point 20) are presented in Figure 5.3. Figure 5.3a compares the measured dispersion curve with the theoretical dispersion curves obtained when only layer moduli were estimated and when both layer thickness and layer moduli were determined. The three curves compare favorably. The RMS errors after completion of the inversion processes were 1.4 and 1.7 for the two cases.

The estimated modulus profiles from the two cases are shown in Figure 5.3b. The moduli were fairly similar. Table 5.1 summarizes the results for all test points at this site. The average, standard deviation and coefficient of variation (COV) for the site are also included in the table. The COVs of the layer moduli when only the moduli of the layers were estimated, in most cases,

were higher than those when both modulus and thickness were estimated. Overall, the modulus of the AC layer was consistent through out the section with a COV of 15% and 11%, for the two inversion schemes. The base layer had a COV of 21% in the first case and increased to 30% for the second case. The COV of subgrade, across the section, decreased from 51% in the first case to 18% in the second case. This exercise clearly demonstrates the importance of either knowing or estimating the thickness of the pavement layers.

Table 5.1 - Results of SASW data reduction process at El Paso District Parking Lot

Point	Inversion of Modulus Only				Inversion of Modulus and Thickness					
	Modulus, ksi			RMS Error	Thickness, in.		Modulus, ksi			RMS Error
	AC	Base	S.G.		AC	Base	AC	Base	S.G.	
1	2455	183	49	1.8	2.0	6.0	1989	251	28	1
2	1743	155	17	0.9	2.0	5.5	1877	179	27	1.1
3	1879	228	7	1.7	2.0	5.1	2143	148	35	2.2
4	1730	99	30	0.8	1.6	5.0	2276	146	34	1.4
5	1468	197	53	3.3	1.8	5.5	2184	138	30	1.1
6	1785	228	26	1.8	1.7	9.0	2117	305	24	1.6
7	1692	228	65	2.6	1.7	9.0	2187	352	23	1.3
8	1810	228	49	1.2	2.3	7.9	2222	303	21	3.7
9	2264	228	7	1.8	2.0	5.7	1991	334	20	1.8
10	2249	225	15	1.1	2.1	5.1	1763	199	26	0.8
11	1390	166	12	0.9	1.3	4.6	2002	147	25	1.5
12	1690	228	17	1.6	1.9	6.3	1907	282	20	0.8
13	1785	228	34	2	1.3	8.6	2089	287	19	1.1
14	1512	228	27	2.4	2.2	7.0	1706	170	19	0.9
15	1404	228	27	2	2.1	5.8	1736	265	27	0.9
16	1545	145	41	1.5	1.7	8.1	1691	229	23	0.8
17	1733	112	30	0.7	1.9	5.1	1682	142	28	0.8
18	1550	167	29	1.8	1.2	3.4	2260	331	25	1.7
19	1932	165	18	1.6	1.5	4.1	2525	296	19	1.3
20	1992	228	36	2.2	1.7	4.0	2201	327	30	1.3
Avg.	1780	195	30	1.7	1.8	6.0	2027	242	25	1.4
Std	274	41	15	0.6	0.3	1.6	222	72	5	0.6
COV	15%	21%	51%	37%	16%	27%	11%	30%	18%	47%

SMART Analysis

SMART estimates the design moduli from seismic moduli as discussed in Chapter 2. The estimated seismic moduli and the nonlinear parameters of the base and subgrade layers were used as input to SMART. The seismic profiles with fixed thickness of the layers were used. Ideally, the nonlinear properties, k_2 and k_3 of the base and subgrade (see Equation 2.4) should be determined from laboratory tests. In the absence of laboratory values, the default k_2 and k_3 values incorporated in SMART for the types of material present at the site were used. Since SMART is based on a nonlinear algorithm, two sets of design modulus values (i.e., conservative and average) were estimated for the base and subgrade layers. As discussed in Abdallah et al. (2003), the conservative design moduli correspond to the minimum modulus measured in each layer; whereas the average moduli correspond to the weighted average moduli directly under the load. For the ACP, the design moduli were determined using the simplified procedure described in Chapter 2.

The average and conservative moduli are presented in Table 5.2. SMART can provide seven theoretical deflections corresponding to the locations of the FWD sensors. The RMS error between the measured FWD deflections and the deflections estimated by SMART are also reported in Table 5.2. This RMS error is an independent means for evaluating the validity of the results from SMART. The average RMS error of 3% was obtained at this site with a maximum RMS error of 7%.

FWD Analysis

MODULUS was used to estimate the moduli of the layers using the FWD measured deflections. The layer thicknesses were set to 2 in. and 6 in. for the AC and base, respectively. The modulus of the ACP was fixed to 500 ksi since the thickness of AC layer was less than 3 in. The FWD deflections measured in the field for this site are presented in Table 5.3. The deflections from the second drop (load close to 9000 lb) were normalized to a 9000-lb load and was used in the analysis.

The backcalculated moduli are presented in Table 5.4 along with the deflection basin fitting mismatch. In MODULUS the mismatch is reported as error per sensor. To uniformly compare the results with the other methods, the RMS errors were determined from the calculated deflection bowls and reported as deflection basin mismatches. The RMS errors are small for all test points with an average of 3%. The average base and subgrade moduli from MODULUS are 88 ksi and 18 ksi respectively. The average base modulus from MODULUS is similar to the results from SMART. The subgrade moduli from MODULUS and SMART are also fairly close.

Table 5.2 - Design moduli from SMART at El Paso District Parking Lot

Point	Modulus (ksi)						RMS Error
	Conservative			Average			
	AC	Base	S.G.	AC	Base	S.G.	
1	625	66	10	625	81	23	1%
2	544	43	8	544	52	19	2%
3	612	75	7	612	91	14	4%
4	493	26	8	493	32	18	5%
5	551	33	9	551	40	20	6%
6	623	118	9	623	150	19	2%
7	554	172	11	554	235	22	3%
8	693	150	9	693	194	19	1%
9	589	110	7	589	139	14	5%
10	544	64	6	544	78	13	3%
11	450	32	7	450	39	16	4%
12	516	123	8	516	160	15	2%
13	450	105	9	450	137	19	1%
14	440	94	8	440	121	17	1%
15	554	87	8	554	108	18	1%
16	424	26	8	424	33	18	0%
17	467	33	7	467	40	17	6%
18	508	31	7	508	38	16	4%
19	528	35	7	528	42	16	1%
20	548	46	7	548	57	16	7%
Avg.	536	73	8	536	93	17	3%
Std. Dev.	69	43	1	69	58	3	2%
COV	13%	59%	15%	13%	62%	14%	68%

Table 5.3 - Measured FWD field data normalized to 9000 lbs from FWD at El Paso District Parking Lot

Point	Deflections (mils)						
	Sensor Spacing						
	0 in.	12 in.	24 in.	36 in.	48 in.	60 in.	72 in.
1	18.5	8.6	4.2	2.5	1.9	1.5	1.1
2	21.6	8.4	4.0	2.5	1.8	1.5	1.1
3	21.7	9.8	4.9	2.9	2.0	1.7	1.2
4	22.2	10.8	5.1	3.2	2.2	1.7	1.4
5	19.9	9.7	4.9	3.2	2.3	1.7	1.4
6	17.0	8.5	4.9	3.3	2.3	1.9	1.4
7	15.5	8.4	4.8	3.1	2.2	1.7	1.3
8	15.5	8.6	5.0	3.1	2.2	1.6	1.3
9	15.4	9.0	5.3	3.5	2.5	1.9	1.5
10	20.6	10.5	6.1	3.7	2.7	2.0	1.6
11	27.2	12.4	6.3	3.9	2.7	2.1	1.7
12	20.8	10.9	5.8	3.5	2.4	1.9	1.4
13	17.7	9.3	5.3	3.3	2.2	1.9	1.4
14	20.4	9.9	5.6	3.3	2.3	1.8	1.4
15	18.3	9.8	5.4	3.5	2.4	1.9	1.5
16	22.1	10.4	5.5	3.4	2.4	1.8	1.5
17	20.7	10.5	5.6	3.5	2.4	1.9	1.5
18	22.5	10.7	5.5	3.3	2.4	1.9	1.5
19	24.8	11.6	5.6	3.5	2.5	1.9	1.4
20	17.9	9.4	5.2	3.3	2.3	1.8	1.4
Mean	20	9.9	5.3	3.3	2.3	1.8	1.4
Std. Dev.	3	1.1	0.5	0.3	0.2	0.2	0.1
C.V.	15%	11%	10%	10%	10%	8%	10%

Table 5.4 – Backcalculated Moduli from FWD at El Paso District Parking Lot

Point	Modulus (ksi) using MODULUS			
	AC	BASE	SUBGRADE	RMS Error
1	500	68	21	2%
2	500	42	22	4%
3	500	54	19	2%
4	500	55	17	3%
5	500	73	18	4%
6	500	120	19	5%
7	500	153	19	3%
8	500	156	19	3%
9	500	187	17	4%
10	500	89	16	3%
11	500	43	14	3%
12	500	78	16	2%
13	500	112	18	4%
14	500	76	17	3%
15	500	110	17	4%
16	500	62	17	3%
17	500	77	17	3%
18	500	59	17	3%
19	500	47	16	2%
20	500	108	18	4%
Avg.	500	88	18	3%
Std. Dev.		40	2	1%
COV		45%	10%	18%

JIM analysis

Performing the analysis using the joint inversion program developed under this project requires data from both the SPA and FWD. The idealized dispersion curve from Step 1 and the measured FWD deflections at each point were input into JIM to calculate the design modulus and thickness of each layer. The conservative and average moduli when only modulus was backcalculated is presented in Table 5.5. The results in the table show a COV of 16% for both the ACP and subgrade layers. The COV for the base moduli was 34%.

Table 5.5 - Design moduli from JIM at El Paso District Parking Lot

Point	Modulus (ksi)						RMS Error
	Conservative			Average			
	AC	Base	S.G.	AC	Base	S.G.	
1	638	54	12	638	67	27	5%
2	597	30	11	597	38	26	4%
3	653	48	9	653	58	21	1%
4	495	26	8	495	32	19	5%
5	578	31	9	578	38	20	6%
6	749	63	9	749	77	20	4%
7	681	63	10	681	76	22	6%
8	752	84	10	752	102	21	3%
9	703	46	8	703	56	18	10%
10	574	54	7	574	66	16	2%
11	443	30	6	443	36	15	2%
12	594	61	8	594	75	18	0%
13	481	61	9	481	76	19	3%
14	494	69	9	494	85	19	1%
15	587	71	8	587	87	18	2%
16	471	69	8	471	86	18	1%
17	440	33	8	440	41	17	6%
18	509	30	8	509	37	17	4%
19	537	31	7	537	38	17	1%
20	600	46	8	600	55	19	5%
Avg.	579	50	9	579	61	19	3%
Std. Dev.	93	17	1	93	21	3	2%
COV	16%	34%	16%	16%	34%	15%	66%

Figure 5.4 compares the results of JIM when moduli were backcalculated versus when both modulus and thickness of each layer were estimated. The conservative estimated were used in the figure for comparison. As reflected in Figure 5.4a, the ACP moduli when both thickness and modulus are estimated are on the average 30% greater (870 ksi) when compared to when only modulus is estimated (580 ksi). The base moduli are similar for both cases and vary from 30 to 70 ksi along the section (see Figure 5.4b). The subgrade moduli represented in Figure 5.4c show little variation between the two inversion schemes with an average modulus close to 9 ksi.

Comparison of Results from the Different Analyses

Results from JIM, SMART and MODULUS are compared in this section. The thickness of the AC and base layers estimated using JIM and SMART are compared in Figure 5.5. For the ACP

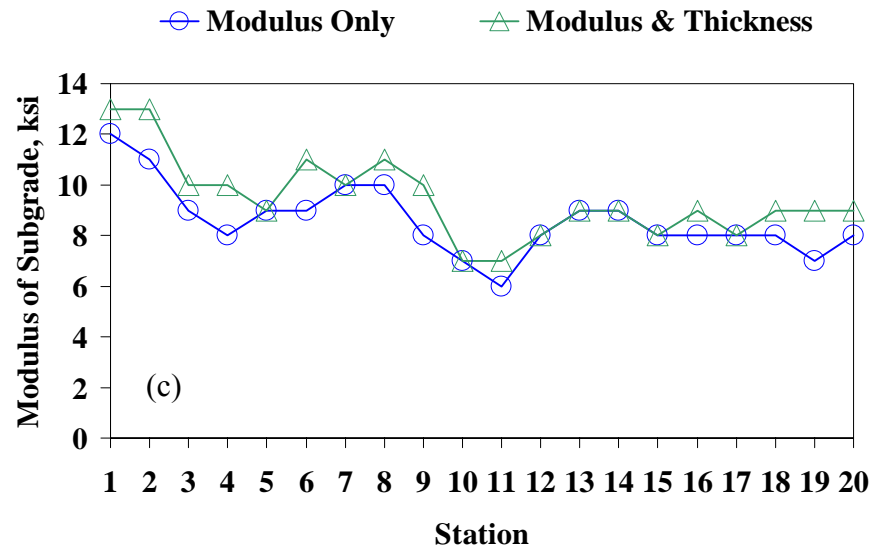
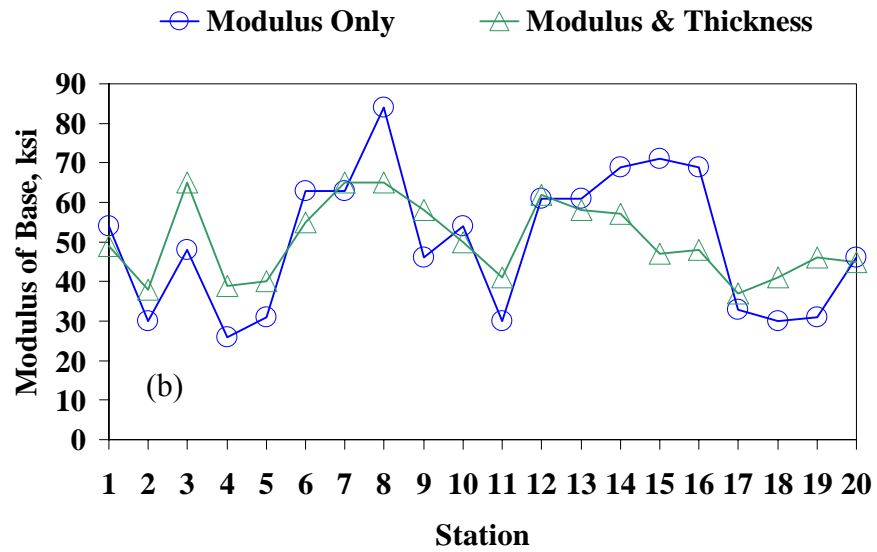
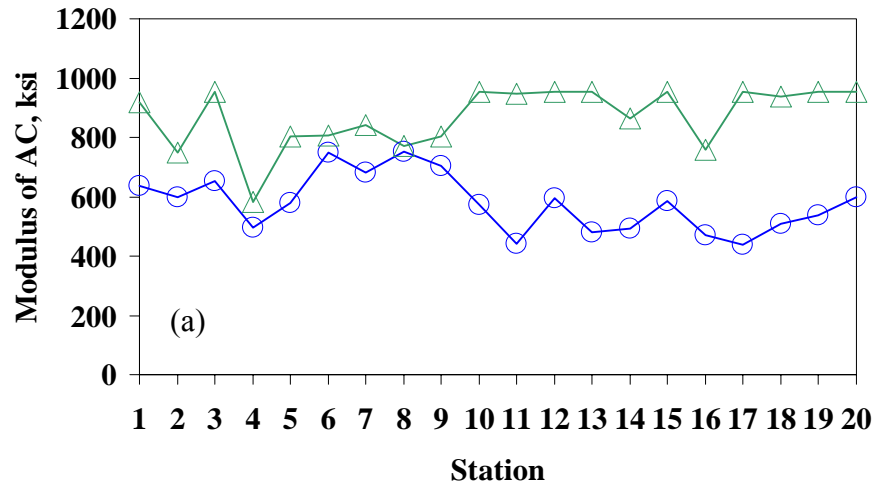


Figure 5.4 - Variations in moduli from JIM along El Paso District Parking Lot

layer the thickness of 1.8 in. (COV 16%) from SMART was similar to the nominal thickness of 2 in. The thickness from JIM for the section was also reasonable with an average thickness of 1.7 in. (COV 16%). For the base layer with a nominal thickness of 6 in., SMART yields an average thickness of about 6 in. with a COV of 28%. Comparatively, JIM estimates an average base thickness of 5.5 in. but with a smaller COV value of 17%.

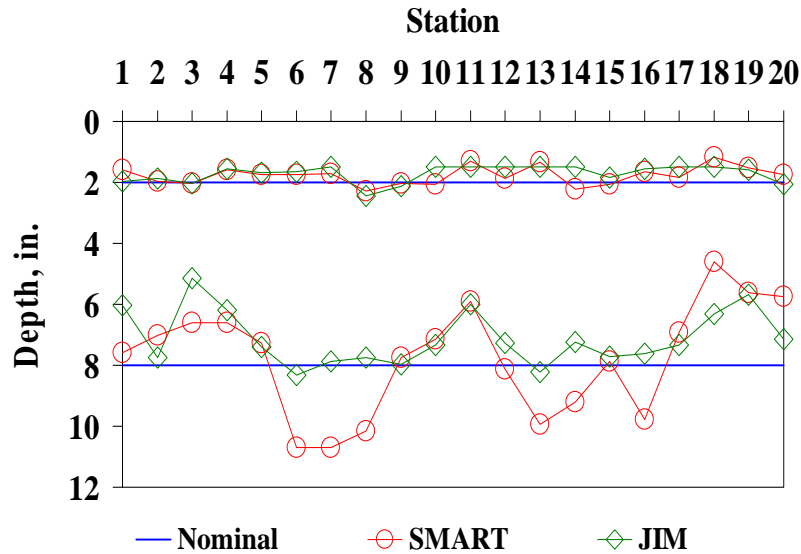


Figure 5.5 - Variations in layer thicknesses from JIM and SMART along El Paso District Parking Lot

Moduli of the ACP, base and subgrade from SMART, MODULUS, and JIM are compared in Figure 5.6. For the ACP layer, as reflected in Figure 5.6a, SMART and JIM yield consistent results across the section with average moduli of 536 ksi and 580 ksi, respectively. The COV of both was less than 16%. The modulus of the ACP layer for the FWD analysis was fixed at 500 ksi.

The conservative moduli from SMART and JIM and the FWD moduli from MODULUS for base layer are reported in Figure 5.6b. The results from FWD and SMART seem to follow the same trend with both showing a peak modulus values between Stations 6 and 10. The average base moduli are 88 ksi and 73 ksi, respectively. Both exhibit large variation in modulus since SMART COV is about 45% and JIM COV about 60% along the section. JIM however seems to yield more consistent moduli through out the section with an average modulus of 50 ksi and a COV of 34%. Even through JIM yields higher moduli at similar locations as compared to SMART and FWD, the variation is not as much. The data used in JIM is identical to the data used in SMART and FWD with the exception that JIM uses both sets of data (dispersion curve and FWD deflection). This may indicate that JIM maybe less sensitive to the misestimation of layer moduli.

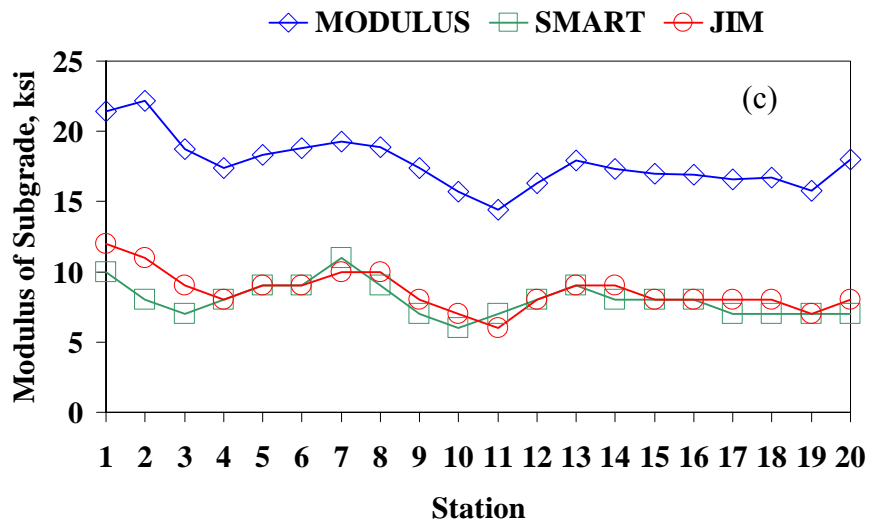
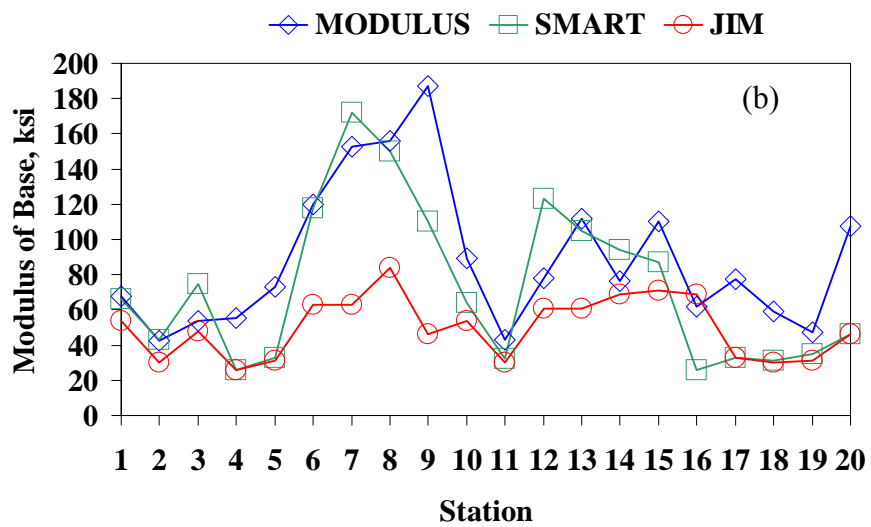
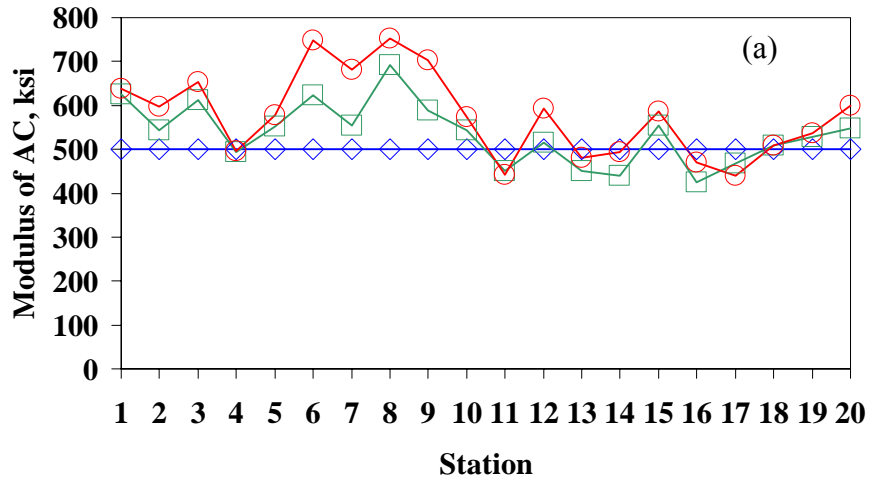


Figure 5.6 - Comparison of moduli from MODULUS, SMART and JIM at El Paso District Parking Lot

Subgrade moduli from the three analyses are compared in Figure 5.6c. The three analyses provide consistent results throughout the section. However, moduli from JIM and SMART are quite close to one another with an average value of 9 ksi and COV of 16%. The FWD moduli are twice the moduli from the other two analyses with an average of 18 ksi and a COV of 10%. Even though not shown here, the FWD moduli closely match the average moduli (instead of the conservative moduli) of both SMART and JIM reasonably well. This indicated that the subgrade moduli from FWD are representative of the deeper sections of the subgrade and may be not conservative.

As indicated before, JIM and SMART can calculate surface deflections corresponding to FWD set up. The RMS errors associated with the basin mismatch between the measured and calculated deflections from JIM, MODULUS and SMART under a 9000 lb FWD load are compared in Figure 5.7. The RMS error provides an indication of the level of convergence of each analysis. Overall the basin mismatch RMS errors are small for all three methods since they are typically less than 5% except for one point where the RMS error from JIM is about 10%.

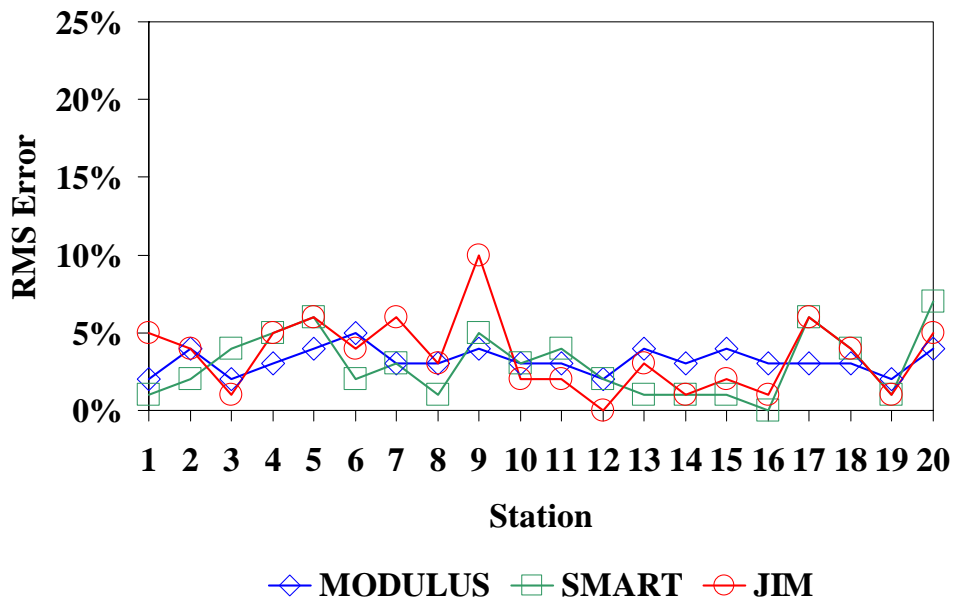


Figure 5.7 - Comparison of deflection basin mismatches at El Paso District Parking Lot

Case Study - Ride Rut Facility at Riverside Annex

The Ride Rut facility located at the Riverside Annex of Texas A&M University was another ideal site at this stage of the project. Figure 5.8 provides an idealized illustration of the pavement cross-section. The site consisted of 2 in. of ACP over a granular base, over an 8-in.-thick lime treated subbase. The subgrade consisted of a highly plastic clay. The test section was 2000 ft long. The base thickness for the first and last 200 ft of the section was nominally 6 in. thick, and for the middle 1600 ft 14 in. thick. As reflected in Figure 6.8, twenty five points were tested at this site. The first five and the last four points were 50 ft apart to cover the 6-in.-thick base, and the middle sixteen points, which were located on the thicker base, were 100 ft apart.

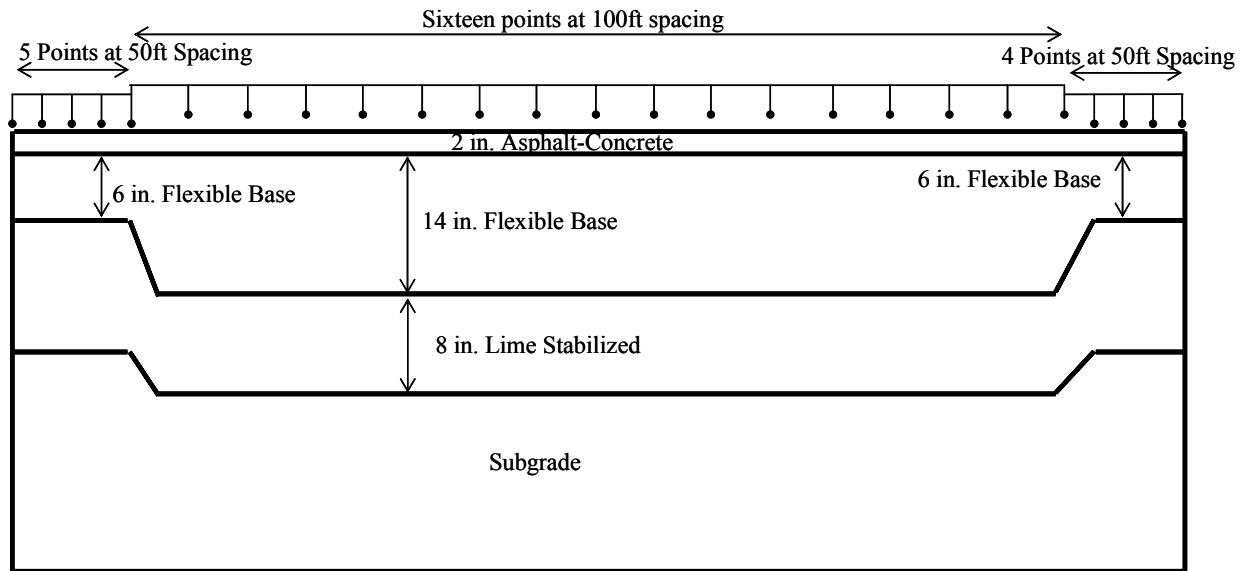


Figure 5.8 - Schematic of the test setup and test section at the Ride Rut facility.

Field Testing

The GPR, FWD, SPA and PSPA were used at this site. This site provided us with the opportunity to test the feasibility of using JIM, as well as to implement the sequential integration process. The NDT devices used at the site are shown in Figure 5.9. Each point was tested with the GPR three times. After the GPR data was collected, the FWD followed by the SPA and PSPA were used at the site. Each device at each point repeated the test three times. A repeatability test was also performed at the 0 ft marker to further demonstrate repeatability of each device.



Figure 5.9 - FWD and SPA at the Ride Rut facility

Data Analysis

The procedure used to analyze the data can be summarized in following steps:

- Step 1: Determine the seismic modulus profile from SPA using SASW software.
- Step 2: Determine design modulus profile using the results of Step 1 in SMART software.
- Step 3: Determine modulus profile from FWD using MODULUS.
- Step 4: Determine the design modulus profile using the measured dispersion curves and the deflection basins using JIM.
- Step 5: Extract discrete thickness for each test location from GPR data using COLORMAP
- Step 6: Determine the modulus of ACP from PSPA data
- Step 7: Use data from the GPR and PSPA as input to MODULUS to conduct sequential analysis.

Each step in the data analysis process is elaborated below.

Conventional Analyses

The results from Steps 1 through 4 are included in Appendix C. A statistical summary of the results are provided in Table 5.5. The layer moduli from the SASW method when the thicknesses were fixed to their nominal values are similar to when the thicknesses were estimated. Since the section tested is an experimental one, extreme care was taken to ensure uniformity and accuracy in thickness. The average estimated AC thickness from the SASW method is 2 in. similar to the nominal thickness with a COV of 12%. The average base thickness from SASW tests for the middle sub-section was about 14 in. with a COV of 42%. For the two sub-sections with thinner base, the average thickness was about 4 in., about 2 in. less than the nominal thickness. The subbase thickness also differed from the nominal thickness. For the middle sub-section the SASW method reported a thickness of about 23 in. and about 12 in. for the thinner sub-sections. This indicates that the compactive efforts during the preparation of the subbase also stiffened a portion of the subgrade.

The conservative and average moduli from SMART as well as backcalculated moduli from FWD are also reported in Table 5.5. The average modulus of AC calculated by SMART is about 560 ksi which is close to 500 ksi assumed for the FWD. The FWD base modulus on average is close to that from SMART obtained under the ‘Average’ condition. This indicates that some unconservatism is built into the modulus of this layer when FWD is used. The average subbase modulus from SMART for ‘Average’ and ‘Conservative’ conditions are similar indicating that the subbase does not experience much of load-induced nonlinearity. The estimated modulus from SMART is on the average 33 ksi which is smaller than 58 ksi reported by MODULUS. The average subgrade modulus from FWD was 18 ksi whereas for SMART it was about 24 ksi. This occurs because the estimated subbase moduli for the subbase are greater with the FWD than from SMART.

Table 5.6 - Results of SASW data reduction process the Ride Rut facility

Analysis Method	Inversion Parameter		Average	Std. Dev.	COV
SASW	Modulus, ksi (modulus only)	AC	1973	337	17%
		Base	106	37	35%
		Subbase	57	22	38%
		Subgrade	24	10	40%
	Modulus, ksi (modulus & thickness)	AC	1932	179	9%
		Base	106	25	23%
		Subbase	66	20	30%
		Subgrade	19	6	32%
	Thickness, in. (modulus & thickness)	AC	2.0	0.3	12%
		Base	3.7/14.1*	1.5/5.9*	41%/42%*
		Subbase	23.1/12.4*	6.6/4.0*	29%/32%*
	SMART	Modulus, ksi (conservative)	AC	590	100
Base			68	21	31%
Subbase			33	12	35%
Subgrade			23	9	39%
Modulus, ksi (average)		AC	590	100	17%
		Base	93	29	31%
		Subbase	34	12	34%
		Subgrade	24	9	39%
FWD	Modulus, ksi	AC	500	0	0%
		Base	96	31	32%
		Subbase	58	43	74%
		Subgrade	18	3	17%

* - values from thin base and thick base, respectively.

JIM analysis

As for the first case study, the joint inversion analyses were conducted in two manners: with thickness fixed and with thickness estimated. The results are summarized in Figure 5.10. The reported moduli are from the “conservative” option of JIM. In Figure 5.10a, ACP moduli are more consistent when thickness is included in the inversion process with only 7% variability. Similar trends are observed for the base and subbase layer. The average moduli of the base were 67 ksi (without thickness estimation) and 73 ksi (with thickness estimation). For the subbase, the average moduli were similar and about 38 ksi for both cases. The subgrade moduli were not only consistent for the two cases but also across the site. The average was 16 ksi with a COV of 18% for both cases.

Layer thicknesses measured with the GPR and calculated with JIM and SMART (SASW analysis) are compared in Figure 5.11. The ACP thickness from JIM, SMART and GPR were very similar and close to the nominal thickness of 2 in. Even though GPR, SMART and JIM show large variability from the nominal thickness, the GPR thickness is more consistent and closer to the nominal thickness of the base. One possible explanation of the difference is the nature of test methods. GPR layer thickness is obtained based on the dielectric properties of the

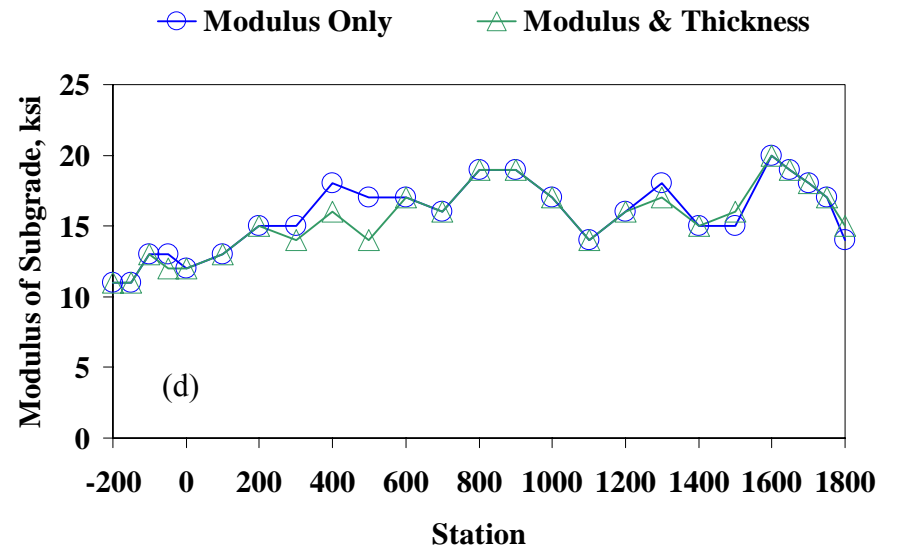
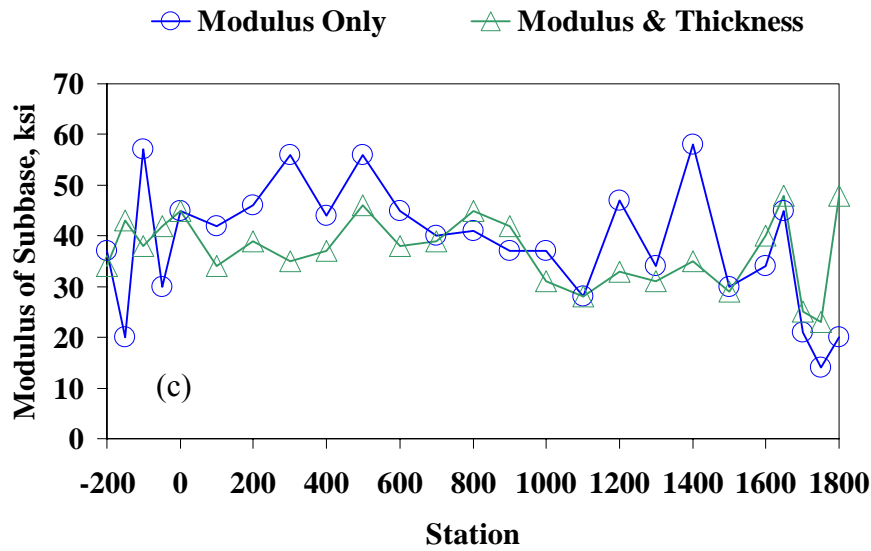
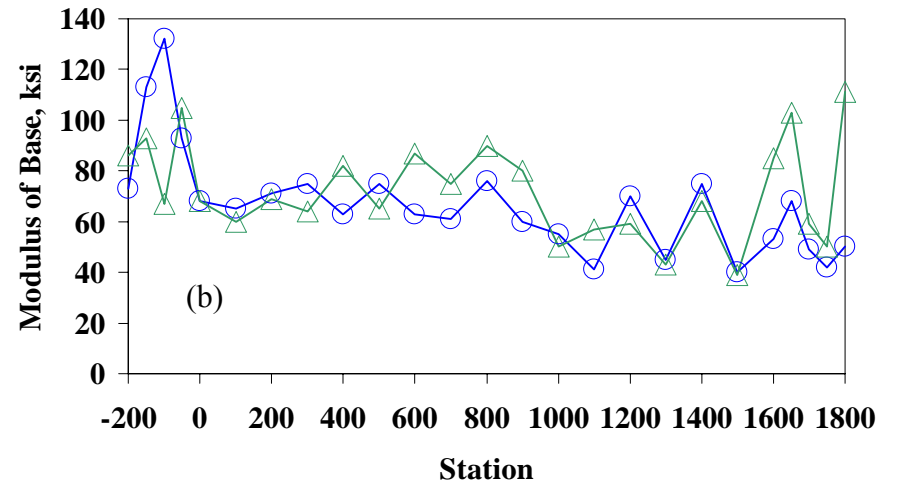
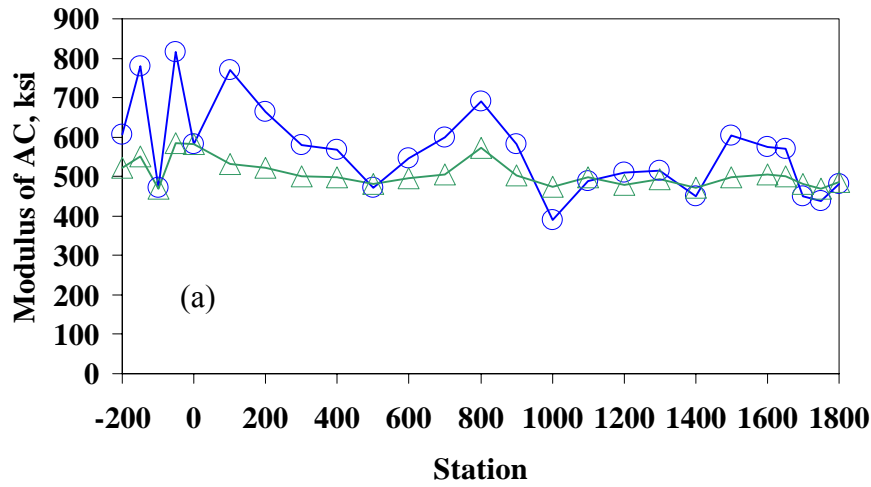


Figure 5.10 - Variation in moduli of pavement layers from JIM at the Ride Rut facility

layers; as such it is primarily impacted by the differences in the geological sources of the materials. The GPR can distinguish the interface between the granular base and clay materials. On the other hand, JIM and SMART rely on mechanical differences in the properties of different layers. Therefore, they estimate the boundaries where the moduli of two adjacent layers are different. Since the moduli of the base and subbase are similar, and since the base was placed in two lifts, it seems that JIM and SMART thicknesses are converging to the thickness of the top base layer.

GPR was not able to identify the bottom of the subbase layer because either the dielectric properties of the base and subgrade were similar or because the interface of the subbase and subgrade were too deep for the GPR antenna used. The subbase thicknesses from JIM and SMART, as shown in Figure 5.11, are greater than the nominal thicknesses. However, the combined thicknesses of the base and subbase correspond reasonably well with those reported as constructed. Once again, this occurs because both JIM and SMART estimate the thicknesses based on the contrast in stiffness. The total thickness of base and subbase from JIM is fairly close to that obtained from SMART.

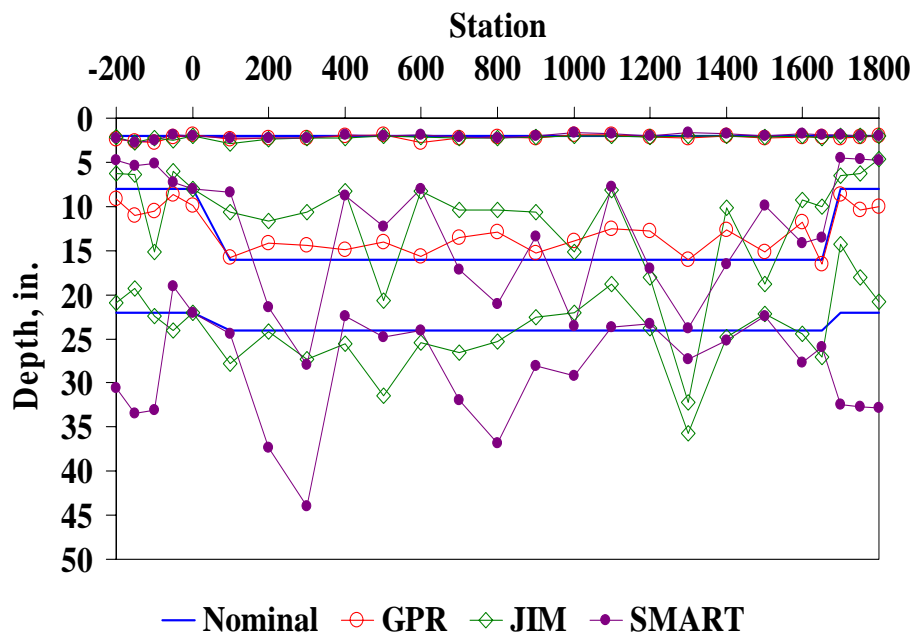


Figure 5.11 - Variations in layer thicknesses from JIM and SMART at the Ride Rut facility

Comparison of Results from Different Analyses

Moduli of different layers obtained from SMART, MODULUS, and JIM are compared in Figure 5.12. Moduli of the ACP from SMART and JIM, as shown in Figure 5.12a, are consistent across the site with average values of 590 ksi (COV of 17%) and 568 ksi (COV 16%), respectively. As indicated before, a modulus of 500 ksi was assumed in MODULUS analysis.

For the base, moduli from MODULUS, JIM, and SMART seem to follow the same trend, as reflected in Figure 5.12b. Moduli from SMART and JIM are similar and lower than those from MODULUS since the conservative values from JIM and SMART were used. The base moduli

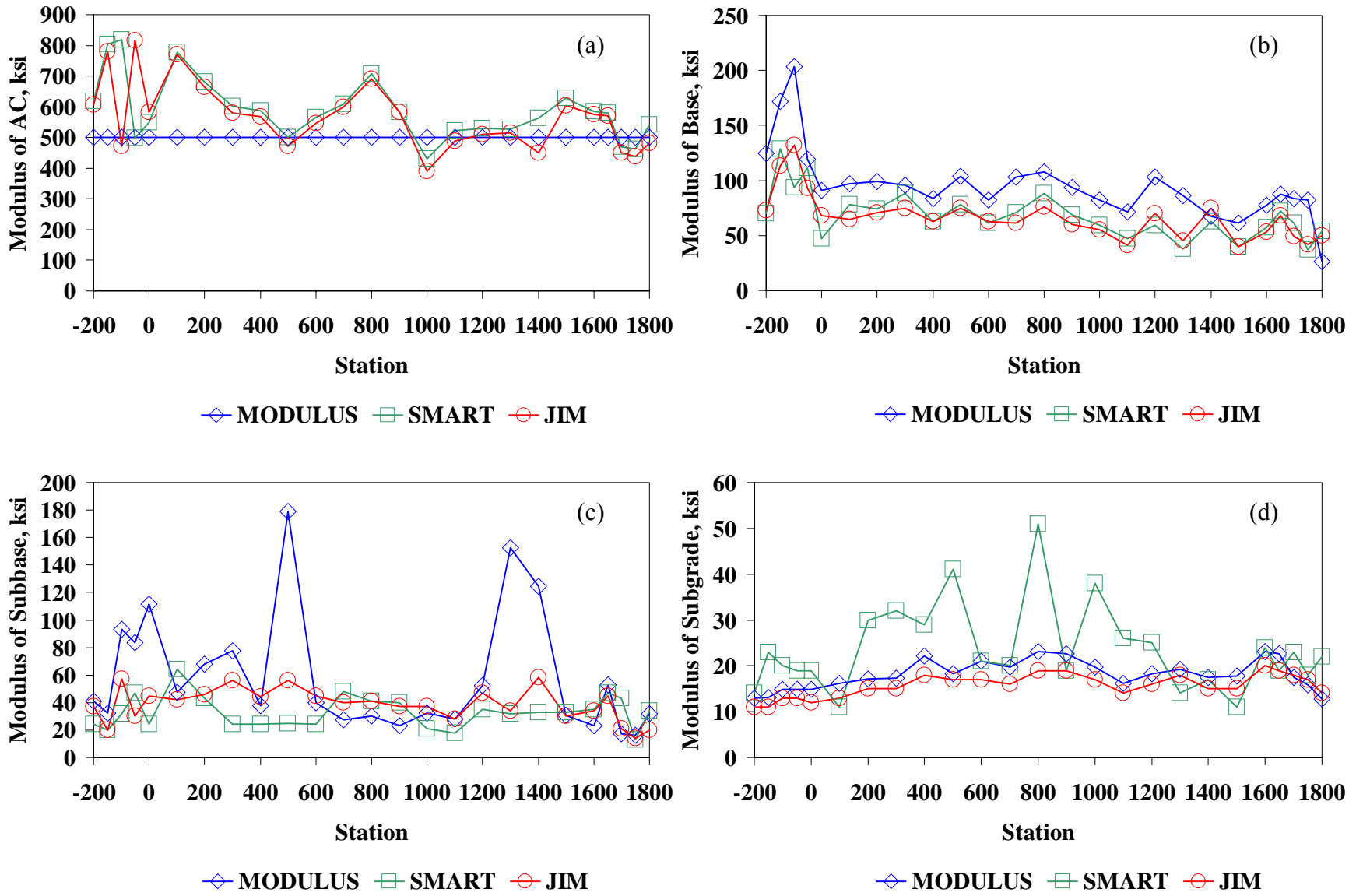


Figure 5.12 - Comparison of moduli obtained from MODULUS, SMART and JIM at the Ride Rut facility

are on the average 96 ksi from MODULUS, 68 ksi from SMART, and 67 ksi from JIM. The COV was close to 35% for all methods. This indicates that SASW method is controlling the modulus of the base.

For the subbase and subgrade results from JIM are fairly consistent throughout the entire site. SMART and JIM provide similar moduli for subbase layer with average values of 33 ksi for SMART and 39 ksi for JIM. MODULUS results are consistent in some areas, but for several points along the site the results are erratic with modulus values close to the base modulus (see Figure 5.12c).

Subgrade moduli from SMART, with an average of 23 ksi, in most cases are greater than those from Jim and FWD. JIM and FWD yield similar trends with average values of 16 ksi and 18 ksi, respectively. The current configuration of SPA allows the estimation of moduli down to a depth of 4 ft to 5 ft. As such, the subgrade moduli from SMART correspond to a thickness of about 2 to 3ft. FWD provides subgrade moduli to much deeper depths than SPA. For this specific site, this may explain the differences between the two analyses. The outcome of JIM for subgrade is clearly controlled by the FWD deflections.

The RMS errors associated with deflection basin mismatch from FWD, JIM and SMART are shown in Figure 5.13. The RMS errors are small for MODULUS and JIM (less than 5%). However, the RMS errors from SMART are much greater. The big RMS errors can be attributed to the differences in the estimated modulus of the subgrade. Again, SMART subgrade moduli are greater because they correspond to the first 2 ft of subgrade which is much stronger at this site.

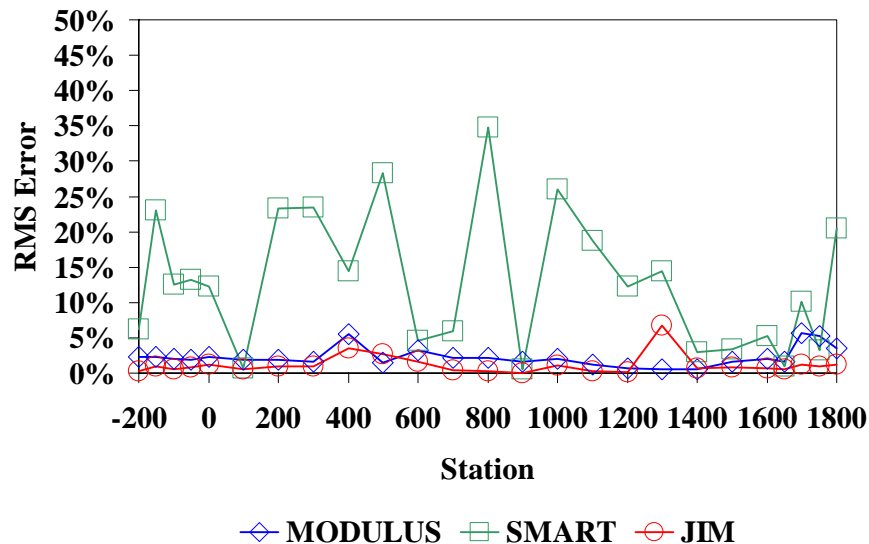


Figure 5.13 - Comparison of deflection basin mismatches at the Ride Rut facility

In general, JIM seems to be the most stable analysis when compared to SMART and MODULUS. It seems that the combination of FWD deflections and SPA dispersion curve into a joint inversion algorithm is advantageous and valuable in determining pavement properties, especially layer moduli.

Sequential Analyses

As part of the feasibility study for integrating NDT data, a sequential analysis was also performed. Parameters that can reliably be obtained with GPR and/or SPA/PSPA are assumed as fixed a priori information in MODULUS to reduce input uncertainty and improve results. Backcalculation process was performed with: a) FWD deflection data only, b) incorporating GPR thickness with FWD deflections, c) incorporating PSPA modulus with FWD deflections, and d) incorporate both GPR thickness and PSPA modulus with FWD deflections.

As shown in Figure 5.14, the moduli from the four studies are quite similar. This is not an ideal site for this exercise because the layer thicknesses are close to the nominal ones, and since the modulus of the AC layer is fortuitously close to 500 ksi typically assumed in MODULUS. Never the less the exercise was carried out to demonstrate this method. Further cases will be analyzed and investigated to determine the full potential of sequential integration.

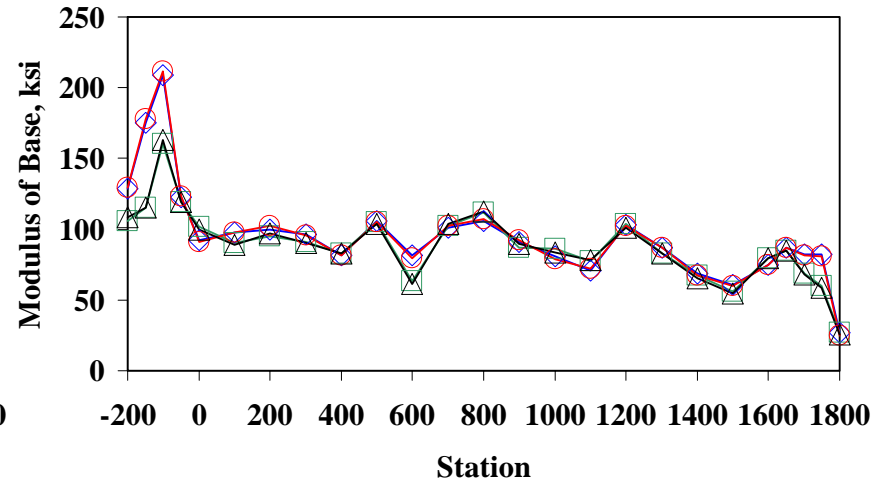
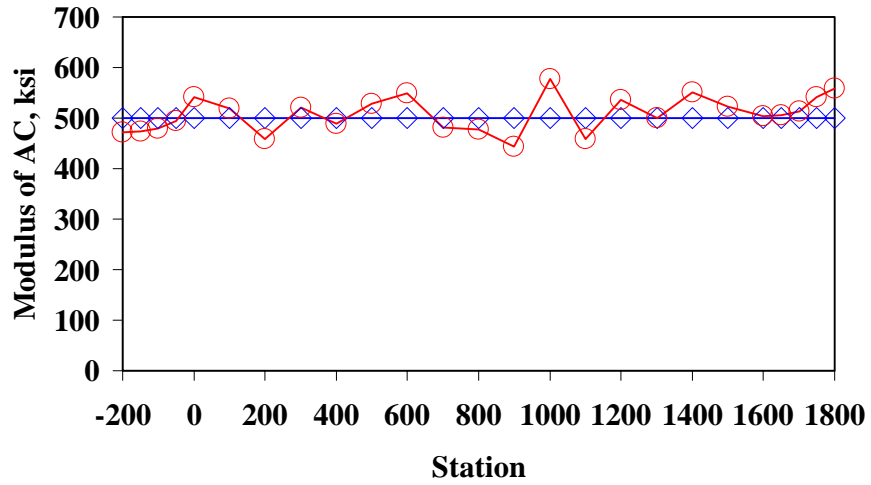
Summary of Study

Nondestructive testing (NDT) methods are typically used to measure the variations in the modulus of different pavement layers. Several NDT devices such as the FWD, the SPA, the PSPA and GPR are currently used for this purpose. Each of these devices has its strengths and shortcomings. The major objective of this study is to develop algorithms that combine the information for these devices and analyze the data jointly.

The results from the two case studies have shown the advantages of data integration. The results have also provided an indication of where to focus research efforts in the project. Several alternatives have proven viable and will be pursued further.

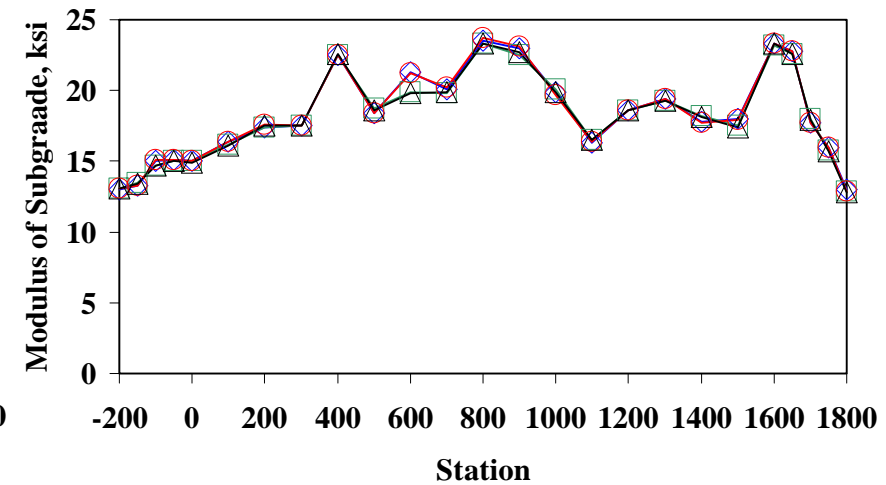
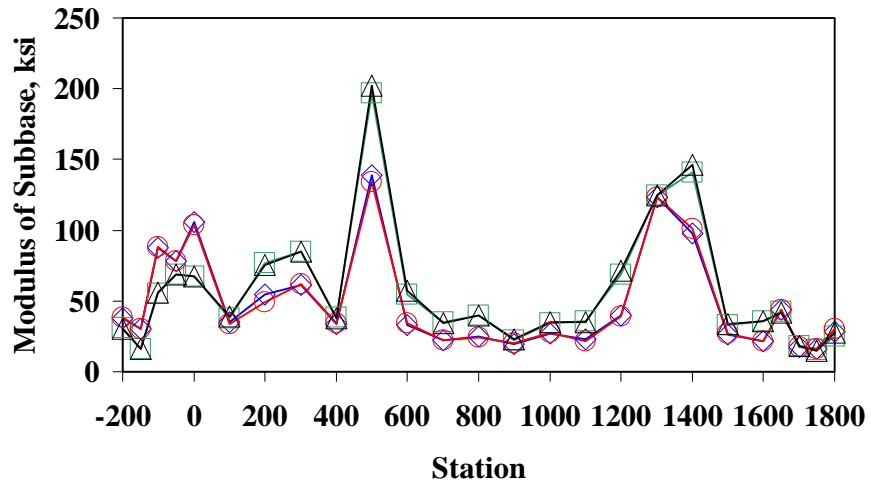
The results of JIM for both sites were very reasonable and comparable to both FWD analysis and seismic analysis. In many instances the results from JIM were more stable than the results of the other analyses.

Data from several other sites in Texas have been gathered and are currently being analyzed. The results of the analyses will be included in the final report. Also the algorithm of JIM is complete and is currently being incorporated into a graphical interface. The processing speed of the JIM is being optimized. The software will allow users to easily retrieve data from the various NDT devices using their current formats. The software will have the capabilities for users to easily match and arrange data for each station. It also will have the flexibility to ignore data from the analyses process based on user's digression.



◆ FWD Only ○ With PSPA

◆ FWD Only □ With GPR ○ With PSPA △ With Both



◆ FWD Only □ With GPR ○ With PSPA △ With Both ◆ FWD Only □ With GPR ○ With PSPA △ With Both

Figure 5.14 - Comparison of moduli from MODULUS based on sequential analysis algorithms at the Ride Rut facility

Chapter 6

Work Plan for Implementing Integration Algorithms

The first phase of this project was to determine the feasibility of data integration. As presented in Chapter 5, data integration based on the NDT equipment available to TxDOT is feasible. The combination of NDT data provides more credibility to the data and provides pavement engineers better means to assess the condition of pavement sections. The research effort here was focused on using the following NDT devices: FWD, GPR, SPA, and PSPA.

The integration techniques proposed by the research team based on the studies performed and discussions carried out with the project management committee are summarized in Figure 6.1. Two analysis tools, MODULUS and SMART are currently used by TxDOT. These two tools are included in the figure to help explain the overall process involved in the development of the data integration tools. The third algorithm shown in the figure is JIM where data from FWD and SPA are used together in an inversion algorithm. The last three processes are all based on sequential integration. Algorithm 4 uses MODULUS for the analysis however the input is not just the FWD deflection, but could also include layer thickness from GPR and moduli from the PSPA/SPA. The fifth algorithm would incorporate layer thickness profiles from GPR into the analysis of SMART. This would be useful in cases where the seismic inversion is only performed to obtain the modulus profile. The final algorithm listed in the figure combines sequential integration with the joint inversion. Layer thickness from GPR and/or modulus of AC layer could be incorporated into the analysis before processing the joint inversion algorithm. These are the set of algorithms that were selected to possibly develop and combine into an integration algorithm.

The flowchart in Figure 6.2 outlines the over proposed plan for data integration under this project. First a test protocol will be established and modified as more sites are visited and more data is collected using the different NDT devices. The test protocol that will be developed will focus on two areas: a) sequence of data collection and b) data alignment from different NDT devices. The test protocol is crucial in the success of the algorithm that will be developed to preprocess NDT data.

Based on the protocol developed, a preprocessing center will be formulated. Preprocessing, simply implies a way to manage data from various NDT devices and ensuring the arrangement of

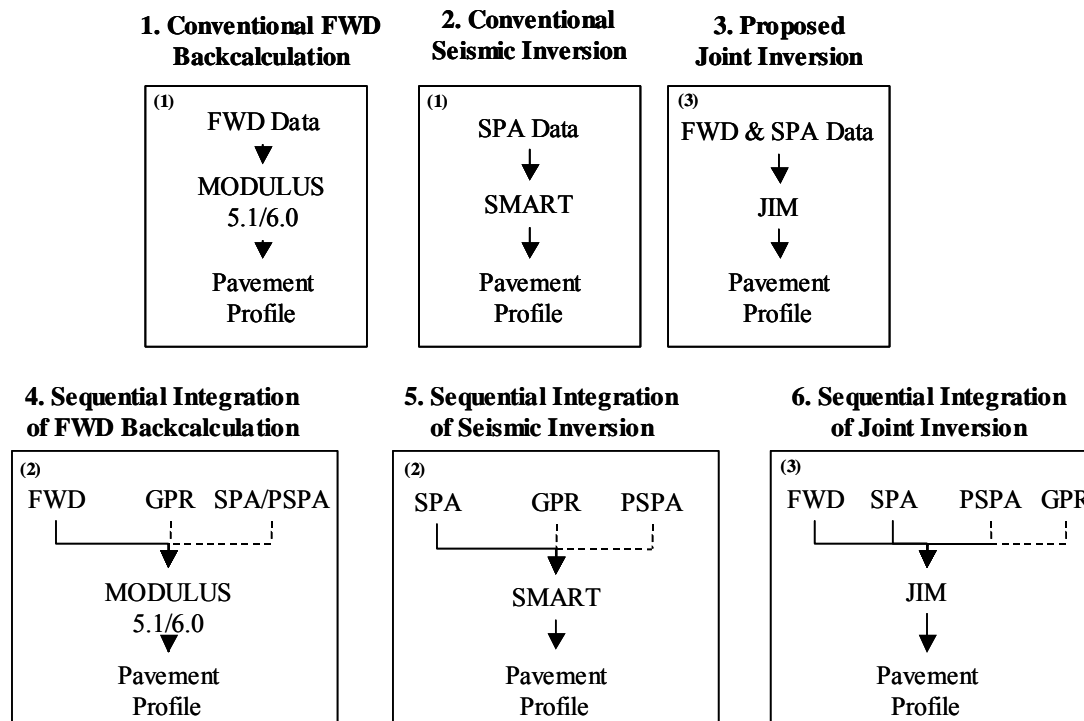


Figure 6.1 - Framework of the proposed integration algorithm

that data to allow for the use of analyses algorithms. After preprocessing is performed, the next step is to provide user with analysis options. Selection of the different analysis algorithms will be based on several factors. One factor depends on the type of data collected. Another factor will be the quality/quantity of data collected. These two factors will be built in and thereby automated in the process. The final factor is based on user selection. Even though several analyses algorithms are available for selection, user still has the final selection on which analyses to consider.

The next step in the figure is the analysis center. This is performed in the background with no user interaction. The results from the analysis will be further processed in a fusion center. The fusion center will require user interaction. The interaction will be limited to the various fusion options that will be developed.

Fusion of the results was briefly introduced in Chapter 2. Several alternatives of fusion methods were investigated. The results were purposely not included in this report so as to not confuse the integration analysis algorithms being developed, (sequential integration, JIM) with the fusion techniques. Fusion uses as input results of the analyses to determine the most representative results.

A separate report will be provided that includes detail information on concepts of data fusion and the applicability of fusion to NDT results of pavement analyses. The report will include several examples of applying data fusion and fused values from the results of the different analyses presented in Chapter 5 of this report.

Finally, the results module (shown in Figure 6.2) will provide the representative pavement stiffness profile. The dashed-box enclosure shows the sections of this proposed integration scheme that will be incorporated into a software tool.

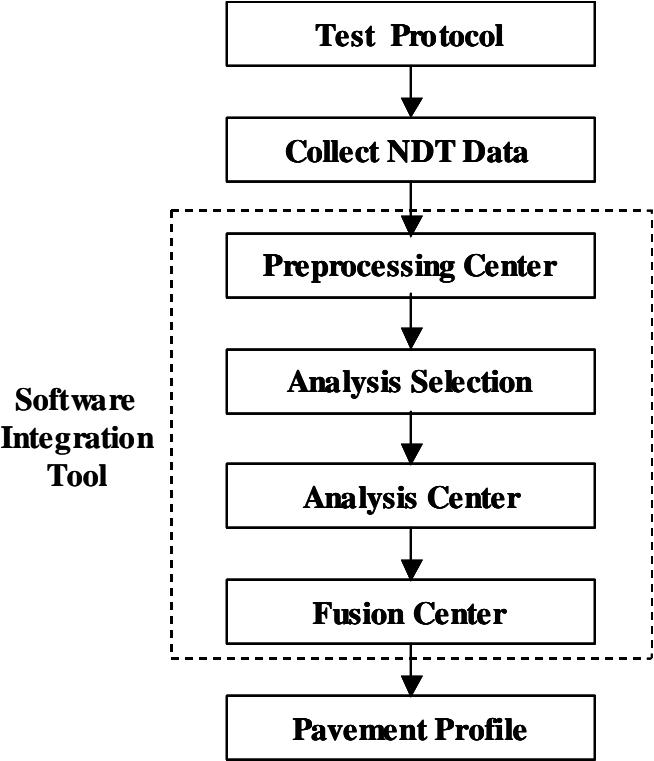


Figure 6.2 - Flowchart of proposed software integration tools

References

Abdallah, I., and Nazarian, S., (2003), "Determination of Nonlinear Parameters of Flexible Pavement Layers from Nondestructive Testing," Research Report 1780-4, Center for Highway Materials Research, the University of Texas at El Paso, TX

Abdallah, I., Nazarian, S. and Yuan, D., (2001), "Integrating Seismic and Deflection Methods to Estimate Pavement Moduli," Journal of Transportation Research Record No. 1755, Washington D.C., pp. 43-50

Abdallah, I., Yuan, D. and Nazarian, S., (2003), "Validation of Software Developed for Determining Design Modulus from Seismic Testing," Research Report 1780-5, Center for Highway Materials Research, the University of Texas at El Paso, TX

Aouad, M. F., Stokoe, K. H., and Briggs, R. C., (1993), "Stiffness of Asphalt Concrete Surface Layer from Stress Wave Measurements," Transportation Research Record 1384, Washington, D.C., pp. 29-35.

Baker, M. R., Crain, K., and Nazarian, S. (1995), "Determination of Pavement Thickness with a New Ultrasonic Device," Research Report 1966-1, Center for Highway Materials Research, The University of Texas at El Paso, Texas.

Barksdale, R. D., Alba, J., Khosla, P. N., Kim, R., Lambe, P. C. and Rahman, M. S., (1997), "Laboratory Determination of Resilient Modulus for Flexible Pavement Design," NCHRP Web Document 14, Federal Highway Administration, Washington, D.C., 486p.

Bush A. J. (1980), "Development of the Nondestructive Testing for Light Aircraft Pavements," Phase I, Evaluation of NDT Device Report No. FAA-RD-80-9, Washington, D.C.

Dobroka, M., Gyulai, A., Ormos, T., Csokas, J. and Dresen, L., (1991), "Joint Inversion of Seismic and Geoelectric Data Recorded in an Underground Coal Mine," Geophysical Prospecting, v. 39 n5, pp. 643-665

Ferry, J.D, (1970), "Viscoelastic Properties of Polymers," 2nd edition, John Willy, New York.

Georgeson, G.E., Lempriere, B.M. and Shrader, J. E., (1989), "Integrated Nondestructive Evaluation Data Reduction System (INDERS)", Joint Army Navy NASA Air Force (JANNAF), Silver Springs, MD.

Hering, A., Misiek, R., Gyulai, A., Ormos, T., Dobroka, M. and Dresen, L., (1995), "Joint Inversion Algorithm to Process Geoelectric and Surface Wave Seismic DATA. Part I: Basic Ideas," *Geophysical Prospecting*, v. 43 n2, pp. 135-156

Ke, L., Nazarian, S., Abdallah, I., and Yuan, D., (2002), "A Sensitivity Study of Parameters Involved in Design with Seismic Moduli," Research Report 1780-2, Center for Highway Materials Research, the University of Texas at El Paso.

Li, Y. and Nazarian, S., (1994), "Evaluation of Aging of Hot-Mix Asphalt Using Wave Propagation Techniques," *Proceedings, Engineering Properties of Asphalt Mixtures And the Relationship to Their Performance*, ASTM STP 1265, Philadelphia, PA, pp.166-179.

Lytton R. L., Roberts, R. L., and Stoffels, S., (1985), "Determination of Asphaltic Concrete Pavement Structural Properties by Nondestructive Testing," NCHRP Report No. 10-27, Texas A & M University, College Station, Texas.

Mirza, M. W., and Witzcak, M.W., (1995), "Development of a Global Aging System for Short and Long Term Aging of Asphalt Cements," *Journal of Association of Asphalt Paving Technologies*, Volume 64, Association of Asphalt Paving Technologies, St Paul, Minnesota, pp. 393-430.

Misiek, R., Leibig, A., Gyulai, A., Ormos, T., Dobroka, M. and Dresen, L., (1997), "Joint Inversion Algorithm to Process Geoelectric and Surface Wave Seismic DATA. Part II: Applications," *Geophysical Prospecting*, v. 45 n1, pp. 65-85

Nazarian, S. and Desai, M. R. (1993), "Automated Surface Wave Method: Field Testing," *Journal of Geotechnical Engineering Division, ASCE*, Vol. 119, No. GT7, New York, NY, pp. 1094-1111.

Nazarian, S., Baker, M., and Crain, K. (1997), "Assessing Quality of Concrete with Wave Propagation Techniques," *Materials Journal*, American Concrete Institute, Farmington Hills, MI, Vol. 94, No. 4, pp. 296-306.

Nazarian, S., Yuan D. and Baker M. R. (1995), "Rapid Determination of Pavement Moduli with Spectral-Analysis-of-Surface-Waves Method," Research Report 1243-1F, Center for Geotechnical and Highway Materials Research, The University of Texas at El Paso, El Paso, TX, 76 p.

Nelson, J.M, Bossi, R.H. and Lancaster, C.A., (1997), "NDE Data Fusion Final Report", Boeing Document No. D658-10844-1, Seattle, WA.

Nelson, J.M., Cruikshank, D. W., and Galt, S., (1989), "A Flexible Methodology for Analysis of Multiple-Modality NDE Data", Review of Progress in Quantitative Nondestructive Evaluation, pp. 819-826.

Osegueda, R.A., Lopez, H., Pereyra, L. and Ferregut, C.M., (2000), "Localization of Damage Using Fusion of Modal Strain Energy Differences," Proc. of International Modal Analysis Conference XVIII, SEM, Vol. I, San Antonio, TX, Feb. 7-10, pp. 695-701.

Saarenketo, T. and Scullion, T., (1994), "*Ground Penetrating Radar Applications on Roads and Highways*," TTI Report 1923-2F, College Station, TX.

Scullion, T., Servos, S., Ragsdale, J. and Saarenketo, T., (1997), "*Applications of Ground-Coupled GPR to Pavement Evaluation*," TTI Report 2947-S, College Station, TX.

Sivaneswaran, N., Pierce, L. M., and Mahoney, J. P., (1999), EVERCALC 5.0, Washington State Department of Transportation. Web page

Uddin W., and McCullough, B. F. (1989), "In Situ Material Properties from Dynamic Deflection Equipment," Nondestructive Testing of Pavements and Backcalculation of Moduli, ASTM, STP 1026, Philadelphia.

Uzan J., and Lytton, R. L., (1990), "Analysis of Pressure Distribution Under Falling Weight Deflectometer Loading," Journal of Transportation Engineering, ASCE, Vol. 116, No. 2, New York, NY, pp. 246-251.

Vozoff, K. and Jupp, D.L.B., (1975), "Joint Inversion of Geophysical Data," Geophys. J.R. ASTR. Soc., v. 42, pp. 977-991.

Witczak, M.W., Bonaquist, R., Von Quintus, H., and Kaloush, K.,(1999) "Specimen Geometry and Aggregate Size Effects in Uniaxial Compression and Constant Height Shear Tests," Journal of Association of Asphalt Paving Technologist, Volume 69, pp 733-793.

Wu H., (2001), "Feasibility of Artificial Neural Network Approach to Inversion of Spectral Analysis of Surface Waves Data for Pavement Structures," Masters of Science Thesis, The University of Texas at El Paso

Yuan D. and Nazarian, S., (1993), "Automated Surface Wave Testing: Inversion Technique," Journal of Geotechnical Engineering, ASCE, Vol. 119, No. GT7, New York, NY, pp. 1112-1126.

Appendix A
Sample Survey

**Pavement Analysis and Design in Texas
Survey Conducted by
The University of Texas at El Paso**

A. PURPOSE OF SURVEY

TXDOT project 4393 “Integration of Nondestructive Testing Data Analysis Techniques” is to develop a tool that will ultimately combine data from all the main nondestructive testing (NDT) devices used by TXDOT to better assess the condition of the pavement. To achieve this goal, the strengths and weaknesses of current processes for testing, analysis, and design with NDT devices need to be determined. The results of this survey should help the researchers of this project focus their efforts in identifying areas of improvement.

B. GENERAL INFORMATION

Name: _____

Title/Position: _____

E-mail: _____

TxDOT Office: _____

Phone No.: _____

Do you mind if we contact you? Yes No

If you do not mind, do you prefer E-Mail Phone

Are you involved with collecting, analyzing or using the results from NDT data?

Yes No

Are you involved with analysis or design of flexible pavements?

Yes No

(If the answer is “no” to both questions, please stop, make suggestion(s) of possible contact(s) and please fax this page back to us.)

Alternate Person(s): _____

Section Q1:Data Collection

Q1.1. Please select NDT devices that you have used for data collection?
 FWD GPR SPA PSPA None

Q1.2. Have you used the data collected with more than one of the NDT devices for the same project?
 Yes No

Please specify which have you used:

Q1.3. Are you satisfied with the current data collection process for;

FWD?	<input type="checkbox"/> Yes	<input type="checkbox"/> No	<input type="checkbox"/> No Opinion
GPR?	<input type="checkbox"/> Yes	<input type="checkbox"/> No	<input type="checkbox"/> No Opinion
SPA?	<input type="checkbox"/> Yes	<input type="checkbox"/> No	<input type="checkbox"/> No Opinion
PSPA?	<input type="checkbox"/> Yes	<input type="checkbox"/> No	<input type="checkbox"/> No Opinion

Q1.4. Based on your experience; do you have any recommendations that will improve the data collection process of any of the NDT devices?
 Yes No

What are your recommendations?

Section Q2:Data Analysis

Q2.1. For what type of project(s) have you performed analysis for flexible pavements using FWD data? (Check all that apply)
 New Reconstruction Repairs/Rehabilitations Other-Specify:




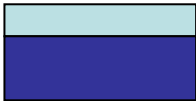
Q2.2. For what type of project(s) have you performed analysis for flexible pavements using GPR data? (Check all that apply)

- New
 Reconstruction
 Repairs/Rehabilitations
 Other-Specify:

Q2.3. For what type of project(s) have you performed analysis for flexible pavements using SPA or PSPA data? (Check all that apply)

- New
 Reconstruction
 Repairs/Rehabilitations
 Other-Specify:

Q2.4. Please select common types of flexible pavement structures in your district and specify typical material type for each layer.

<input type="checkbox"/> 	HMA _____ Base _____ Subgrade _____	<input type="checkbox"/> 	HMA _____ HMA _____ Base _____ Subgrade _____
<input type="checkbox"/> 	HMA _____ Base _____ Subbase _____ Subgrade _____	<input type="checkbox"/> 	HMA _____ Subgrade _____

Other(Specify)

Q2.5. Have you encountered any limitations in the current flexible pavement analysis programs?

- Yes
 No

if yes, please specify situations or cases where this occurred:

Q2.6. What source(s) of information do you use to provide the thickness of each layer in backcalculation?

Q2.7. What source(s) of information do you use to provide the initial minimum and maximum values of modulus for each layer in backcalculation?

Q2.8. What source(s) of information do you use to provide the Poisson's ratio of each layer in backcalculation?

Q2.9. In the case where the thickness of the AC layer is less than 3 in., what do you use for the minimum and maximum values of AC modulus in FWD data backcalculation?

Q2.10. Have you used GRP results in modulus backcalculation?

- Yes No

Q2.11. Have you used seismic results in FWD modulus backcalculation?

- Yes No

Q2.12. Based on your experience; do you have any recommendations you feel might improve the data analysis process?

- Yes No

What are your recommendations?

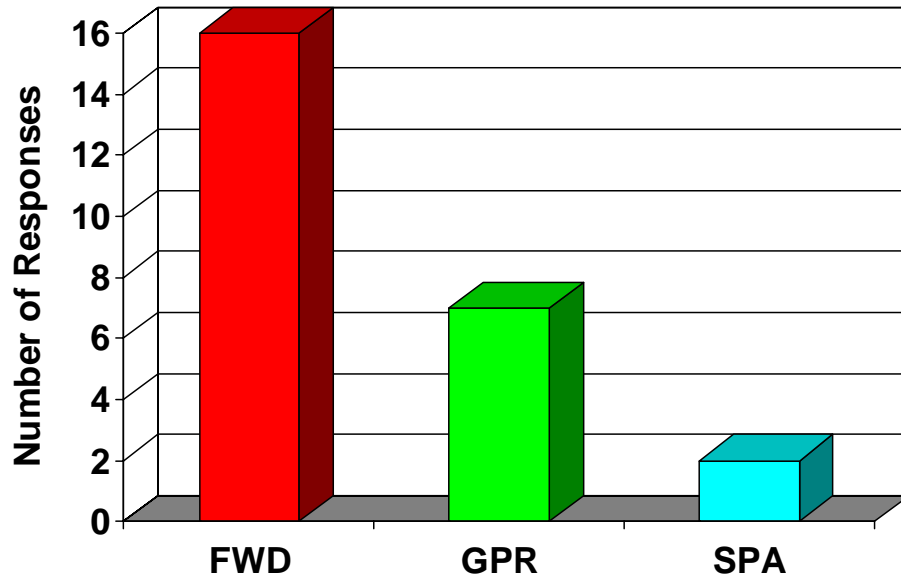
Q2.13. Can you identify any specific project(s) that you are not particularly happy with the results of the traditional stand alone analysis but you think that an integrated approach might help?

Yes No

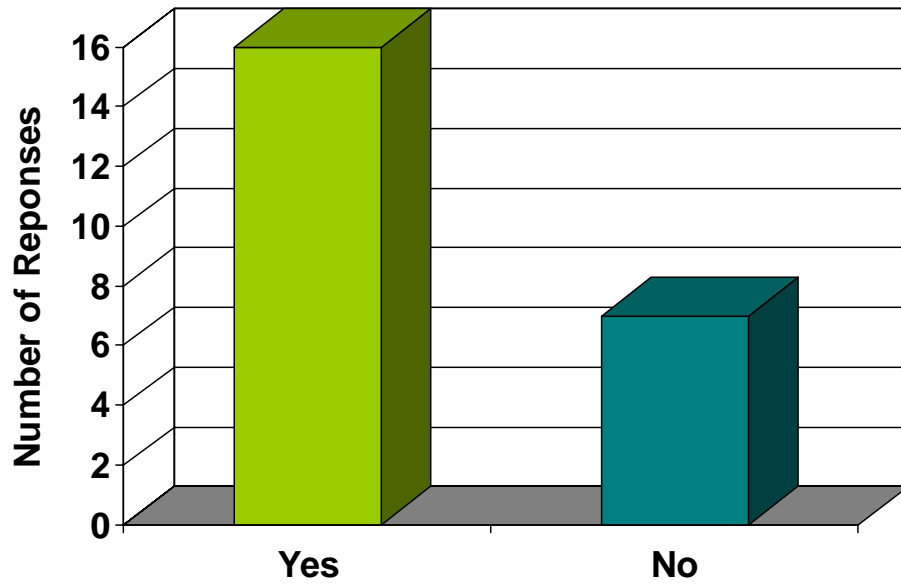
Could you specify the site(s) and provide information about them?

Appendix B
Results of Survey

Q1.1 - Please select NDT devices that you have used for data collection?

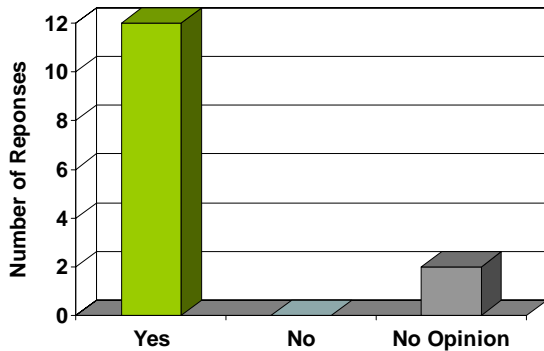


Q1.2 - Have you used the data collected with more than one of the NDT devices for the same project?

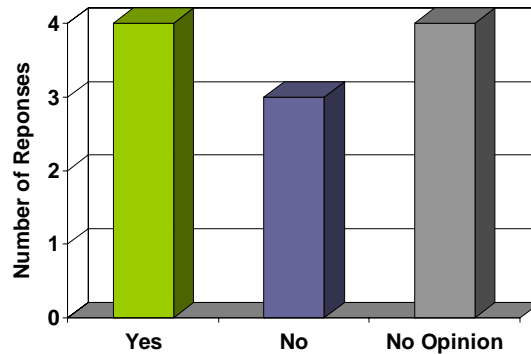


Q1.3 - Are you satisfied with the current data collection process for

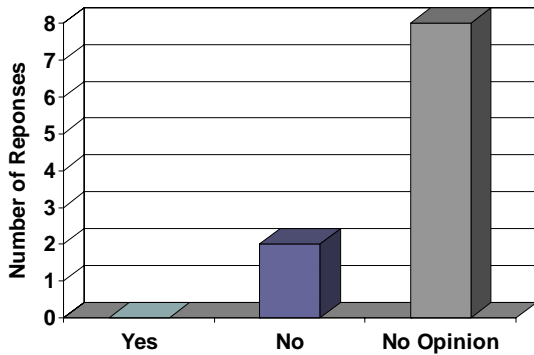
(a) FWD



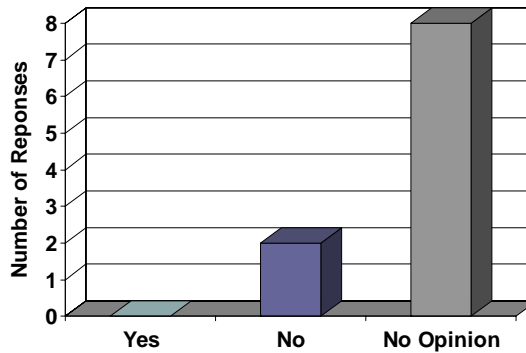
(b) GPR



(c) SPA



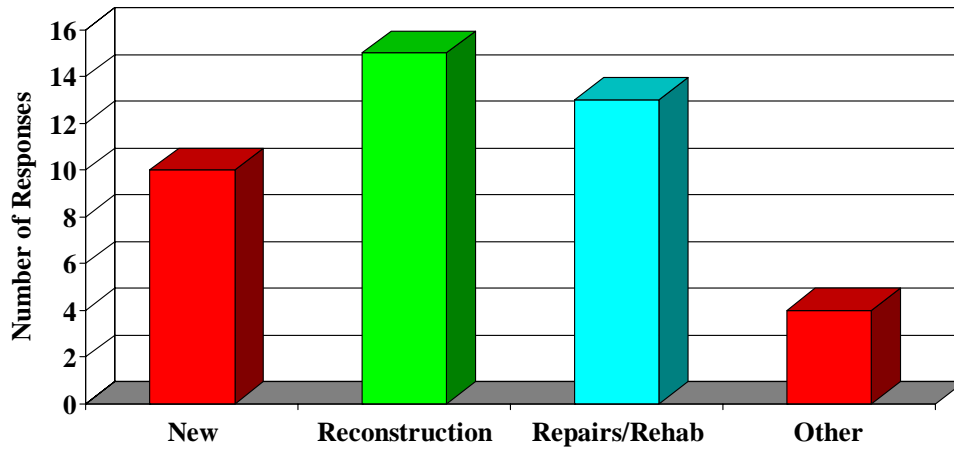
(d) PSPA



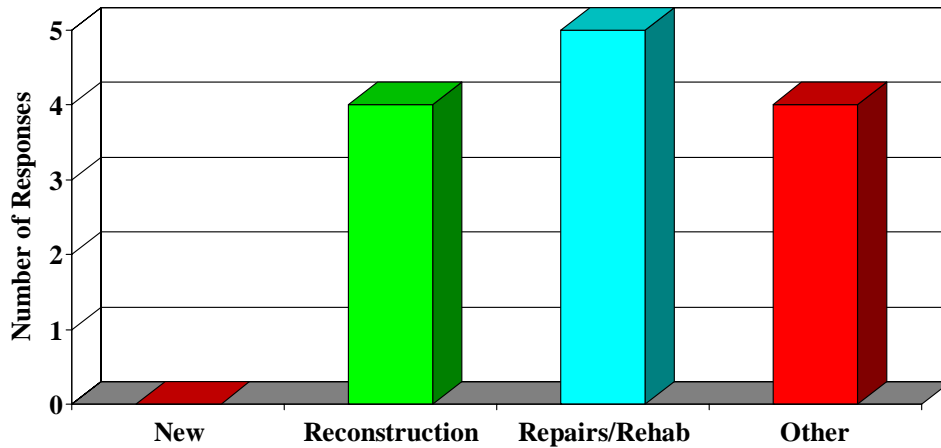
Q1.4 - Improve the data collection process of any of the NDT devices?

- GPR - for project level testing, collect data without the reference marker required input (just the DMI reading). Would like more test comments to be input into the file. For example, take the hand notes we currently collect and input so that it stays with the data file. Both GPR and FWD, be able to use GPS data that is currently collected with the data to tie the testing to project locations, perhaps generate a map of testing locations
- For the GPR, there needs to be an easier system for linking the video to the DMI. For the SPA and PSPA, the biggest problem is that there are too few of these devices in the inventory to ever develop confidence in their use.
- Combine all of them into one machine
- Design a more user-friendly operating program for use with the FWD.
- We would be interested in other methods in the future

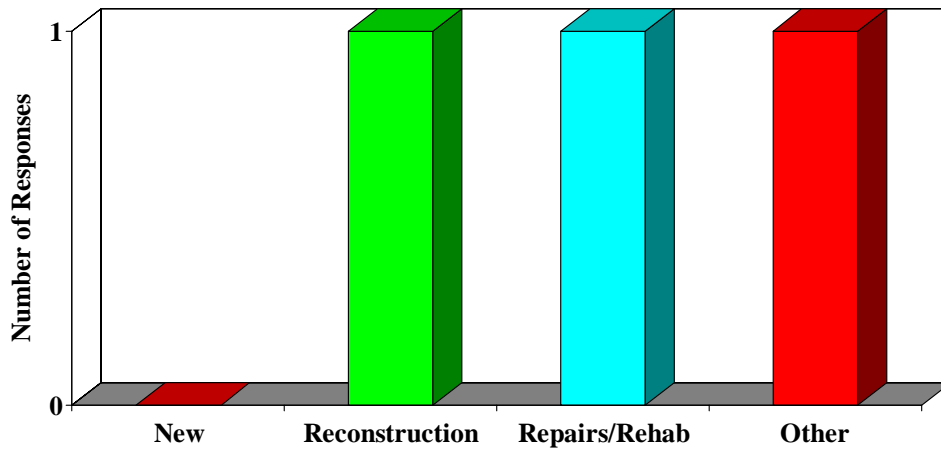
Q2.1 - Performed analysis for flexible pavements using FWD data



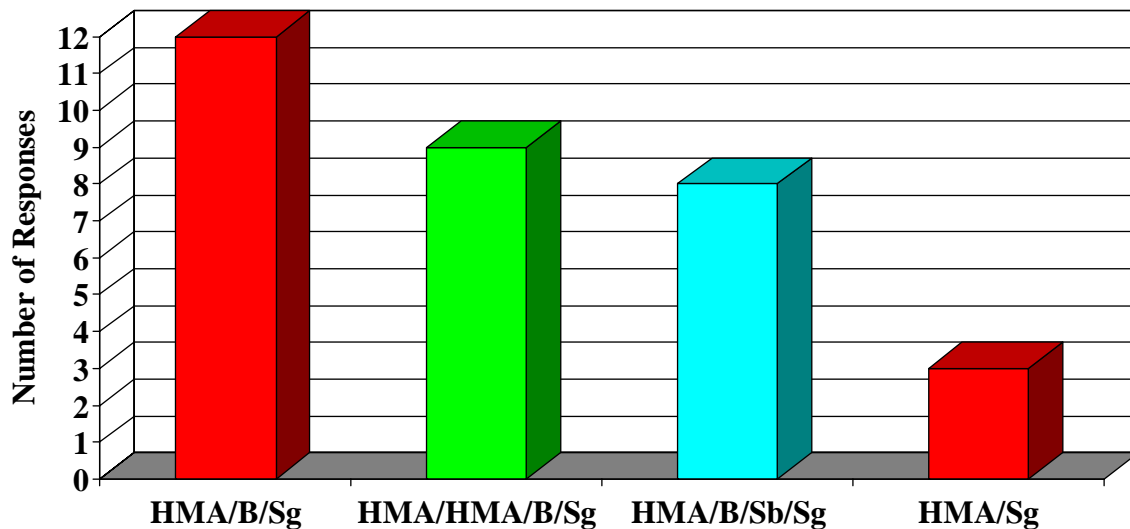
Q2.2 - Performed analysis for flexible pavements using GPR data



Q2.3 - Performed analysis for flexible pavements using SPA data



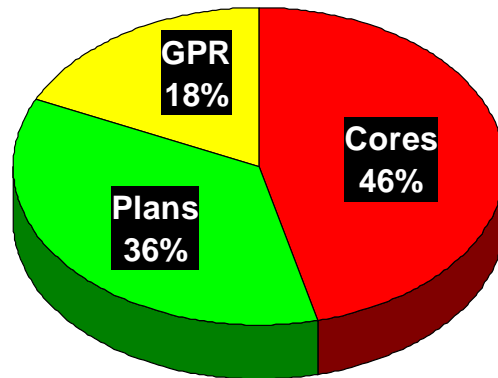
Q2.4 – Pavement Structure in Your District



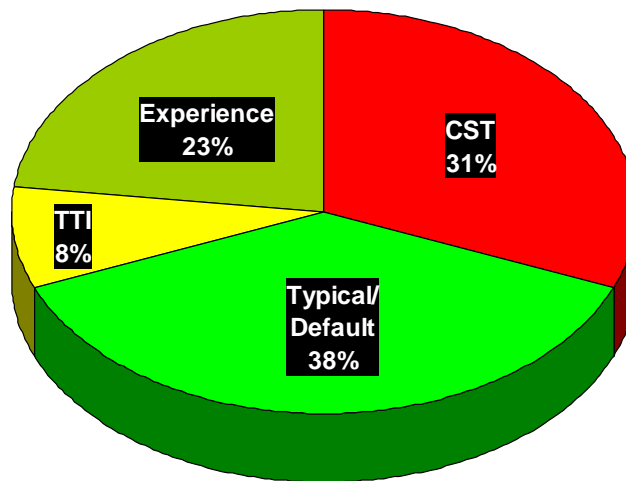
Q2.5 - Limitations in the current flexible pavement analysis programs?

- Can't see what you[re] doing. It's much like hydraulics, very analytical, not practical. We need something that will accurately tell us what need to be done to accurately add strength to our pavements.
- When using cement treated subbase, followed by flexible base and HMA surface.
- Overlay of concrete with HMAC
- FWD program required a lot of manual interpretation - to achieve proper results; perhaps the algorithms could be written in the program to make the adjustments and interpretation as necessary.
- When we have semi-rigid pavements. Such as cement treated base or thick hot mix. This usually occurs at an ESAL level of approximately 3 million, when there isn't enough justification for concrete pavement, however the flexible becomes very thick.
- Very user unfriendly
- MODULUS - ACP layer must be at least 3.0" thick. Shallow bedrock prevents reasonable solution when run under "default" program generated values. SPA - no user friendly analysis software. PSPA - new analysis software looks promising, but lack of familiarity with use because too few devices are available for routine use.
- Design of ACP overlays in general and specifically on top of concrete pavement. Design of Heavily Cement Stabilized Bases.
- Rehab - Number of Layers Exceeds Capability
- Cement stabilized situations - we are careful to not create too stiff a subgrade by using 3-4% cement max. The FPS-19W programs are limited by a max 100-150 ksi modulus or you will be beyond a flexible pavement situation.
- Analyzing pavements where we have used flyash treated salvage materials.

Q2.6 - What source(s) of information do you use to provide the thickness of each layer in backcalculation?



Q2.7 - Source for initial minimum and maximum values of modulus for each layer in backcalculation?



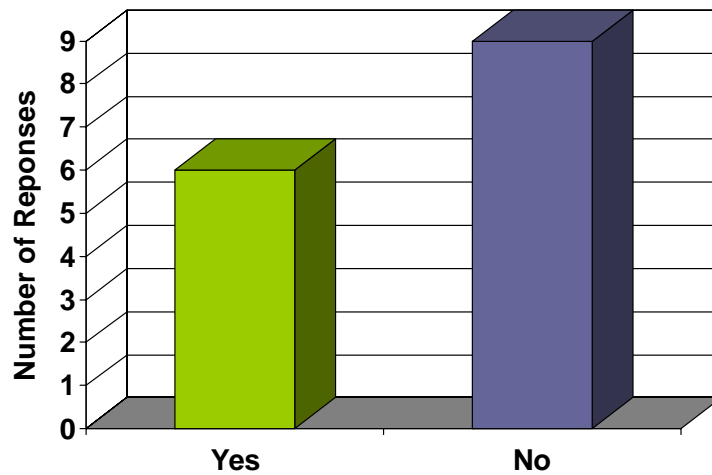
Q2.8 - Source for Poisson ratio of each layer in backcalculation?

- Experience
- General Guideline
- Not highly sensitive
- Select Rehabilitation for Flexible Pavements
- Pavement Sections / Construction Division
- Standard Charts
- Default Values
- Ranges Provided by TTI

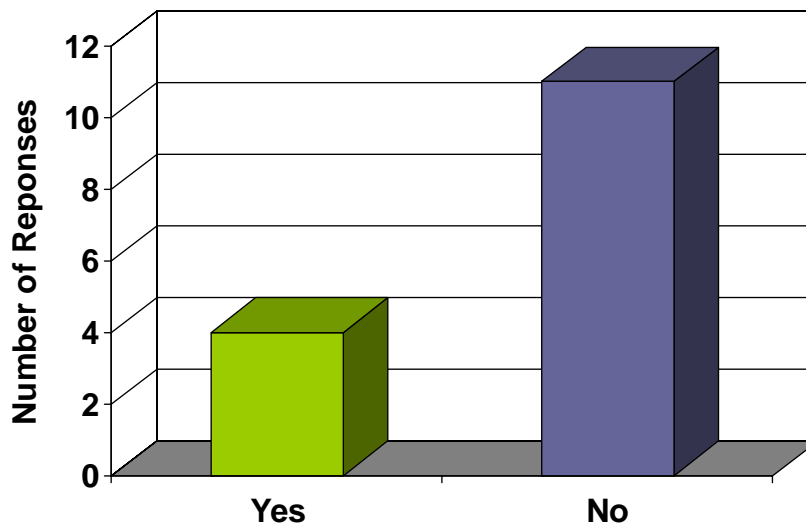
Q2.9 - In the case where the thickness of the AC layer is less than 3 in., what do you use for the minimum and maximum values of AC modulus in FWD data backcalculation?

- Depends on pavement temperature
- 250,000 psi for min & max
- 300-800,000 [psi]
- 500 [ksi] for both
- use default values
- min: 15,000 psi max: 500,000 psi
- 400,000 psi

Q2.10 - Have you used GPR results in modulus backcalculation?



Q2.11- Have you used Seismic results in FWD modulus backcalculation?



Q2.12 - Recommendations you feel might improve the data analysis process?

- The research I've read on GPR seems promising.
- I believe the process can be integrated to make it easier and more efficient to achieve pavement analysis and design.
- Something that will allow you to view the GPR, FWD and coring data in reference to each other.
- More user friendly program; program that can function of use all data relevant to a pavement design instead of the current process of using MOD 5.1 etc.
- Overcome shallow bedrock limitations in MODULUS. Overcome extreme variability in 4-layer solutions in backcalculation. With SPA, develop user-friendly analysis program. Increase population of SPA, PSPA.
- Using GPR & Seismic to determine & verify layer thicknesses. Plans are not usually accurate. Using adjusted seismic moduli as seed values for backcalculation. If backcalculating 4 layers or more one layer can be fixed with a modulus value adjusted determined from SPA.
- come up with easy an accurate method to determine layer thickness
- I would be interested in other options than what we are now doing to gain additional background to help make better pavement design decisions.

Q2.13 - Can you identify any specific project(s) where you are not particularly happy with the results of the traditional stand-alone analysis but you think an integrated approach might help?

- Any roadway currently under design in our District.
- No, but I think the approach should be integrated and I will start using it for routine analysis and design, if it is available
- Projects that the existing pavement thickness varies. Pavements that have a lot of patches.
- Forensic investigation, LP375 (Ft. Bliss), El Paso Co. 2.0" CMHB overlay, 1.5" Ty D HMAC, 12" flex base, shallow bedrock. Forensic investigation, IH 20, Ward Co. 1.0" plant mix seal, 3.0" Ty C HMAC, 4" new flex base, shallow bedrock
- I do not have a specific project, but the integrated approach will definitely help.
- The stand alone procedures give decent results. Integrating all of them will save money and provide pavement engineers with a tool to better analyze and manage their pavements
- Our current project on US380 in Garza county. We recently collected SPA/GPR data in November.

Appendix C

Results of Data Analysis Using SMART, MODULUS, and JIM for the Ride Rut facility

Table C.1 - Results of SASW data reduction process for the Ride Rut facility

Point	Inversion of Modulus Only				Inversion of Modulus and Thickness					
	Modulus, ksi			RMS Error	Thickness, in.		Modulus, ksi			RMS Error
	AC	Base	Sg.		AC	Base	AC	Base	Sg.	
1	2455	183	49	1.8	2.0	6.0	1989	251	28	1
2	1743	155	17	0.9	2.0	5.5	1877	179	27	1.1
3	1879	228	7	1.7	2.0	5.1	2143	148	35	2.2
4	1730	99	30	0.8	1.6	5.0	2276	146	34	1.4
5	1468	197	53	3.3	1.8	5.5	2184	138	30	1.1
6	1785	228	26	1.8	1.7	9.0	2117	305	24	1.6
7	1692	228	65	2.6	1.7	9.0	2187	352	23	1.3
8	1810	228	49	1.2	2.3	7.9	2222	303	21	3.7
9	2264	228	7	1.8	2.0	5.7	1991	334	20	1.8
10	2249	225	15	1.1	2.1	5.1	1763	199	26	0.8
11	1390	166	12	0.9	1.3	4.6	2002	147	25	1.5
12	1690	228	17	1.6	1.9	6.3	1907	282	20	0.8
13	1785	228	34	2	1.3	8.6	2089	287	19	1.1
14	1512	228	27	2.4	2.2	7.0	1706	170	19	0.9
15	1404	228	27	2	2.1	5.8	1736	265	27	0.9
16	1545	145	41	1.5	1.7	8.1	1691	229	23	0.8
17	1733	112	30	0.7	1.9	5.1	1682	142	28	0.8
18	1550	167	29	1.8	1.2	3.4	2260	331	25	1.7
19	1932	165	18	1.6	1.5	4.1	2525	296	19	1.3
20	1992	228	36	2.2	1.7	4.0	2201	327	30	1.3
Avg.	1780	195	30	1.7	1.8	6.0	2027	242	25	1.4
Std Dev.	274	41	15	0.6	0.3	1.6	222	72	5	0.6
COV	15%	21%	51%	37%	16%	27%	11%	30%	18%	47%

Table C.2 - Design moduli from SMART for the Ride Rut facility

Point	Modulus (ksi)								RMS
	Conservative				Average				
	AC	Base	Sb	Sg	AC	Base	Sb	Sg	
1	618	70	24	14	618	104	25	14	9%
2	803	129	20	23	803	168	21	24	15%
3	819	94	32	20	819	136	34	20	11%
4	497	111	47	19	497	133	52	20	4%
5	549	47	24	19	549	73	25	19	7%
6	778	78	64	11	778	105	65	12	3%
7	681	74	43	30	681	104	43	30	14%
8	602	88	24	32	602	118	25	32	8%
9	588	63	24	29	588	90	26	29	12%
10	500	78	25	41	500	108	27	41	13%
11	566	61	24	21	566	86	25	21	4%
12	610	71	48	20	610	97	49	20	4%
13	708	88	41	51	708	123	42	52	12%
14	583	69	40	19	583	98	41	19	0%
15	430	59	21	38	430	85	23	38	12%
16	523	47	18	26	523	69	19	26	11%
17	529	59	35	25	529	84	35	25	9%
18	528	38	32	14	528	40	33	14	15%
19	562	63	33	17	562	89	34	17	2%
20	629	40	33	11	629	49	34	11	4%
21	584	57	35	24	584	75	35	24	5%
22	580	72	47	19	580	102	48	20	0%
23	470	61	43	23	470	65	45	23	2%
24	461	37	13	18	461	54	13	18	7%
25	541	54	34	22	541	67	35	22	3%
Avg.	590	68	33	23	590	93	34	24	7%
Std. Dev.	100	21	12	9	100	29	12	9	5%
COV	17%	31%	35%	39%	17%	31%	34%	39%	62%

Table C.3 - Measured FWD field data normalized to 9000 lbs for the Ride Rut facility

Point	Deflections (mils)						
	Sensor Spacing						
	0 in.	12 in.	24 in.	36 in.	48 in.	60 in.	72 in.
1	16.7	10.7	6.6	4.3	3.4	2.6	2.1
2	15.9	10.8	6.6	4.2	3.4	2.5	2.1
3	11.7	8.0	5.4	3.7	3.1	2.3	1.9
4	13.8	8.5	5.6	3.7	3.1	2.3	1.9
5	14.2	8.4	5.5	3.7	3.1	2.4	2.0
6	12.7	7.5	4.7	3.3	2.8	2.2	1.8
7	11.8	6.9	4.2	3.0	2.6	2.1	1.7
8	11.9	6.7	4.2	3.0	2.6	2.0	1.7
9	12.3	7.1	3.4	2.4	2.2	1.8	1.5
10	10.4	5.6	3.7	2.7	2.5	2.0	1.7
11	12.7	6.7	3.8	2.6	2.2	1.7	1.5
12	12.2	7.0	4.2	2.8	2.4	1.8	1.4
13	11.2	6.4	3.6	2.4	2.0	1.6	1.2
14	12.5	6.7	3.9	2.6	2.0	1.5	1.2
15	13.4	7.0	4.3	2.8	2.3	1.7	1.4
16	15.5	8.5	5.1	3.5	2.8	2.1	1.7
17	11.8	6.5	4.3	3.0	2.5	1.8	1.4
18	11.4	5.7	3.6	2.7	2.4	1.8	1.5
19	13.4	6.5	4.1	2.9	2.6	2.0	1.5
20	15.9	8.1	4.6	3.0	2.6	1.9	1.5
21	13.4	6.9	3.7	2.5	2.0	1.5	1.2
22	11.8	5.9	3.6	2.5	2.0	1.5	1.2
23	18.9	10.3	4.8	2.8	2.0	1.5	1.2
24	20.1	11.1	5.4	3.0	2.2	1.6	1.3
25	27.71	12.43	5.92	3.7	2.76	1.95	1.56
Mean	14.1	7.8	4.6	3.1	2.5	1.9	1.6
Std. Dev.	3.6	1.8	0.9	0.5	0.4	0.3	0.3
C.V.	26%	23%	20%	17%	17%	17%	17%

Table C.4 - Results of backcalculated design modulus values for the Ride Rut facility

Point	Modulus (ksi) using MODULUS				RMS
	AC	BASE	Subbase	SUBGRADE	
1	500	124.4	40.8	12.9	2%
2	500	171.9	32.2	13.1	2%
3	500	203.5	93.5	14.8	2%
4	500	119.4	83.5	14.9	2%
5	500	90.8	111.5	14.8	2%
6	500	97.1	47.2	16.1	2%
7	500	99.3	68	17.2	2%
8	500	95.5	77.6	17.3	2%
9	500	83.6	38	22.1	6%
10	500	104	179.1	18.2	1%
11	500	82.3	39.7	21.1	3%
12	500	103	27.7	19.8	2%
13	500	107.5	30.3	23.2	2%
14	500	93.4	23	22.6	2%
15	500	81.9	32.4	19.7	2%
16	500	71.4	27.9	16.1	1%
17	500	103.1	52.4	18.3	1%
18	500	86	152.4	19.2	1%
19	500	67.7	124.3	17.5	1%
20	500	61.1	30.6	17.8	2%
21	500	77.4	23.3	23.2	2%
22	500	87.6	52.9	22.6	2%
23	500	83.5	17.5	17.5	6%
24	500	82.4	16.3	15.8	5%
25	500	26	31.7	12.7	4%
Avg.	500	96	58	18	2%
Std. Dev.	0	31	43	3	1%
COV	0%	32%	74%	17%	53%

Table C.5 - Design moduli from JIM for the Ride Rut facility

Point	Modulus (ksi)								RMS
	Conservative				Average				
	AC	Bas	Sb	Sg	AC	Base	Sb	Sg	
1	605	59	29	14	605	93	32	14	5%
2	790	105	19	14	790	139	20	14	5%
3	481	96	42	17	481	135	47	17	6%
4	786	106	28	16	786	146	29	17	6%
5	583	59	29	16	583	77	31	17	7%
6	764	84	19	18	764	112	20	18	6%
7	672	69	41	19	672	98	42	20	7%
8	589	64	37	20	589	92	38	20	7%
9	566	60	38	25	566	77	39	26	10%
10	486	89	73	22	486	97	75	22	8%
11	561	54	28	25	561	79	29	25	9%
12	599	71	24	23	599	97	25	23	8%
13	684	77	38	27	684	108	38	28	9%
14	576	69	28	28	576	96	30	28	10%
15	411	54	21	24	411	77	22	24	8%
16	507	43	28	18	507	56	29	18	7%
17	503	71	22	23	503	99	23	23	8%
18	517	36	14	28	517	55	16	29	15%
19	455	61	34	21	455	89	35	21	8%
20	643	40	30	21	643	44	30	22	8%
21	583	52	24	28	583	77	26	29	9%
22	575	66	34	28	575	94	35	28	9%
23	468	51	20	25	468	78	22	25	9%
24	431	49	13	23	431	72	15	23	8%
25	476	50	19	18	476	77	21	18	8%
Avg.	572	65	29	22	572	91	31	22	8%
Std. Dev.	103	19	12	4	103	24	12	5	2%
COV	18%	28%	41%	20%	18%	27%	39%	21%	24%

